Regulation and Pharmacology of the Mitotic Kinesin Kif15

By

Megan Dumas

Dissertation

Submitted by the Faculty of the

Graduate School of Vanderbilt University

in partial fulfillment of the requirements

for the degree of

DOCTOR OF PHILOSOPHY

in

Cell and Developmental Biology

May 31st, 2019

Nashville Tennessee

Approved:

Ryoma Ohi, Ph.D.

Irina Kaverina, Ph.D.

Marija Zanic, Ph.D.

Matthew J. Lang, Ph.D.

Gary A. Sulikowski, Ph.D.

For Kathy & Donald Dumas

ACKNOWLEDGEMENTS

First, I would like to thank my mentor Dr. Ryoma “Puck” Ohi for all of his guidance, support, and friendship over the years. Being in Puck’s lab taught me both the fun and beauty of science and I am forever grateful to have studied the mitotic spindle during my graduate career. I also would like to thank Dr. Marija Zanic, whose support and encouragement were paramount to my success at Vanderbilt and whose lab welcomed me as their own. I would like to thank my Ohi lab mates Dr. Emma Sturgill, Dr. Sophia Gayek, Dr. Jennifer Landino and Dr. Stephen Norris. Each of you have taught me what it means to be a scientist and each of you have helped me in numerous ways throughout graduate school. And to my Zanic lab mates, Dr. Elizabeth Lawrence, Dr. Goker Arpag, Veronica Farmer, Claire Strothman, Nikki Rodgers, and Cayetana Arnaiz. Thank you for the support, camaraderie, and welcoming me into your lab family. And lastly, my best friend, my sister, Dr. Nora Foegeding! I could not have gotten any luckier having you as my room mate when I moved to Nashville. Words can not describe how important your friendship and support have been throughout my time at Vanderbilt.

I want to thank my mother and father for their unconditional love, support, and encouragement. You both are incredible parents and I am grateful to have you both to learn from every day.

TABLE OF CONTENTS

Page

ACKNOWLEDGMENTS iii

LIST OF TABLES vi

LIST OF FIGURES vii

LIST OF ABBREVIATIONS ix

Chapter

I. Introduction 1

The Cell Cycle and Mitosis 1
The Mitotic Spindle 2
Tubulin and Dynamic Instability 3
Spindle MT Structure 4
Forces Within the Spindle 6
Dynein 7
Kinesins 7
Spindle Assembly: Nucleation of MTs 9
Spindle Assembly: Centrosome Separation 10
Regulation of Mitotic Kinesins 14
Targeting Mitosis for Chemotherapies 16
MT Targeting Compounds 17
Next Generation Anti-Mitotics 18
Summary 20

II. Materials and Methods 22

Protein Expression and Purification 22
MT Gliding Assay and Image Analysis 23
ATPase Assay Screening Conditions 24
Steady State ATPase Assay 25
Cell Culture, Transfections, and Immunoblotting 26
Generation of K5I-Resistant RPE-1 Cells 27
Co-pelleting Assays 27
Co-Immunoprecipitation Assays 28
Spindle Assembly Assay and Fixed-Cell Imaging 29
Compound Synthesis Information 30

III. Regulation of Kif15 via Cis and Trans Mechanisms 32

Introduction 32
C-terminal Inhibition of Kif15 Resides Within its last 100 Amino Acids 34

KBP Inhibits Kif15 and Kif18A MT Gliding 34
KBP Binds Directly to Kif15 and Kif18A 36
KBP Blocks MT Binding of Kif15 and Kif18A 37
KBP Overexpression Prevents Kif15-Driven Spindle Stabilization 39
Discussion 40

IV. Identification of GW108X: A Novel Kif15 Inhibitor 42

Introduction 42
Assay Quality Conditions 43
Screening the GlaxoSmithKline Published Kinase Inhibitor Set 44
First Round of Structure-Activity Relationship (SAR) Analysis 48
Second and Third Round of SAR: Modifications to Phenol and Furan Group 50
Discussion 51

V. GW108X is a Reversible, Non-ATP Competitive Inhibitor of Kif15 55

Introduction 55
GW108X is a Reversible Inhibitor 56
GW108X has a High Preference for Kif15 56
GW108X is a Non-Competitive ATP Inhibitor 57
GW108X Inhibits Spindle Assembly in K5I Resistant Cells 58
Discussion 62

VI. Kif15-IN-1 is an ATP Competitive Inhibitor of Kif15 65

Introduction 65
Kif15-IN-1 Displays Sub-Micromolar IC_{50} 66
Kif15-IN-1 is Reversible and Competes with ATP 67
Kif15-IN-1 Decreases Mitotic Spindle Length 68
Kif15-IN-1 Prevents Spindle Assembly in KIRC-1 Cells 68
Discussion 68

VII. Concluding Remarks 72

Targeting Kif15 Intramolecular Interactions 72
Targeting Kif15 Pharmacologically 73

Appendix

A.1. Structure-Activity Relationship Analysis of GW108X, VU669, & VU724 Analogs 77
A.2. Can GW108X or its Derivatives Prevent K5I resistance in RPE-1 cells? 84

References 88

LIST OF TABLES

Table Page

4.1 Statistical Analysis of Assay Development and Screening Conditions.....46

LIST OF FIGURES

Figure Page

1.1 Schematic of MT populations with the mitotic spindle 5

1.2 Schematic of spindle assembly and centrosome separation by Eg5 11

3.1 C-terminal amino acids required for Kif15 auto-inhibition 35

3.2 KBP inhibits Kif18A and Kif15 MT gliding 36

3.3 Direct interaction between KBP and the motor domains of Kif15 and Kif18A 37

3.4 KBP interferes with Kif18A-N480 and Kif15-N420 MT binding 38

3.5 Full length kinesin motors display complex KBP regulation 39

3.6 KBP overexpression inhibits Kif15-driven spindle stabilization 40

4.1 Testing the ADP-Glo ATPase assays conditions 44

4.2 Screening the GSK PKIS 45

4.3 Summary of the top five compounds from PKIS screen 47

4.4 Characterization of top five compounds in MT gliding assay & IC_{50} of GW108X 48

4.5 Summary of lower scoring compounds (from top 10) from PKIS 49

4.6 SAR analysis for GW108X derivatives 50

4.7 SAR analysis of the second round of GW108X derivatives 52

4.8 SAR analysis of third round of GW108X derivatives 53

5.1 GW108X is a reversible Kif15 inhibitor and has a high preference for Kif15 57

5.2 GW108X is a non-competitive ATP inhibitor 58

5.3 RPE-1 cells maintain spindle bipolarity when treated with GW108X 60

5.4 GW108X prevents spindle assembly in KIRC-1 cells....61

5.5 Monopolar spindles dominant 2 hours after GW108X removal....62

6.1 Sub-micromolar IC_{50} of Kif15-IN-1 in MT gliding assay....66

6.2 Kif15-IN-1 is a reversible, ATP competitive inhibitor of Kif15....67

6.3 Kif15-IN-1 has no effected on Kif15 localization or protein levels in RPE-1 cells....69

6.4 Kif15-IN-1 prevents spindle assembly in KIRC-1 cells....70

A1.1 SAR analysis of GW108X structural analogs....78

A1.2 SAR analysis of VU669 structural analogs....80

A1.3 SAR analysis for VU724 structural analogs....83

A2.1 Combined STLC and GW108X treatment....85

A2.2 Resistant colony formation with STLC & varying incubations with compound 2 ...87

LIST OF ABREVIATIONS

GSK	GlaxoSmithKline
PKIS	Published Kinase Inhibitor Set
MT	Microtubule
SAR	Structure-Activity Relationship
FL	Full Length
K5I	Kinesin-5 Inhibitor
LZ	Leucine Zipper
AMPPNP	Adenylyl-imidodiphosphate
SEM	Standard error of the mean
SD	Standard deviation
KBP	Kinesin-binding protein
K-MTs	Kinetochore microtubules
NEB	Nuclear envelope breakdown
MTOC	Microtubule organizing center
SAF	Spindle assembly factor
KIRC	K5I resistance cell
OE	Over expressed
CRC	Concentration response curve

CHAPTER 1

INTRODUCTION

The Cell Cycle and Mitosis

Cell division is a fundamental process that is required for life. It is a beautiful orchestration of biochemical events that gives cellular life the ability to pass on its genetic material, allowing organisms to grow and reproduce. Cell division relies on the cell cycle machinery, an incredibly complex network of proteins that prepares and primes the cell to duplicate and segregate its genome. Cell division is arguably one of the most important events that takes place in our body, as the cell has to handle the genome with both care and efficiency. As such, several diseases arise due to faulty cell division, such as cancer.

The cell cycle has four distinct phases, each depending on the success of the previous to be initiated. The first phase is called G1, a period of cell growth and microenvironment monitoring to determine if conditions are suitable for cell division. This is followed by a DNA synthesis phase, where the cell duplicates the genome in preparation to divide. DNA duplication is followed by another, shorter growth phase (G2) where the cell continues to synthesis proteins required for cell division. The cell cycle culminates in mitosis, whose major events include release of DNA from the nucleus and the creation of the mitotic spindle (Alberts et al. 2008).

Despite mitosis being the shortest phase in the cell cycle, lasting roughly 30 minutes, it is the most critical step. Mitosis itself consists of different stages, beginning with prophase and prometaphase, where the chromosomes condense, the nuclear envelope breaks down, and the mitotic spindle is built. This is followed by metaphase, where the duplicated chromosomes align

at the equator of the mitotic spindle. Once chromosome alignment is achieved, the cell physically separates the sister chromatids during anaphase, pulling them to opposite ends of the cell concurrent with cytokinetic ring constriction at the cell equator (Asbury 2017; Green et al. 2012). Within the two new daughter cells, the chromosomes decondense and the nuclear envelope reforms during telophase (Alberts et al. 2008). Mitosis concludes with cytokinesis, the cleavage and physical separation of the two new daughter cells (Green et al. 2012).

The cell spends an enormous amount of energy and resources preparing to divide, ramping up protein production to support the duplication of organelles and the genome. To prevent waste and protect the integrity of division, the cell has evolved numerous safeguards to guarantee a successful cell cycle. These checkpoints consist of biochemical switches that induce an all-or-none response signaling cascade (Nurse 2000). Cells use binary responses to control the cell cycle because it is equally dangerous to prematurely initiate cell cycle signaling pathways as it is to halt them half way through. Major check points monitor the success of DNA replication, the attachment status of chromosomes to the spindle, as well as microenvironment conditions (Barnum and O'Connell 2014).

The Mitotic Spindle

The term mitosis was coined by Walter Fleming in 1882 from the Greek *mitos* which means "thread" and the Latin *osis*, which means "act" or "process". Though many exciting events comprise mitosis, many who study it are captivated by a macromolecular machine called the mitotic spindle. The spindle is an impressive structure, whose fleeting existence in mitosis makes it even more of a mystery. The "living spindle" was first visualized in 1937 and later the structure was confirmed by Inoue in 1953 using polarized light microscopy (Inoué 1953). The fibers that comprise the mitotic spindle are called microtubules (MT). MTs are a complex cytoskeletal

polymer whose main role in interphase is to provide cytoplasmic organization through organelle positioning and vesicle cargo trafficking (Alberts et al. 2008). In addition, interphase MTs are crucial for cell motility. At the leading edge of the cell, polymerizing MTs activate Rac1 to stimulate actin polymerization within the lamellipodia and at the rear of the cell, MTs target focal adhesions to stimulate their disassembly (Kaverina, Krylyshkina, and Small 1999; Kaverina, Rottner, and Small 1998; Waterman-Storer et al. 1999). In mitosis, MTs assume a new responsibility, creating anchor points between the chromosomes and the spindle pole.

Tubulin and Dynamic Instability

MTs are composed of αβ-tubulin heterodimers that self-assemble in a head-to-tail fashion to create a protofilament (Borisy and Taylor 1967). Lateral non covalent interactions between tubulin protofilaments leads to the creation of a hollow, cylindrical tube that is the MT (Alberts et al. 2008). The β subunit of the tubulin dimer contains an exchangeable nucleotide binding pocket that can bind and hydrolyze GTP. During MT assembly, GTP-tubulin adds on to the growing end of the polymer and creates a protective GTP-tubulin cap and subsequent GTP hydrolysis leads to a predominantly GDP-tubulin lattice (Carlier et al. 1984; Mitchison and Kirschner 1984). GTP-hydrolysis within the structure leads to a 'bending' of the tubulin dimer and compaction of the MT lattice. This compaction generates strain within the lattice and acts as a storage of energy that is released during depolymerization (Alushin et al. 2014). MTs exhibit a unique feature called dynamic instability that allows individual polymers to switch between periods of growth and shrinkage within a steady state population (Mitchison and Kirschner 1984). MTs also have an intrinsic polarity due to the nature of tubulin protofilament assembly. The α subunit of the incoming tubulin dimer interacts with the exposed β subunit in the protofilament, creating a polar

structure with exposed α and β subunits at either end. These ends are classified as the minus and plus end of the MT, respectively. The structural polarity of the polymer results in functional differences between the two ends of the filament, with the plus end generally being more dynamic then the minus end (Walker et al. 1988). This inherent property of MTs, along with dynamic instability, results in the creation of dynamic networks within the cell that have the dual ability to explore cellular space as well as create stable structures when needed. Furthermore, this dynamicity of MTs imparts the ability to drastically rearrange their cellular network at the onset of mitosis, disassembling the interphase MT array in a matter of minutes. Not surprisingly, the dynamic property of MTs is essential during mitosis. Efficiency and adaptability of the MTs within the spindle is crucial for spindle formation as well correcting erroneous chromosome connections.

Spindle MT Structure

Tens of thousands of MTs make up the mitotic spindle and sub populations of MTs take on distinct functions. The spindle is a bipolar structure with microtubule organizing centers (MTOCs), or centrosomes, at opposite ends. In general, the minus ends of the MTs are focused and embedded in the centrosomes, with the dynamic plus ends free to explore cytosolic space (Doxsey 2001). The majority of the spindle MTs grow towards the center of the structure and fall into three categories: interpolar, bridging, and kinetochore MTs. Kinetochore MTs (K-MTs) are bundles of parallel MTs that form a mechanical link to the chromosome via the protein complex called the kinetochore (Hinshaw and Harrison 2018). These bundles are the most stable MT population in the spindle, with a lifetime in the order of minutes (Zhai et al. 1995). Bridging MTs, also known as bridging fibers, are bundles of anti-parallel MTs that connect sister K-MTs. During metaphase, bridging fibers help balance the interkinetochore tension and during anaphase, produce

sliding forces to separate the sister chromatids (Kajtez et al. 2016; Vukušić et al. 2017). Interpolar MTs grow from opposite centrosomes and overlap in the cell middle, creating an anti-parallel array (Mastronarde et al. 1993). This population of MTs comprises the majority of the MT density within the spindle and is more dynamic then their K-MT counterpart, with a half-life of less than one minute (Zhai et al. 1995). Despite their rapid turnover, interpolar MTs provide structural integrity for the spindle. Last but not least, there are astral MTs, a population of non-bundled MTs that grow towards the cell cortex rather than the cell middle. Astral MTs interact with actin and the molecular motor dynein at the cell cortex and are required for proper spindle orientation (Laan et al. 2012).

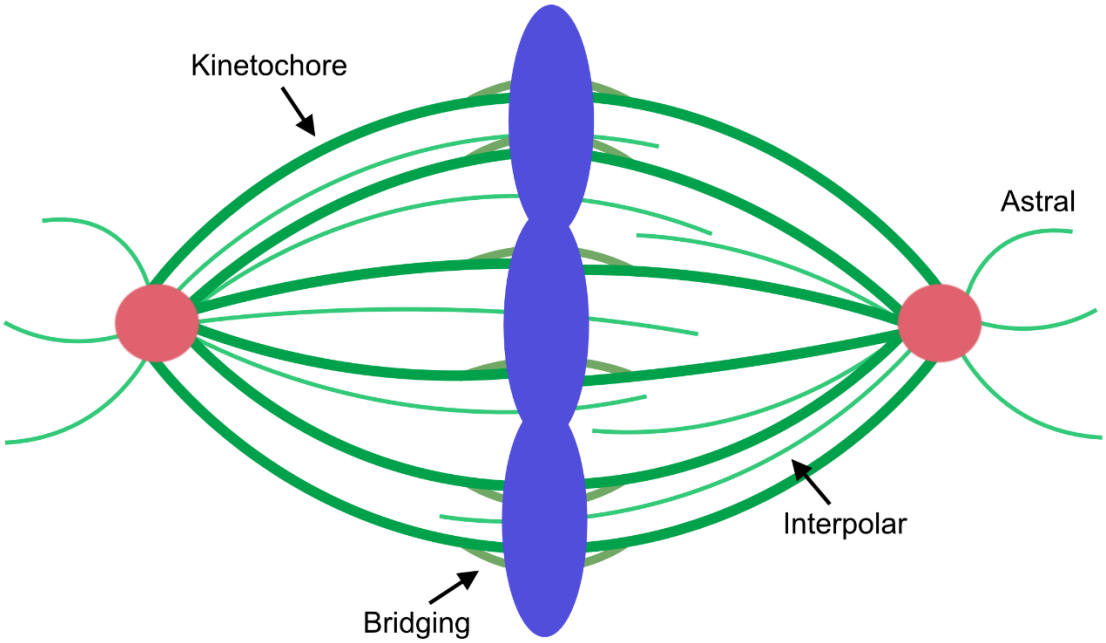

Figure 1.1 Schematic of MT populations within the mitotic spindle. Kinetochore, bridging, and interpolar MTs are all located within the spindle mass. Astral MTs grow away from the spindle center and interact with the cell cortex.

Forces Within the Spindle

Upon observing mitosis in a living cell, it becomes clear that it is a force driven process. One might notice the constant motion of the chromosomes, the subtleties in spindle positioning, or the polymerization and depolymerization of the MTs. These movements, in part, can be attributed to another intrinsic property of MTs: their ability to produce forces within cells. MTs can produce both pushing and pulling forces during their polymerization and depolymerization, respectively. Tubulin dimers add to the growing plus end of the MT during polymerization, which is able produce force against boundaries *in vitro* (Dogertom and Yurke 1997). This force generation model, referred to as the Brownian ratchet mechanism, attributes thermal fluctuations to the occasional insertion of new subunits at the growing end, even in the presence of an external resisting force (Mogilner and Oster 1999; Peskin, Odell, and Oster 1993). In cells, plus end polymerization in the spindle midzone uses this property to drive chromosomes further apart in late anaphase (Scholey et al. 2016). Depolymerization of MTs occurs when the stabilizing GTP-tubulin cap is lost, resulting in rapid release of the bent GDP-lattice. Cells harness the forces generated from MT depolymerization to pull on sister chromatids during metaphase and importantly anaphase, when chromatids must reach the new daughter cell (Asbury 2017; Khodjakov and Rieder 1996; Lombillo et al. 1995).

While the MTs that compose the mitotic spindle can inherently produce forces on their own, the mechanical processes observed in mitosis would not be possible without the orchestration of molecular motors. Molecular motors are broadly classified as enzymes that harness the energy from ATP hydrolysis to generate force inside the cell. The precise coordination and balance of forces generated by these motors is crucial for the success of the spindle.

Dynein

In 1965, the first MT based motor to be discovered for its role in cilia bending was dynein, named after the Greek word *dyne*, meaning force (Gibbons and Rowe 1965). Dynein is a AAA+ ATPase motor that walks towards the minus end of the MT and requires the activator dynactin to bind to cargo and walk processively inside the cell (Gill et al. 1991). During interphase, dynein is the sole retrograde transport motor, bringing endocytic vesicles towards the cell center either for recycling or degradation (Alberts et al. 2008). Dynein localizes to specific areas within the cell during mitosis, including the spindle and nuclear membrane, where its force generation properties help shape the mitotic spindle. At prophase, dynein is recruited to the nuclear envelope (NE) to facilitate NE breakdown as well as provide forces to separate the duplicated centrosomes (Raaijmakers et al. 2012). Dynein is also localized to the centrosomes. Here, dynein's ability to cross-link MTs and walk towards the minus end is used to support spindle pole focusing and clustering (Heald et al. 1996; Tanenbaum et al. 2013). In doing so, dynein activity at the poles generates inward directed forces that counteracts the outward forces that dominant during centrosome separation. When dynein activity is perturbed during mitosis, either via interfering antibodies or small molecule inhibitors, spindles are disorganized and display unfocused poles (Firestone et al. 2012; Gaglio et al. 1997). Dynein is also crucial for spindle positioning as hinted above, where cortical dynein pulls on astral MTs on either end of the spindle (Laan et al. 2012).

Kinesins

A second MT based motor named kinesin was discovered 20 years after dynein. Ron Vale and colleagues used the giant squid axon to study the mechanism of fast axonal transport and isolated the ATP dependent motor that powered this process (Vale et al.1985). Kinesins are a large

superfamily of molecular motors, consisting of 15 family members and 45 different kinesins in mammals. In general, kinesins are composed of 3 major tertiary structures, simply named the "head", "stalk", and "tail" domains. The globular "head" domain houses the ATPase and MT binding regions of the motor and is followed by a coiled-coil "stalk" domain that is important for dimerization. Kinesins diverge most in their "tail" region, which generally specifies the kinesins function or localization (Hirokawa and Tanaka 2015). Similar to dynein, kinesins use the mechanochemical coupling of ATP hydrolysis to generate forces within the cell. The kinesin ATPase cycle is tightly coupled to MT binding, with the motor domain cycling between low and high MT affinity states (Cross and McAinsh 2014). When no nucleotide is bound to the active site, kinesins exist in an 'apo' or rigor state and interact strongly with the MT. ATP binding and hydrolysis weaken the motors affinity for the MT, allowing the kinesin to unbind and interact with a new site on the MT lattice. After phosphate release, ADP in the active site shifts the motor into a weak MT binding state, with the motor returning to the 'apo' state upon removal of ADP from the active site and re-binding to the MT lattice (Cross and McAinsh 2014). The majority of kinesins are plus end directed motors, with the exception of Kinesin-14s and Kinesins-13s. HSET is a member of the minus-end directed Kinesin-14 family that localizes to the centrosomes during mitosis while MCAK is a kinesin-13 family member that depolymerizes MTs (Desai et al. 1999; Walczak et al. 1997). In interphase, kinesins are vital for anterograde transport of vesicles as well as organelle positioning. For example, when MTs are depolymerized, the Golgi complex undergoes fragmentation and lysosomes freely diffuse (Ba et al. 2018; Thyberg and Moskalewski 1985). The force generation ability of kinesins is also harnessed in mitosis and will be discussed below.

Spindle Assembly: Nucleation of MTs

Spindle assembly begins when the interphase MT network disassembles at the onset of mitosis. This breakdown provides the soluble tubulin that is required to create the mitotic spindle *de novo*. Quick and efficient MT nucleation is key to building the spindle under the time constraints of cell division. As such, the nucleation capacity of the centrosomes increases substantially during mitosis, presumably through the recruitment of γ-tubulin and the γ-tubulin ring complex (γ-TURC). γ-tubulin is a member of the tubulin family found in all eukaryotes and is highly enriched at MTOCs (Oakley et al. 1990; Oakley and Oakley 1989). The γ-TURC is a ring structure composed of γ-tubulin and other proteins that act as a template to build a MT and together with γ-tubulin, is required for MT nucleation (Zheng et al. 1995). The MT catastrophe frequency also increases substantially during mitosis (Verde et al. 1992). Changing this parameter of dynamic instability allows the MTs within the spindle to quickly explore the cell volume at the onset of mitosis. This exploration is central to the "search and capture" model, where upon nuclear envelope break down (NEB), the dynamic MTs emanating from the centrosomes can search and engage the sister chromatids (Holy and Leibler 1994).

Centrosomes were long believed to be the only microtubule organizing center (MTOC) in cells. In retrospect, it would be unwise to not have back up methods to create a structure as important as the spindle. As such, it is now understood that spindle assembly is extremely robust and cells employ several mechanisms to protect the spindle. The most obvious clue that cells harness other pathways to create a mitotic spindle comes from observing female oocyte meiosis. Ooctyes lack centrosomes and instead depend on an acentrosomal spindle assembly pathway to create a bipolar spindle (Bennabi et al 2016). The acentrosomal pathway relies on MT nucleation originating from chromosomes. Several spindle assembly factors (SAFs) are sequestered in the

nucleus by α/β importins and their release depends on the small GTPase Ran and its guanine nucleotide exchange factor RCC1 (Kalab and Heald 2008). RCC1 is highly enriched on the chromatids, resulting in a high concentration of Ran-GTP and subsequent release of SAFs near the chromosomes (Kalab et al 2002). For example, the protein TPX2 is an importin cargo and its release promotes MT nucleation and downstream signaling pathways that promote spindle assembly (Gruss and Vernos 2004). In addition, the acentrosomal pathway depends on MT motors to sort and organize MTs into a bipolar structure (Heald et al. 1996). Though the acentrosomal spindle assembly pathway is generally masked in centrosome containing cells, ablation of the centrosome does not interfere with formation of a bipolar spindle, signifying that back up mechanisms can be employed and dominate when needed (Khodjakov et al. 2000).

MT nucleation also occurs inside the spindle. This process is mediated by a protein called augmin, which binds to MTs within the spindle and recruits the γ-TURC (Goshima et al. 2008). The interaction between a spindle MT and augmin promotes branching of MTs off of one another, adding MT density to the spindle. This population of nucleated MTs is crucial for spindle function. When augmin nucleation is removed from HeLa cells, spindle MT density decreases and mitotic progression is impaired (Uehara et al. 2009).

Spindle Assembly: Centrosome Separation

The iconic bipolar geometry of the spindle may be its most important feature. While other characteristics of the spindle are indeed crucial for mitosis, any cell attempting to divide with a structure other than a bipole will fail. Bipolarity is achieved only when the minus ends of the spindle MTs are focused at the two centrosomes. The consequences of bipolarity failure can be seen in both monopolar and multipolar cells. Monopolar spindles are rosette structures whose

centrosomes are enclosed by a radial array of MTs and DNA due to centrosome separation failure. Syntelic chromosome attachments dominate and without equal tension on both sister kinetochore, the spindle assembly checkpoint (SAC) is activated, leading to apoptosis (Kapoor et al. 2000; Tao et al. 2005). Conversely, cells that form multipolar spindles are in danger of producing aneuploid progeny with uneven chromosome distribution (Kwon et al. 2008). Aneuploid cells are highly unstable and display chromosome instability, a hall mark of cancer (Ganem et al. 2007; Salmela and Kallio 2013). Both monopolar and multipolar mitoses are equally disastrous for the cell and as such, several pathways have evolved to add robustness to the bipolar spindle to promote its correct formation.

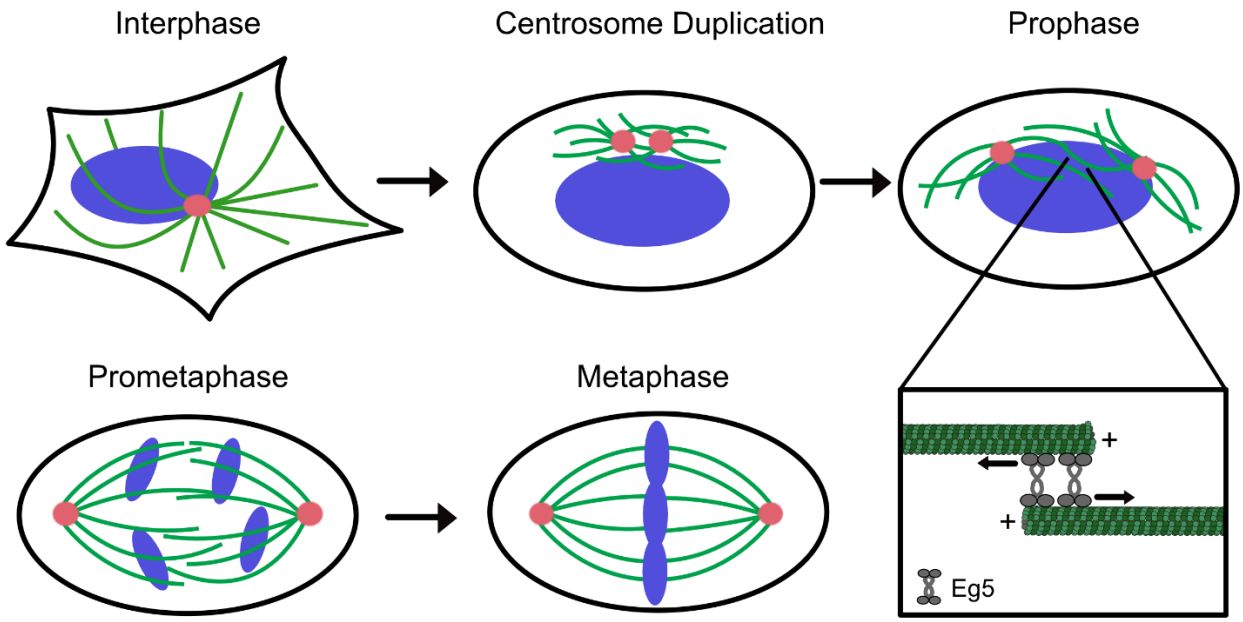

Figure 1.2 Schematic of spindle assembly and centrosome separation by Eg5. During interphase, the MT network spans the cell and acts as a 'highway' for cargo carrying molecular motors. When the cell cycle is initiated, the centrosomes duplicate and an increase in MT nucleation and MT dynamics leads to the formation the mitotic spindle. Eg5 is able to bind to the anti-parallel MT overlap formed between the two centrosomes and provides the pushing forces required for separation (inset).

After centrosome duplication, sister centrosomes remain in proximity of each other on the nuclear envelope and must separate before NEB. The main outward force generator involved in centrosome separation is the mitotic kinesin-5 family member Eg5 (Blangy et al. 1995; Sawin et al. 1992). Eg5 is a tetrametric kinesin that has two motor domains on opposite ends of the molecule, allowing Eg5 to engage two MTs at once (Le Guellec et al. 1991). As a plus end directed motor, Eg5 acts as a MT slider when its motor heads are bound to anti-parallel MTs or a MT crosslinker when bound to parallel bundles (Kapitein et al. 2005). Eg5 localizes to the NE during prophase, where it can bind and slide MTs within the nascent antiparallel overlap being formed by the sister centrosomes (Figure 1.2, Sawin and Mitchison 1995). Recent work suggests that Eg5 also acts as a MT polymerase that dwells at the MT plus end, promoting MT growth and preventing catastrophe, essentially generating its own track (Chen and Hancock 2015). This novel finding aligns with the function of Eg5 during mitosis, allowing the motor to dwell on antiparallel overlaps to facilitate outward pushing forces while also creating longer MT tracks. During prometaphase and metaphase, Eg5 remains bound to the spindle and is enriched near the poles (Sawin and Mitchison 1995; Sturgill and Ohi 2013). At first, this seems like an odd localization for an anti-parallel MT slider. One explanation comes from the observation that bipolar spindles do not collapse if an Eg5 inhibitor is added after bipolarity is achieved, suggesting that Eg5 is not required for spindle bipolarity maintenance. Moreover, Eg5 has been shown to be functional on parallel MTs and may play a role in pole maintenance (Groen et al. 2008; Kapitein et al. 2005).

Several specific and potent kinesin-5 inhibitors (K5I) have been developed over the past 20 years and have been utilized by clinicians and basic researchers alike (Kozielski 2012). Researchers have taken advantage of these small molecules to study auxiliary spindle assembly pathways in somatic cells that do not rely on Eg5 activity for centrosome separation. To date, four

different groups have generated K5I resistant cell (KIRC) lines and all of them share one unifying feature: they require the mitotic kinesin Kif15 for viability (Dumas et al. 2018; Ma et al. 2014; Raaijmakers et al. 2012; Saeki et al. 2018; Sturgill et al. 2016; Sturgill and Ohi 2013). Before this universal requirement for Kif15 in K5I resistance had been revealed, the kinesin-12 family member Kif15 was first likened to Eg5 due to its ability to rescue spindle bipolarity when overexpressed in K5I treated cells and later for its anti-parallel MT sliding capabilities (Reinemann et al. 2017; Tanenbaum et al. 2009). Kif15 was first discovered in *Xenopus* as a plus end directed kinesin, containing an N-terminal motor domain followed by a coiled-coil stalk (Boleti et al. 1996). Within its coiled-coil stalk lies a non-motor MT binding site that allows Kif15 to engage with two MTs (Sturgill et al. 2014). In *C. elegans*, Eg5 is not required for bipolar spindle formation and instead relies on Kif15 in both oocyte meiosis and mitosis (Bishop, Han, and Schumacher 2005; Segbert et al. 2003; Wignall and Villeneuve 2009).

In human tissue culture cells, Kif15 is essential for spindle bipolarity maintenance, rather than generation of centrosome separation forces (Tanenbaum et al. 2009; Vanneste et al. 2009). Kif15 localizes to K-MTs, acting as a K-MT stabilizer and length regulator while also antagonizing the outward forces generated by Eg5 (Sturgill and Ohi 2013). However it is Kif15, rather than Eg5, that assumes a dominant role in spindle bipolarity maintenance. HeLa metaphase spindles maintain spindle bipolarity when treated with an Eg5 inhibitor, but collapse to monopoles if Kif15 is knocked down (Sturgill and Ohi 2013; Tanenbaum et al. 2009). Cells treated with a K5I can adapt to loss of Eg5 activity by over expressing Kif15 (Sturgill and Ohi 2013; Tanenbaum et al. 2009). When over expressed, Kif15 redistributes to non-K-MTs, where it is able to compensate for loss of Eg5 by sliding anti-parallel MTs apart to separate the centrosomes (Sturgill and Ohi 2013).

Despite being an antiparallel MT slider, centrosome separation via Kif15 is temporally and mechanically distinct then the Eg5 driven pathway. In HeLa cell derived KIRCs, centrosomes fail to separate by NEB and form a monopolar intermediate. On the path to bipolarity, monopolar spindles break radial symmetry to create a radial fan-shaped monoester, which then undergoes "reverse jackknifing", where one spindle pole rotates 180°. Even though this alternative spindle assembly pathway accomplishes the end goal of bipolarity, it is not efficient, as evidenced by nearly 50% of cells undergoing apoptosis (Sturgill and Ohi 2013).

Regulation of Mitotic Kinesins

Kinesin motors are vital mechanical movers in the cell that have crucial functions in both interphase and mitosis. Since kinesins consume ATP, a central energy source for the cell, their activity must be controlled to prevent fruitless ATP hydrolysis. In addition, controlling when and where kinesins become active allows the cell to effectively harness their power when needed, preventing the disaster of kinesin hyperactivity. Kinesin activity is kept in check several ways. Though both interphase and mitotic motors are subjected to the same regulatory mechanisms, mitotic motors will be discussed as examples for each.

Globally, mitotic motors are regulated through control of protein levels during the cell cycle and cyclin dependent phosphorylation, similar to non-kinesin mitotic proteins (Verhey and Hammond 2009). Beyond this, a common regulatory mechanism exploited by several kinesins is autoinhibition. Autoinhibition is a *cis* regulatory mechanism, with the C-terminal tail of the kinesin interacting with the motor domain. This folded conformation effectively shuts down ATPase and MT binding activity of the motor. Autoinhibition is a particularity effective method since the inhibitory component is attached to the motor itself, allowing for quick and precise inhibition.

Though this mechanism is most studied in the transport motor kinesin-1, mitotic motors also use autoinhibition to regulate their activity within the spindle (Hackney and Stock 2000; Kaan et al. 2011). For example, the chromosome congression kinesin CENP-E is directly regulated in this manner, with phosphorylation by Cdk1 relieving inhibition and allowing the motor to bind MTs at the onset of mitosis (Espeut et al. 2008). Similarly, Kif15 is directly regulated by its C-terminal tail. What makes Kif15 autoinhibition unique is that Kif15 harbors a second non-motor MT binding site within its coiled-coil tail, which imparts a preference for MT bundles over single filaments (Sturgill et al. 2014). Together, self-regulation and a preference for bundled MTs in an active conformation ensures that the motor is restricted to K-MTs during mitosis. Kif15 is cytosolic during interphase, but does not bind to MTs, suggesting that its autoinhibition is relieved upon mitotic entry. Indeed, Kif15 phosphorylation by Aurora A kinase promotes its localization to the spindle during mitosis (van Heesbeen et al. 2017). Furthermore, Kif15 has a potential Cdk1 phosphorylation site, but direct phosphorylation by Cdk1 has not been confirmed (Boleti et al. 1996).

Interactions in *trans* between kinesins and their binding partners, or "receptors", can recruit kinesins to their proper spindle location. A classic example of a "receptor" that targets several kinesins is the midzone associated protein PRC1. PRC1 interacts with the N-terminal region of Kif4a, a chromokinesin that regulates midzone MT length (Kurasawa et al. 2004; Subramanian et al. 2013). During anaphase, PRC1 also targets the transport kinesin MKLP-1 and MKLP-2 to the spindle midzone, both of which are required for successful cytokinesis (Neef et al. 2006). Kinesins that regulate MT dynamics during mitosis are often recruited to the plus end of the MT through interactions with MT end binding protein EB1 (Mimori-Kiyosue et al. 2000). For example, the MT depolymerase MCAK binds to EB1 and becomes enhanced at MT tips (Lee et al. 2008).

Post translational modifications can also control kinesin activity in cells. Phosphorylation is the most studied modification and can regulate kinesin activity in several ways. The majority of phosphorylation events occur in the regulatory non-motor regions of the kinesin, thus either interfering or promoting an activity or localization (Welburn 2013). For example, MCAK phosphorylation by Aurora B kinase dampens its MT depolymerization activity during mitosis, presumably through interfering with its ability to bind MTs. When MCAK phosphorylation by Aurora B is blocked, MCAK activity is unchecked and monopolar spindles dominant (Ohi et al. 2004). On the other hand, phosphorylation of Eg5 by Cdk1 promotes its localization to the spindle and is also required for spindle bipolarity (Blangy et al. 1995; Sawin and Mitchison 1995). Phosphorylation can also relieve autoinhibitory interactions, such as described above for CENP-E (Espeut et al. 2008).

Finally, mitotic kinesins can be sequestered in the nucleus to prevent their activity during interphase. For example, Kinesin-14 family member HSET and MKLP-1 are sequestered to the nucleus via their interactions with nuclear importins, ensuring that they are only released when needed after NEB (Goshima and Vale 2005; Liu and Erikson 2007).

Targeting Mitosis for Chemotherapies

Plants that contain active MT targeting compounds, such as the extract from the toxic blooming flower autumn crocus, have been used to treat human conditions since the Ancient Egyptians (Florian and Mitchison 2016). It would be many millenia later when the compound from that flower would be isolated by scientists and named Colchicine. Colchicine binds to curved tubulin dimers and forces them to remain curved, leaving them unable to polymerize (Barbier et

al. 2010). Though not used a chemotherapy, Colchicine's ability to arrest mitosis ignited the field with curiosity about cell division in different tissues and organisms (Florian and Mitchison 2016).

MT Targeting Compounds

Many of the first chemotherapeutics discovered in the United States target microtubules and are still routinely used to treat certain cancers. The first class of MT targeting compounds was the vinca alkaloids, discovered in the 1950s from natural products (Noble, Beer, and Cutts 1958). Vinca alkaloids such as vinblastine bind to the tubulin dimer and have been used primarily to treat lymphomas and germ cell malignancies. The sequestration of tubulin dimers by vinca alkaloids eliminates the pool of polymerization competent tubulin, effectively shutting down MT dynamics (Florian and Mitchison 2016).

The most famous and successful MT targeting compound is Paclitaxel or Taxol. Taxol was discovered in the 1960s, isolated from the bark of the Pacific Yew tree, but its complex structure and low purification yield left many researchers uninterested (Wani et al. 1971). A decade later, pivotal work by Susan Horwitz and her graduate student Peter Schiff demonstrated Taxol acted by binding to and stabilizing MTs, unlike any other MT targeting drug to date (Schiff et al. 1979). Taxol is still used to treat a variety of cancers such as ovarian, breast, and non-small lung cell cancers (Florian and Mitchison 2016).

While the success of MT-targeting agents in the clinic should be celebrated, it is interesting to note that the reason for their success remains a mystery. MT-targeting agents are thought to function by targeting rapidly dividing cells by interfering with MT and mitotic spindle dynamics, leading to mitotic arrest. Indeed, a common side effect associated with taxol treatment is neutropenia, demonstrating taxols toxicity to proliferative tissue in the body (Rowinsky et al.

1993). However, the proliferation rate of solid tumors that Taxol is commonly used to treat is relatively low, begging the question of how Taxol is able effectively stop tumor growth (Mitchison 2012). Furthermore, it was demonstrated in samples from breast cancer patients and cell lines that clinically relevant Taxol concentrations do not induce mitotic arrest and instead, forced cells to undergo mitosis with multipolar spindles (Zasadil et al. 2014). This suggests that the success of Taxol is due to its ability to induce chromosome missegregation, leading to cell death. Regardless of clinical mechanism, Taxol remains the most successful chemotherapy in history (Walsh and Goodman 2010).

It is also worth noting that MT-targeting agents do have negative side effects for the patients that take them. The most common are neutropenia and peripheral neuropathy (Rowinsky et al. 1993). The fact remains that MTs are needed for a variety for cellular functions, and cells that rapidly divide such as neutrophils, or rely on their MT network for long distance signaling such as neurons, will be negatively affected.

Next Generation Anti-Mitotics

To minimize collateral damage, next generation anti-mitotics target proteins with mitotic-specific functions, such as kinases required for mitotic progression or kinesins that assemble the mitotic spindle. From the first category, mitotic kinases such as Aurora A, Aurora B, and Plk1 are all current targets for chemotherapeutics and have active clinical trials (clinicaltrials.gov). Aurora A and B are kinases vital for mitotic progression, phosphorylating key spindle assembly factors and SAC components, respectively (Perez et al. 2015). The mitotic kinase Plk1 is a workhorse kinase during mitosis, playing a role in centrosome maturation, chromosome alignment, and cytokinesis (Combes et al. 2017).

The spindle itself is a mitosis specific machine, acting as the mechanical structure that supports and drives mitosis forward. With this in mind, several inhibitors have been discovered that target mitotic kinesins that aid in spindle assembly and function. Several inhibitors exist for kinesins, but only Eg5 and CENP-E inhibitors have been used in clinical trials, discussed below.

The first Eg5 inhibitor discovered was monastrol, named for its ability to cause mono-asters in mammalian tissue culture cells (Mayer et al. 1999). In fact, monastrol was the first selective kinesin inhibitor to be discovered, kicking off a wave of excitement in both the clinical and basic biology fields. Cell biologists jumped on the opportunity to use K5Is to understand the role Eg5 played in spindle assembly, while pharmaceutical companies were hoping to finally have found an anti-mitotic that would wreck the spindle without causing neurotoxicity. Several pharmaceutical companies such as AstraZeneca, Bristol-Myers Squibb, and Merck all had competing K5I discovery programs, reflecting the excitement and promise around Eg5 and K5I scaffolds. To date, over 50 Phase I & II clinical trials testing different K5Is have been completed and millions of dollars have been spent studying and optimizing these compounds (Kozielski 2012). Despite their initial promise of becoming a block-buster chemotherapy, K5Is have largely failed in the clinic. Some reports documented stabilization of tumor growth, but none reported regression in tumor size. Though K5Is are inefficient as a monotherapy, there are currently active clinical trials for the treatment of multiple myeloma using the K5I ARRY-520 in combination with a proteasome inhibitor (Carfilzomib) or Pomalidomide and Dexamethasone, an anti-angiogenic and corticosteroid, respectively. The CENP-E inhibitor GSK-923295 is an allosteric rigor inhibitor that has been used in a single Phase 1 clinical trial, where its pharmacokinetics and dose-limiting toxicities were reported (Chung et al. 2012).

Several reasons for K5I failure have been hypothesized. The most obvious reason would be development of mutations within the K5I binding site of Eg5, rendering the small molecule inactive (Talapatra et al. 2013). This is a common downfall for several cancer drugs, as the genetic instability of tumors allows for selection for resistance mutations (Mansoori et al. 2017). Another possibility, which was discussed earlier, is that the success of anti-mitotics depends on the proliferation rate of the target tumor as well as retention time of the small molecule. Monopolar spindles have been observed from tumor samples from patients that were administered a K5I, indicating that K5Is indeed disrupt spindle assembly (Kantarjian et al. 2012). Another hypothesis is that tumor cells may overcome Eg5 inhibition by employing alternative spindle assembly mechanisms. Indeed, work from KIRCs suggests monopolar spindles are an intermediate structure in the Kif15-driven spindle assembly pathway (Sturgill and Ohi 2013). Mechanisms that overcome K5I treatment in tissue culture cells involve over expression of Kif15 or expression of a MT bundler, thus increasing Kif15s substrate in the cell. In both tumor and non-tumor derived cell culture lines, K5I resistance depends on Kif15, regardless of the resistance mechanism (Sturgill et al. 2016).

Summary

This study strives to understand how Kif15 is regulated both naturally and pharmacologically. The first chapter details studies that focus on how Kif15 is regulated by auto-inhibition and direct interactions with kinesin-binding protein (KBP), a regulatory protein recently characterized to bind several kinesins. Understanding how Kif15 is regulated in cells may provide potential insights into the mechanisms that drive K5I resistance as well as methods to exploit natures regulation for therapeutic use.

The majority of this dissertation focuses on identifying and characterizing small molecule inhibitors of Kif15. The drive to discover Kif15 inhibitors is two-fold. First, the clinical potential of combining K5Is with a Kif15 inhibitor has been discussed as a method to fully inhibit spindle assembly (Kozielski 2012; Sturgill et al. 2016). While this potential is exciting and supported by preliminary research, this hypothesis cannot be tested without a Kif15 inhibitor. Second, kinesin inhibitors have been instrumental in furthering our understanding of kinesin function. Currently, Kif15 silencing by siRNA or knock-out by CRISPR (and other methods) are the only options to experimentally disrupt Kif15 activity in cells. While these methods are fundamental for cell biology research, they pose several limitations and do not provide the precision of small molecule inhibition. Clinical value aside, a small molecule inhibitor for Kif15 will provide a powerful tool to study Kif15 activity and function in mitosis.

We screened a library of kinase inhibitors with the goal of identifying privilege scaffolds for Kif15 inhibition. We identified GW108X, an oxindole kinase inhibitor that inhibits Kif15 activity *in-vitro* and blocks spindle assembly when combined with K5Is. A commercially available Kif15 inhibitor, Kif15-IN-1, is also characterized and compared to GW108X. Importantly, we discovered that GW108X and Kif15-IN-1 are non-ATP competitive and ATP competitive inhibitors, respectively. This difference in inhibitory mechanism suggests that these two inhibitors are targeting different, druggable sites on Kif15.

CHAPTER 2

MATERIALS AND METHODS

Protein Expression and Purification

His_6-GFP-Kif15-FL, His6-Kif15-N700, His_6-HSET, Kif18A-N480-GFP-His6, and Kif18A-FL-GFP-His6 purifications have been described previously (Norris et al. 2018; Reinemann et al. 2017; Stumpff et al. 2011; Sturgill et al. 2014). His_6-Kif15-N420 was purified identically to His_6-Kif15-N700 except that the protein was dialyzed overnight into 10 μM ATP before being frozen. The activity of each His_6-Kif15-N420 protein prep was tested by approximating the ATP to ADP conversion rate before use in small molecule screening. In brief, a standard curve measuring the luminescence with known ADP:ATP ratios was generated using the ADP-Glo assay (described below). The assay was then run with different concentrations of His_6-Kif15-N420 and the luminescence values were compared to the standard curve to approximate ADP generation. The concentration of His_6-Kif15-N420 that generated ~20-30% ATP to ADP conversion rate was used for screening.

GST-KBP was expressed in BL21DE3 cells with 0.4 mM IPTG overnight at 16ºC. Cells were pelleted and flash frozen in liquid nitrogen and stored at -80ºC. For purification, pellets were resuspended in lysis buffer (1xPBS, 500 mM NaCl, 5 mM β-mercaptoethanol (β-ME), 1% NP40 and protease inhibitors (Complete Protease Inhibitor Cocktail tablets, Sigma-Aldrich). Lysate was incubated with 1 mg/mL of lysozyme for 30 minutes on ice, followed by sonication. Lysate was clarified by centrifugation at 35,000 rpm for 1 hour at 4ºC in a Ti 45 rotor (Beckman). Clarified supernatant was incubated with 2 mL of glutathione-agarose (Sigma-Aldrich) for 1 hour at 4ºC and washed with ~200 mLs of wash buffer (1xPBS, 500 mM NaCl and 5 mM β-ME). Protein was

eluted with 1 M Tris (pH 8.0), 3 M KCl and 200 mM glutathione and peak fractions were buffered exchanged into storage buffer (10 mM K-HEPES pH 7.7, 100 mM KCl and 1 mM DTT) using a PD 10 desalting column (GE Healthcare). Protein concentration was determined using Bradford assays and powdered sucrose was added 10% w/v before the protein was aliquoted, frozen in liquid nitrogen, and stored in -80ºC.

MT Gliding Assay and Image Analysis

Flow chambers were assembled using a glass slide, a No. 1.5 glass coverslip and double-sided tape to create a ~20 µl chamber. Approximately 1-1.5 µM of His_6-Kif15-N700 was incubated in the chamber for 3 minutes to allow non-specific absorption of the motor to the coverglass surface. The chamber was then washed with 60 µl of wash buffer (WB, [BRB80, 1 mM MgATP, 0.5 mg/ml casein]) and then incubated with 1% Pluronic F-127 for 1 minute to passivate the surface. The chamber was then washed with 60 µl of WB and then incubated with 0.5-1 µM of Alexa-594 labelled MTs (1:10, labeled:unlabeled tubulin) for 3 minutes. Lastly, the chamber was washed with 60 µl of flow cell buffer (WB plus 70 mM β-ME, 0.035 mg/ml catalase, 0.2 mg/ml glucose oxidase, 4.5 mg/ml glucose) and then imaged by epifluorescence microscopy. All compounds were added to FCB and then introduced into the flow cell. Images were acquired with a Nikon Elements controlled Eclipse 90i (Nikon) equipped with a 60X 1.4 NA (Nikon) objective and a Cool Snap HQ2 CCD camera (Roper). Time lapse sequences spanned 2 minutes with acquisitions captured every 2 seconds. Image J was used for image analysis and for GW108X, GW108X derivatives and Kif15-IN-1 experiments, MT velocity was calculated by measuring the distance a MT travelled in 20 seconds.

For wash out/wash in experiments, time lapse sequences spanned 5 minutes with acquisitions captured every 5 seconds. MT velocity was calculated by measuring the distance the MT travelled in 1 minute before wash in, after compound addition, and after wash out.

MT gliding velocity with KBP was calculated by measuring the distance the MT travelled in total during the 2 minute movie (120 seconds). The average velocity of control slides from one experimental day was calculated and used to calculate the percent inhibition using the following equation,

$$\%\ Inhibition = 100 - \left(\left(\frac{V_x}{V_u}\right) * 100\right)$$

where *Vx* is the velocity of a single MT and $V\mu$ is the average velocity of control MTs from that experimental day.

ATPase Assay Screening Conditions

The Promega ADP Glo™ Kinase Assay kit was used to detect the ATPase activity of His_6-Kif15-N420 and was adapted for use in high throughput format. Uniformity and reproducibility of the assay was evaluated by plating positive and negative reactions (+/- ATP, respectively) containing His_6-Kif15-N420, MTs and reaction buffer (10 mM K-HEPEs pH 7.7, 100 mM KCl, 1 mM DTT, 1 mM $MgCl_2$, 20 µM taxol) in every other well of a 384 well plate. Z-factor (Z') was calculated as follows where *p* is positive control and *n* is negative controls:

$$Z' = 1 - \frac{3(\sigma_p + \sigma_n)}{|\mu_p - \mu_n|}$$

For screening the GlaxoSmithKline Published Kinase Inhibitor Set (Drewry et al 2014), 10 µM of compound was shot into a 384 well plate (Greiner Bio-One) and incubated with 30 nM of His_6-Kif15-N420 + 5 µM MTs for 15 minutes. The reaction was then incubated with 10 µM ATP

for 20 minutes to stimulate the ATPase activity of His_6-Kif15-N420. Next, the kit reagent ADP-Glo was added to stop the ATPase reaction and deplete unconsumed ATP. After 40 minutes of incubation with ADP-Glo, the second kit reagent, Kinase Detection Reagent, was added to convert the ADP generated by His_6-Kif15-N420 to ATP. This ATP is then used to fuel a luciferase reaction and after 30 minutes, luminescence is measured using a luminometer (BioTek). Positive and negative control reactions were incubated with DMSO and either contained or lacked ATP, respectively. All reactions were performed at room temperature. Concentration response curves were performed as described above, except with varying concentrations of compounds.

Analysis of experimental days was performed in Waveguide (Vanderbilt HTS facility). To ensure assay quality, the Z' and coefficient of variation (% CV) for the positive, negative and compound wells were calculated for each plate. The % inhibition, Z-score and B-score were calculated for each compound. The top 5 hits from the screen reproducibly exhibited % inhibition > 60%, Z-score < -3 and B-score < -8.

Steady State ATPase Assay

Enzyme-coupled ATPase rates were quantified by NADH absorbance decay at 340 nm using a Multi-Mode Micro Plate Reader (Molecular Devices Flexstation 3), with 10-20 nM active dimeric His_6-Kif15-N700 motors. Motors and inhibitors were pre-incubated for 30 minutes to ensure steady state before ATP was added to initiate the ATPase reaction. Velocities were fit to an unweighted Michaelis-Menten curve, and these fitted K_M and k_{cat} were used to plot a line to the data in the Lineweaver-Burk plots.

Cell Culture, Transfections, and Immunoblotting

TP53$^{-/-}$ RPE-1 cells (Izquierdo et al. 2014, a gift from Bryan Tsou, Memorial Sloan Ketterling Cancer Center) were cultured in DMEM containing 10% FCS, penicillin and streptomycin. KIRC-1 cells were cultured in the same media with the addition of 10 µM STLC (Sigma-Aldrich).

siRNA transfections were performed using HiPerfect (QIAGEN). The following Kif15 siRNA was used: 5' – GGACAUAAAUUGCAAAUAC – 3' (Dharmacon).

TP53$^{-/-}$ RPE-1 and KIRC-1 cells were grown in a 6-well dish (Denville) and were washed with PBS, trypsinized, and were resuspended and incubated in lysis buffer (Roche Protease Inhibitor cocktail tablet, 1% NP-40, 6 mM Na_2HPO_4, 4 mM NaH_2PO_4, 150 mM NaCl, 2 mM EDTA, 50 mM NaF, 4 µg/mL leupeptin, 0.1 mM Na_3VO_4) for 15 minutes on ice. Extracts were clarified at 4ºC for 15 mins at 13K rpm and diluted 1:5 in 5x sample buffer (SB, 100 mM Tris-Cl, pH 6.8, 4% SDS, 20% glycerol, 200 mM DTT and 200 µg/ml bromophenol blue) and boiled. Samples were loaded at 25-27 µg total protein onto a TGX Stain-Free 10% Acrylamide gel (Bio-Rad), resolved by SDS-PAGE and transferred to a PVDF membrane for immunoblotting.

PVDF membranes were blocked with Odyssey blocking buffer (LI-COR Biosciences) diluted 1:1 in PBS for 1 hour at RT and probed with α-Kif15 at 1 µg/ml, DM1α (Abcam) at 1:5000, or mouse-KBP (Abnova) 1:1000 overnight at 4ºC (Sturgill and Ohi 2013). Membrane was washed 3x for 10 minutes with PBST and incubated with secondary antibodies conjugated to Alexa Fluor 700 (Invitrogen) or IRDye-800 (LI-COR) at 1:5000 for 1 hour at RT. Membrane was washed with PBST and PBS and bound antibodies were detected using an Odyssey fluorescence detection system (Mandel Scientific).

Generation of K5I-Resistant RPE-1 Cells

We generated K5I-resistant *TP53*$^{-/-}$ RPE-1 cells as previously described (Sturgill and Ohi 2013). The KIRC-1 cell line is a single clonal isolate. The properties of KIRC-1 and other K5I-resistant *TP53*$^{-/-}$ RPE-1 isolates will be described elsewhere.

Co-pelleting Assays

MT-co-pelleting was performed by incubating 700 nM of KIF18A-N480-GFP-His_6 or 1 µM of His_6-KIF15-N420 with 2 µM of GST-KBP in reaction buffer (10 mM K-HEPES pH 7.7, 50 mM KCl, 10 mM DTT, 1 mM $MgCl_2$ and 20 µM taxol (Sigma-Aldrich)) for 10 minutes at room temperature to promote their interaction. KIF18A-N480-GFP-His_6, His_6-KIF15-N420, and GST-KBP were clarified by spinning at 90k rpm for 10 minutes at 4ºC prior to use in assay. Next, 1 µM of taxol stabilized MTs and 1 mM AMPPNP (Sigma-Aldrich) was added to each reaction and incubated at room temperature for 15 minutes. The reaction was then spun over 150 µL of sucrose cushion (10 mM K-HEPES pH 7.7, 50 mM KCl, 20 µM taxol, 40% w/v sucrose) at 60k rpm for 20 minutes at 26ºC. 50 µL of supernatant was removed and mixed 1:1 with 2x sample buffer. The remaining supernatant was removed and the supernatant/cushion interface was washed 2x with reaction buffer. The cushion was then removed and the pellet was gently washed with reaction buffer before being resuspended in 100 µl of 1x SB. Both supernatant and pellet samples from each reaction was boiled, vortexed and 30 µL was run on a 10% SDS-PAGE gel. The gel was then stained with Coomassie for ~30 minutes and destained overnight before imaging. ImageJ was used to quantify the integrated intensity of each protein band. Integrated intensity of the supernatant and pellet lanes for each reaction was combined to give yield a total protein integrated intensity value, which was used to calculate the percent of protein in the supernatant.

KIF18A-FL-GFP-His_6 and His_6-GFP-KIF15-FL co-pelleting experiments were performed as described above, except proteins were detected using Western blots instead of Coomassie. For KIF18A-FL-GFP-His_6 experiments, 120 nM of kinesin and 342 nM of GST-KBP was used. For His_6-GFP-KIF15-FL experiments, 135 nM of kinesin and 384 nM of GST-KBP was used. Blots were cut ~70 kDa and the top portion was probed with rabbit-His (MBL, 1:1000) and mouse-KBP (Abnova, 1:1000) and the bottom with α tubulin (DM1α, Abcam).

Co-Immunoprecipitation Assays

Glutathione agarose slurry (Pierce) was washed with binding buffer (BB, 10 mM K-HEPES pH 7.7, 50 mM KCl, 1 mM DTT, 100 µM ATP, 0.1% NP-40) and incubated with 250 nM GST-KBP for 1 hour at 4ºC with rotation. Agarose was then washed 3x with BB and incubated with 20 mg/mL BSA for 30 minutes at 4ºC with rotation. Agarose was washed 3x with BB and incubated with 50 nM KIF18A-N480-GFP-His_6, KIF18A-FL-GFP-His_6, His_6-KIF15-N420 or His_6-GFP-KIF15-FL for 1 hour at 4ºC with rotation. Agarose was pelleted and supernatant was removed and saved, and the agarose pellet was resuspended in BB. Agarose was then washed 5-10x in BB. After washing, agarose was resuspended in 1x sample buffer (50 mM Tris-Cl, pH 6.8, 2% SDS, 6% glycerol, 1% βME and 200 µg/mL bromophenol blue) and boiled. Samples were loaded onto a TGX Stain-Free 10% Acrylamide gel (Bio-Rad), resolved by SDS-PAGE and transferred to a PVDF membrane for immunoblotting.

PVDF membranes were blocked with Odyssey blocking buffer (LI-COR Biosciences) diluted 1:1 in PBS for 1 hour at RT and probed with rabbit-His (MBL, 1:1000) and mouse-KBP (Abnova, 1:1000) overnight at 4ºC. Membrane was washed 3x for 10 minutes with PBST and incubated with secondary antibodies conjugated to Alexa Fluor 700 (Invitrogen) or IRDye-800

(LI-COR) at 1:5000 for 1 hour at RT. Membrane was washed with PBST and PBS and bound antibodies were detected using an Odyssey fluorescence detection system (Mandel Scientific).

Spindle Assembly Assay and Fixed-Cell Imaging

For spindle assembly assays, *TP53*$^{-/-}$ RPE-1 and KIRC-1 cells were treated with 25 µM GW108X, Kif15-IN-1 or DMSO for 24 hours. Cells were fixed in methanol at -20ºC for 10 minutes and then labeled with the following primary antibodies: FITC-conjugated mouse anti-α-tubulin (DM1α; Sigma-Aldrich), 1:500; and rabbit anti-Kif15 (α-Kif15), 1:2000. Secondary antibodies conjugated to Alexa-594 (Invitrogen) were used at 1:500. Fixed cells were incubated with primary and secondary antibodies for 1 hour each at room temperature. DNA was counterstained with 5µg/ml Hoechst 33342 and stained cells were mounted in Prolong Gold (Invitrogen).

Images were acquired using a 60X 1.4 NA objective (Olympus) on a DeltaVision Elite imaging system (GE Healthcare) equipped with a Cool SnapHQ2 charge-coupled device (CCD) camera (Roper). Optical sections were collected at 200 nM intervals and processed using ratio deconvolution in SoftWorx (GE Healthcare). Further image processing was done in ImageJ. Acquisition parameters were same across cell lines and conditions.

For Kif15 and tubulin spindle intensities, an oval ROI was drawn around the spindle to measure the integrated fluorescence of a sum intensity projection for both the tubulin and Kif15 channels. Four smaller ROI ovals were made around the spindle to measure background fluorescence. The four background measurements were averaged and subtracted from the spindle ROI intensity for their respective channel. These values were used to calculate the Kif15:tubulin ratio.

For spindle collapse assays with KBP-OE, cells were collected in G2 overnight with 9 μM RO-3306 (Axxora), washed 5X with DMEM supplemented with FBS and pen/strep, then treated for 90 minutes with 5 μM MG132, followed by 90 minutes with 5 μM MG132 + 10 μM DMSO or 10 μM STLC (Sigma-Aldrich). Cell fixation is the same as described above.

Compound Synthesis Information

Complete description of compound synthesis and characterization have been previously published (Dumas et al. 2018). All reactions requiring anhydrous conditions were conducted in flame dried glass apparatus under an atmosphere of argon. THF, Et_2O, CH_2Cl_2, DMF, benzene and acetonitrile were dried by passage through an activated alumina column under argon. DMSO was distilled from CaH_2 at 15 mm Hg and stored over activated 4Å molecular sieves. Anhydrous MeOH was freshly distilled from calcium hydride. Preparative chromatographic separations were performed on silica gel (35-75 μm); reactions were followed by TLC analysis using silica plates with fluorescent indicator (254 nm) and visualized with a UV lamp or phosphomolybdic acid. All commercially available reagents were purchased from TCI or Aldrich and used as received unless stated otherwise. Optical rotations were measured with a polarimeter using a 1 mL capacity cell with 1 dm path length. Infrared spectra were recorded using a thin film supported on KBr discs or dispersed in a KBr pellet. ^{1}H and ^{13}C NMR spectra were recorded in Fourier transform mode at the field strength specified on either a 300 or 400 spectrometer. Spectra were obtained on $CDCl_3$ or DMSO-d_6 solutions in 5 mm diameter tubes, and chemical shifts in ppm are quoted relative to the residual signals of chloroform (δH 7.26 ppm, or δC 77.0 ppm). Multiplicities in the ^{1}H NMR spectra are described as: s = singlet, d = doublet, t = triplet, q = quartet, m = multiplet, br = broad;

coupling constants are reported in Hz. Low (MS) and high (HRMS) resolution mass spectra are reported with ion mass/charge (*m/z*) ratios as values in atomic mass units.

CHAPTER 3

REGULATION OF KIF15 VIA *CIS* AND *TRANS* MECHANISMS

Megan E. Dumas[1] and Ryoma Ohi[2,3]

[1] Department of Cell and Developmental Biology, Vanderbilt University, Nashville TN
[2] Department of Cell and Developmental Biology, University of Michigan Medical School, Ann Arbor MI
[3] Life Sciences Institute, University of Michigan, Ann Arbor MI

A modified version was previously published as:

Malaby, HLH., Dumas, ME., Ohi, R., and Stumpff, J. (2019) Kinesin-binding protein ensures accurate chromosome segregation by buffering KIF18A and KIF15. *JCB,* 218.

Introduction

Kinesins are molecular motors that use ATP hydrolysis to drive mechanical processes inside cells. Regulation of these enzymes is crucial to prevent hyperactive kinesin activity and prevent futile ATP hydrolysis. As described in the introduction, cells employ a variety of methods to regulate the ATPase cycle of kinesin family members, including autoinhibition. Kif15 uses autoinhibition to regulate both its activity and spindle localization (Sturgill et al. 2014). The region of inhibition has been broadly narrowed down to the last 400 AAs, but the specific residues required for inhibition remain unknown. Understanding Kif15 autoinhibition is important not only to understand how the activity of this motor is regulated, but to gain a deeper insight into the Kif15 inhibitor designed by nature.

A recent study demonstrated that the regulatory protein kinesin-binding protein (KBP) can bind the motor domain of several human kinesins, including the mitotic kinesins Kif15 and Kif18A (Kevenaar et al. 2016). KBP was first identified in patients with Goldberg-Shprintzen syndrome, a disorder that effects the central and enteric nervous system (Alves et al. 2010; Brooks et al. 2005). Kevenaar et al focused on the interaction between KBP and Kif1A, a kinesin-3 family motor involved in neuronal transport. Mechanistically, KBP regulates Kif1A by interfering with the motors ability to bind MTs. Previous studies with Kif1B, another kinesin-3 family member, report that MT binding and motility of the kinesin is *increased* in the presence of KBP (Wozniak et al. 2005). Additionally, a recent study that examined the interaction between Kif15 and KBP reported that KBP promotes Kif15's localization to the spindle and that KBP knockdown comprises K-MT stability and chromosome alignment (Brouwers et al. 2017). While the function of KBP between these studies remains contradictory, it has become clear that KBP-motor interactions must be addressed when considering regulation of the kinesins predicted to interact with KBP (Kevenaar et al. 2016).

However, the ability of KBP to regulate the mitotic motor Kif18A remains unknown. Kif18A is a kinesin-8 family member that is enriched at the tip of K-MTs and helps regulated K-MT length and is required for chromosome congression (Mayr et al. 2007; Stumpff et al. 2008). Kif18A regulates K-MT dynamics by suppressing K-MT oscillations, thus ensuring that chromosomes remain within the metaphase plate (Du e al. 2010). Furthermore, while it is clear that Kif15 is self-regulated, how KBP could be affecting this regulation remains an important question. To understand KBPs interaction and regulation of the mitotic motors Kif15 and Kif18A, we employed mostly *in vitro* assays to ask *if* and *how* KBP effects the activity of these motors.

C-terminal Inhibition of Kif15 Resides Within its Last 100 Amino Acids

Previous work has demonstrated that Kif15 is self-repressed by a region in its C-terminal tail called Coil-2 (Sturgill et al. 2014). Coil-2 contains 400 amino acids (AA) and is predominately a coiled-coil, with a leucine zipper (LZ) motif at the end of the C-terminus (Figure 3.1 A, Boleti et al. 1996; Sturgill et al. 2014). To narrow down the region required for auto-inhibition, sequential protein fragments containing 100 AA were purified for use in the MT gliding assay. A previously characterized truncated Kif15 construct, Kif15-N700, was used for all MT gliding assays (Sturgill et al. 2014). The most C-terminal protein fragment F4 inhibited Kif15-N700 MT gliding in a dose-dependent manner (Figure 3.1 B). This inhibition was specific to F4, as F3 was unable to inhibit Kif15-N700 MT gliding even at high concentrations (Figure 3.1 B).

To confirm in cells, deletion constructs lacking either the C-terminal 100 AA or LZ (GFP-Kif15-Δ100, GFP-Kif15-ΔLZ) were generated and expressed in HeLa cells. Even in the presence of AMPPNP, Kif15-FL remains auto-inhibited and does not bind MTs (Sturgill et al. 2014, Figure 3.1 C). In contrast, both Kif15-Δ100 and Kif15-ΔLZ permit binding to interphase MT, suggesting relief of auto-inhibition (Figure 3.1C). Interestingly, removal of the LZ allows Kif15 to bind interphase MTs, but to a lesser extent when compared to Kif15-Δ100. This suggests that the LZ contributes to auto-inhibition, but that other sequences within the coiled-coil are required for complete inhibition of the motor.

KBP Inhibits Kif15 and Kif18A MT Gliding

To understand if KBP can regulate Kif15 and Kif18A activity, we analyzed MT gliding of the dimeric motor constructs Kif15-N700 and Kif18A-N480 in the presence of bacterially purified GST-KBP. Using the same motor concentration, 250 nM GST-KBP inhibited Kif18A MT gliding

by 90% and Kif15 MT gliding by 76% (Figure 3.2 B & D). This difference of inhibition is visualized in Figure 3.2 A and C, which shows the first and last frames of representative movies pseudo colored in red and green, respectively. Addition of 500 nM GST-KBP increases inhibition of Kif15 MT gliding slightly, increasing from 75% to 82%. The high % inhibition observed with

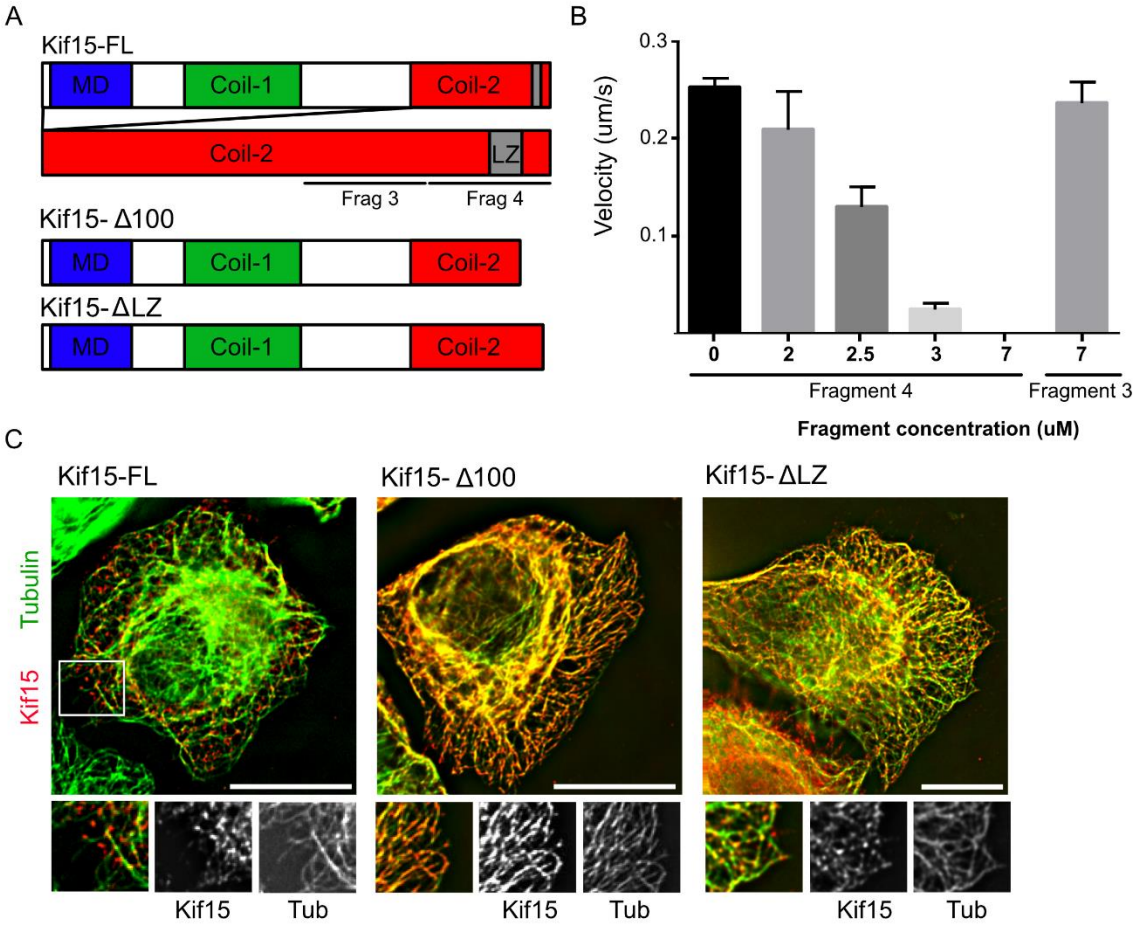

Figure 3.1 C-terminal amino acids required for Kif15 auto-inhibition. A) Schematic of Kif15-FL, Kif15-Δ100, Kif15-ΔLZ constructs and Coil-2 tail fragments. Blue highlights N-terminal motor domain, green highlights Coil-1, red highlights the C-terminal region Coil-2 and grey represents the leucine sipper. Kif15-Δ100 lacks the last 128 AAs and Kif15-ΔLZ lacks the last 30 AAs of Kif15s C-terminal tail. B) Average MT gliding velocity of Kif15-N700 in the presence of Fragment 4 and Fragment 3. C) Representative single focal planes of HeLa cells expressing Kif15-FL (left), Kif15-Δ100 (middle) or Kif15-ΔLZ (right) infused with AMPPNP. Corresponding zoomed images are below and show the merged, tubulin, and Kif15 channels. Scale bar, 10 µm.

Kif18A-N480 suggests that KBP may have a higher affinity for Kif18A over Kif15.

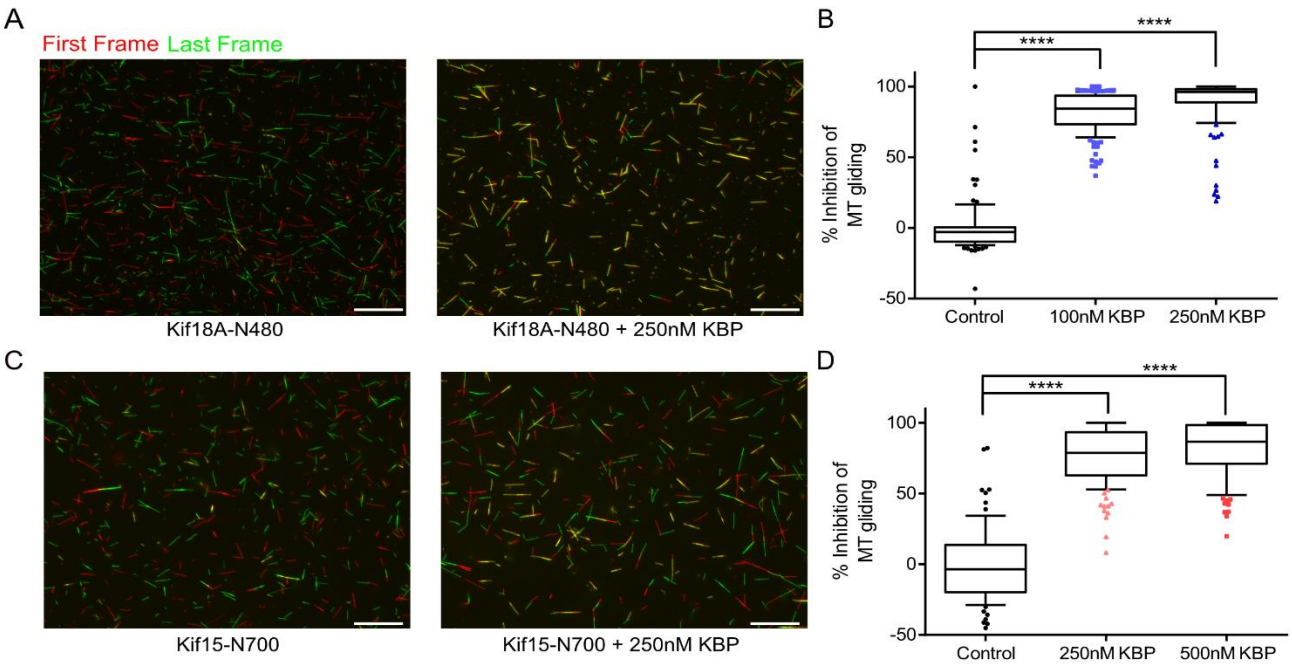

Figure 3.2 KBP inhibits Kif18A and Kif15 MT gliding. A) Representative fields from MT gliding assay with Kif18A-N480 showing the first frame (red) and last frame (green) of MTs in the presence or absence of GST-KBP. B) Quantification of percent inhibition of MT gliding for Kif18A-N480 alone (n = 95) or with 100 nM (n = 147) or 250 nM (n = 123) GST-KBP. C) Representative fields from MT gliding assay with Kif15-N700 showing the first frame (red) and last frame (green) of MTs in the presence or absence of GST-KBP. D) Quantification of percent inhibition of MT gliding for Kif15-N700 alone (n = 76) or with 250 nM GST-KBP (n = 125) or 500 nM GST-KBP (n = 92). N = total number of MTs measured from triplicate independent experiments. Scale bars, 20 µm.

KBP Binds Directly to Kif15 and Kif18A

To determine if KBP directly interacts Kif15 and Kif18A, we performed co-immunoprecipitation of purified GST-KBP with the dimeric motor constructs Kif15-N420 and Kif18A-N480. First, glutathione agarose beads were functionalized with GST-KBP and incubated with or without Kif15-N420 or Kif18A-N480. Both Kif15-N420 and Kif18A-N480 only pellet when GST-KBP is present, indicating a direct interaction between KBP and the motor domains of these constructs (Figure 3.3 A & B). We next tested the ability of KBP to bind the physiologically relevant full length (FL) constructs of Kif15 and Kif18A. In the presence of GST-KBP, Kif18A-FL completely pellets with the beads (Figure 3.3 C). Kif15-FL is autoinhibited by its C-terminal

tail and not surprisingly, KBP is unable to interact with the Kif15-FL motor domain (Figure 3.3 D).

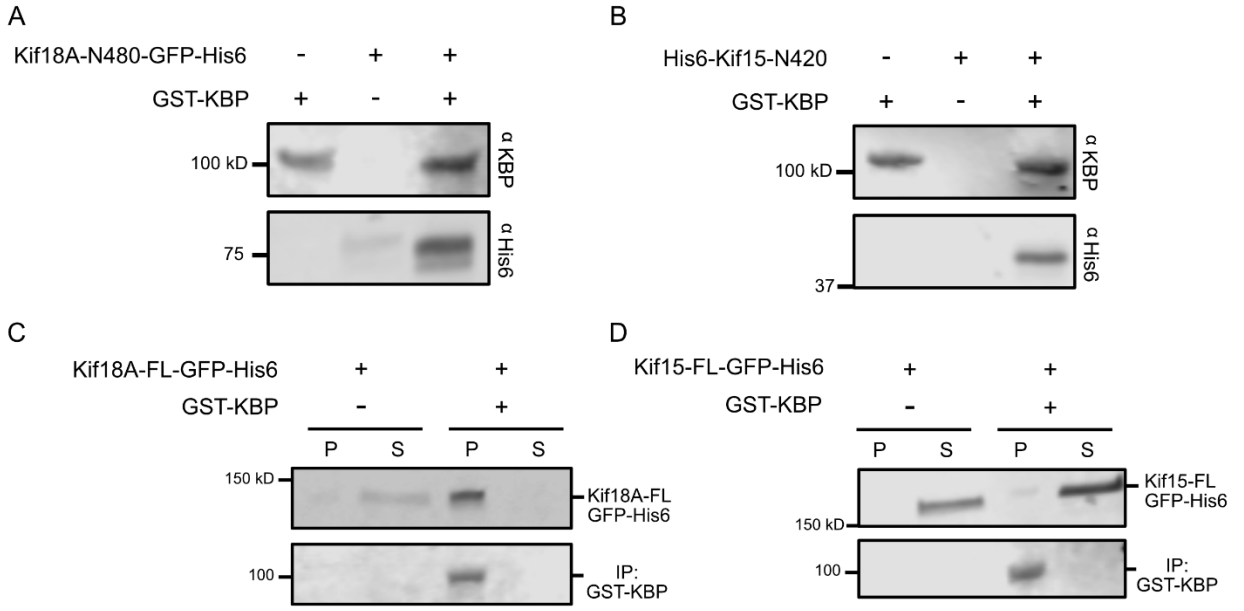

Figure 3.3 Direct interaction between KBP and the motor domains of Kif15 and Kif18A. Representative western blots from co-IP experiments using various Kif18A and Kif15 purified proteins. For all experiments, 50 nM of kinesin and 250 nM KBP was used. A) Co-IP with Kif18A-N480 and GST-KBP. B) Co-IP with Kif15-N420 and GST-KBP. C) Co-IP with Kif18A-FL and GST-KBP. D) Co-IP with Kif15-FL and GST-KBP. All blots were probed with antibodies targeting 6xHis (α His) and KBP (α KBP).

KBP Blocks MT Binding of Kif15 and Kif18A

After confirming direct interaction between KBP and the motor domains of Kif15 and Kif18A, we next tested if this interaction blocked MT binding using the MT co-pelleting assay. We continued to use the minimal dimeric motor constructs which lack secondary MT binding sites for both kinesins, ensuring any MT binding effects are due to KBP:motor interactions. In control conditions, 9% of Kif18A-N480 protein is detected in the supernatant, with the majority of protein pelleting with the MTs. In the presence of KBP, 86% of Kif18A-N480 is now detected in the supernatant (Figure 3.4 A). Interestingly, even though KBP is able to interact with full length Kif18A (Kif18A-FL, Figure 3.3 C), it is unable to shift Kif18A-FL to supernatant in the co-

pelleting assay (Figure 3.5 A). This is likely due to secondary MT binding elements within Kif18A's tail (Weaver et al. 2011).

The MT co-pelleting assay is not ideal for probing pellet to supernatant shifts for Kif15. Even in the presence of AMPPNP, 48 ± 2% of Kif15-N420 is reproducibly found in the supernatant. This result suggests that Kif15-N420 likely has a low K_{on} rate for MTs, which is further supported by this constructs inability to glide MTs in the MT gliding assay (Sturgill and Dumas, unpublished). Regardless, there was a significant shift of Kif15-N420 to the supernatant in the presence of KBP, reproducibly increasing to 67 ± 2% (Figure 3.4 B). As predicted, Kif15-FL was unable to bind MTs *in vitro* (Figure 3.5 B).

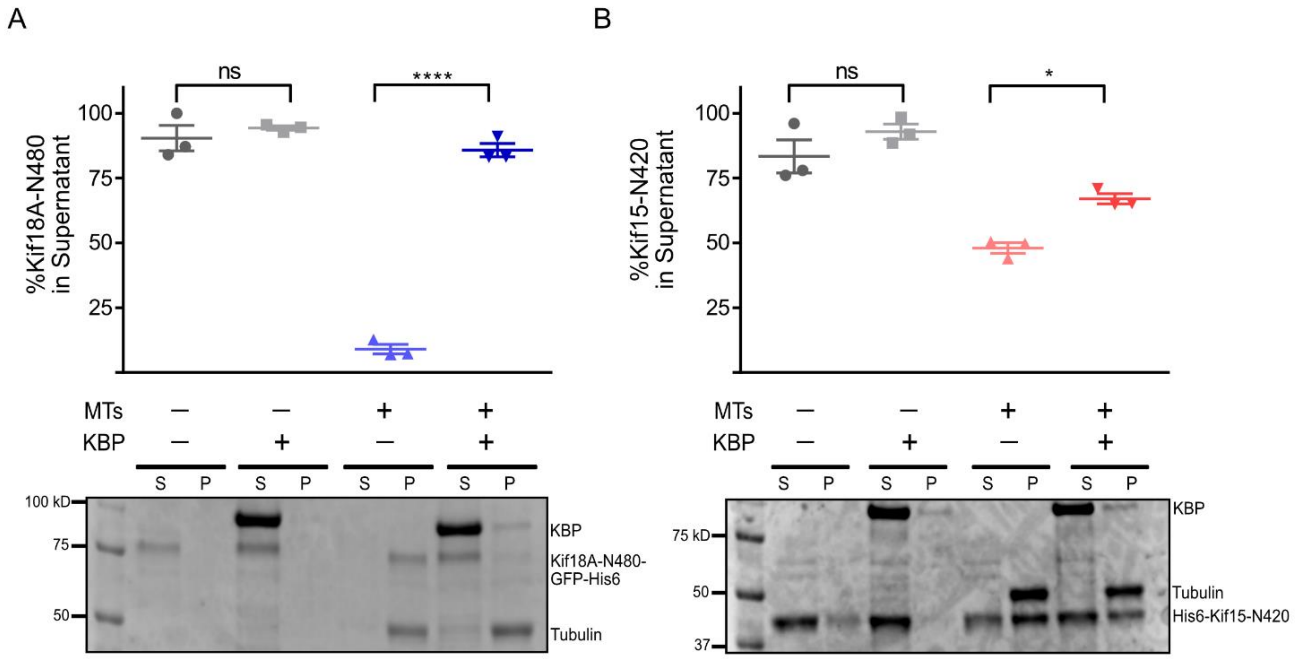

Figure 3.4 KBP interferes with Kif18A-N480 and Kif15-N420 MT binding. A) Results from co-pelleting assay with Kif18A-N480 or B) Kif15-N420 in the presence or absence of KBP and/or MTs. P, pellet; S, supernatant. Bottom: representative Coomassie gels Top: quantification of percentage of kinesin motor present in supernatant fractions. Data was obtained from three independent experiments. ns, not significant, ****, adjusted P < 0.0001, *, adjusted P = 0.031 with 95% confidence interval by one-way ANOVA with Tukey's multiple comparisons test. Error bars represent SEM.

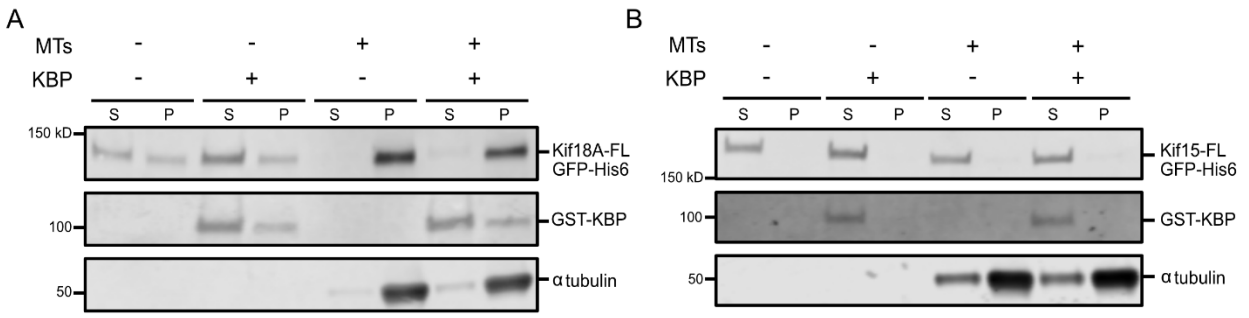

Figure 3.5 Full length kinesin motors display complex KBP regulation. A) Co-pelleting assay with Kif18A-FL, KBP, and/or MTs. Image is western blot probed with antibodies targeting 6xHis (α His), KBP (α KBP), and tubulin (DM1α). B) Co-pelleting assay with Kif15-FL, KBP and/or MTs. Image is western blot probed with antibodies targeting 6xHis (α His), KBP (α KBP), and tubulin (DM1α).

KBP Overexpression Prevents Kif15-Driven Spindle Stabilization

We next asked if KBP had an effect on Kif15 function in cells. In HeLa cells, Kif15 is required for spindle bipolarity maintenance in the absence of Eg5. HeLa metaphase spindles remain bipolar when treated with the Eg5 inhibitor STLC but collapse to monopoles when Kif15 is knocked down via siRNA (Tanenbaum et al. 2009). To determine if KBP interferes with Kif15 mediated spindle stability, spindle structures were scored from HeLa cells transfected with mCherry alone or mCherry-KBP and whose metaphase spindles were treated with DMSO or STLC. The percent of monopolar spindles increased twofold in cells expressing mCherry-KBP, indicating KBP interferes with Kif15 mediated spindle bipolarity (Figure 3.6). Endogenous Kif15 remains localized to the metaphase spindle when KBP is over expressed (OE) due to its second non motor MT binding site (Malaby et al. 2019). Though Kif15 localization is not severely disrupted when KBP is OE, an increase in monopolar spindles upon STLC addition indicates that KBP is indeed blocking motor MT binding, rendering Kif15 unable to resist inward directed forces that cause spindle collapse.

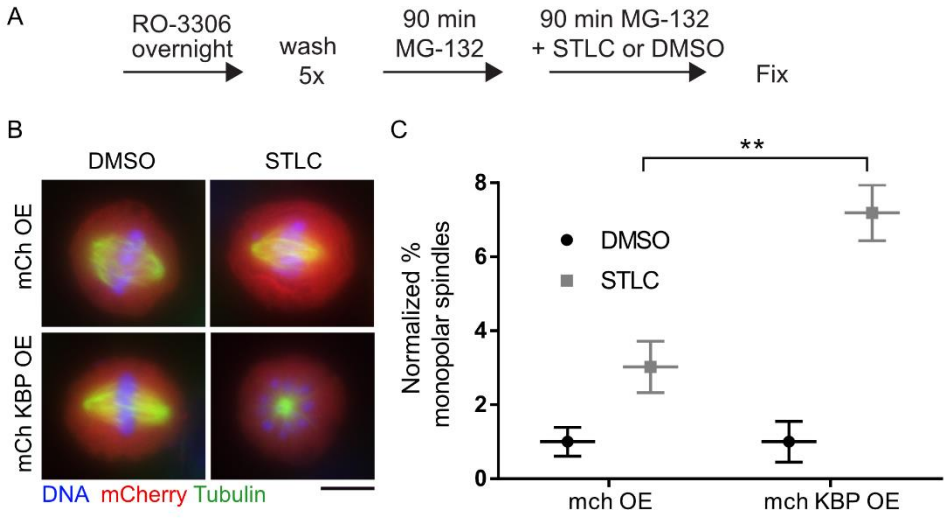

Figure 3.6 KBP overexpression inhibits Kif15-driven spindle stabilization. A) Schematic of spindle collapse assay. B) Metaphase cells expressing mCherry (mCh) only or mCh-KBP treated with DMSO or STLC. Scale bar, 10 µm. C) Quantification of the percentage of mitotic cells with monopolar spindles, normalized to the DMSO condition. Error bars represent SD. Data was obtained from three independent experiments with the following cell numbers: mCh only DMSO (103), mCh only STLC (134), mCh-KBP DMSO (200), and mCh-KBP STLC (269). **, adjusted P = 0.0058 with 95% confidence interval by two-way ANOVA with Tukey's multiple comparisons test.

Discussion

The creation and maintenance of the mitotic spindle is a highly controlled process that relies on the precise regulation of force generating motors to achieve steady state (Dumont and Mitchison 2009). Metaphase spindles are dynamics structures yet they reach a stable, steady state length. This steady state is crucial for the integrity of the spindle and mitosis itself, with any imbalance leading to cell division failures. Cells *must* have reliable methods to control the activity of force generating motors regulating the spindle to ensure bipolarity and mitotic success. This reliance on the precise regulation of molecular motors seems risky, and indeed, protein concentration can vary between cells up to 30% (Sigal et al. 2006). Changes in the concentration of a mitotic motor puts the cell at risk for loss of spindle steady state. To overcome these fluctuations in protein levels, we hypothesize that KBP acts as a "buffer" within the cell and provides fine tuning of mitotic kinesin activity. Our data confirms that KBP is able to bind and

regulate Kif15 and Kif18A activity. Though the data is not shown here, our recent publication in collaboration with the Stumpff lab demonstrates that altered KBP expression in cells disrupts the activity of both motors, leading to chromosome alignment defects and lagging chromosomes (Malaby et al. 2019).

CHAPTER 4

IDENTIFICATION OF GW108X: A NOVEL KIF15 INHIBITOR

Megan E. Dumas[1], Nicole D. Kendrick[1], Somnath Jana[2], Alex G. Waterson[2,3,4], Joshua A. Bauer[5], Gary Sulikowski[3], and Ryoma Ohi[6,7]

[1] Department of Cell and Developmental Biology, Vanderbilt University, Nashville TN
[2] Vanderbilt Institute of Chemical Biology, Nashville TN
[3] Department of Chemistry, Vanderbilt University, Nashville TN
[4] Department of Pharmacology, Vanderbilt University, Nashville TN
[5] Department of Biochemistry, Vanderbilt University, Nashville TN
[6] Department of Cell and Developmental Biology, University of Michigan Medical School, Ann Arbor MI
[7] Life Sciences Institute, University of Michigan, Ann Arbor MI

A modified version was previously published as:

Dumas, ME., Chen, GY., Kendrick, ND., Xu, G., Larsen, SA., Jana, S., Waterson, AG., Bauer, JA., Hancock, W., Sulikowski, GA., and Ohi, R. (2018) Dual inhibition of Kif15 by oxindole and quinazolinedione chemical probes. *Bioorg Med Chem Lett.* 29(2): 148-154.

Introduction

Small molecule screening is a popular method to discover target compounds for either tool or therapeutic usage. Screening thousands of compounds is a viable option for targets with little or no structural data and is widely an unbiased approach. Indeed, large small molecule screens have led to the discovery of several kinesin inhibitors (Catarinella et al. 2009; Mayer et al., 1999; Qian et al., 2010). Small molecule screens can be broken down into two general categories: cell-based phenotypic or biochemical target-based assays (Coussens et al. 2017). Cell-based assays

rely on a predictable phenotype to score compound effectiveness and due to their unbiased nature, it can take months to discover the cellular target of the compound. Alternatively, target based approaches utilize an *in-vitro* assay that contains purified components of the target of interest. Downsides of this approach stem from the uncertainty of cell permeability properties of the lead compounds and their ability to reach the desired target inside cells. With these considerations in mind, and our ability to purify active Kif15 constructs from bacteria, we decided to pursue small molecule inhibitors of Kif15 using a target-based approach.

Kinases are a highly targeted group of enzymes for cancer therapeutics due to their diverse roles in cellular signaling pathways that stimulate cell proliferation and survival (Manning et al. 2002). There are currently over three thousand ongoing Phase I-III clinical trials for new kinase inhibitors and several pharmaceutical companies have devoted departments for kinase discovery research (Bhullar et al. 2018). As such, kinase inhibitor libraries are widely available to research institutions and offer a unique opportunity for investigators interested in targeting proteins that hydrolyze ATP. Kinesins also hydrolyze ATP, but instead of transferring the phosphate to a substrate, these enzymes translate ATP hydrolysis into mechanical movement. We took advantage of the kinase inhibitor resources at Vanderbilt University and hoped to identify a privileged scaffold that inhibited Kif15.

Assay Quality Conditions

To search for Kif15 inhibitors, we used an *in-vitro* ATPase assay with purified components. The luminescence-based ADP-Glo^{TM} Kinase assay was chosen for its low assay volume and ability to detect low concentration of ATP (Zegzouti et al. 2011, Figure 4.1 A). To select for compounds that bind to the motor domain of Kif15, we used the dimeric motor construct Kif15-N420. Like

other kinesins, Kif15-N420 required the presence of MTs to stimulate ATPase activity. To test the uniformity and reproducibility of the assay conditions, described below, positive (+ ATP), negative (- ATP), and control compound (VU0656487) reactions with Kif15-N420 were plated every third row (Figure 4.1 B). During preliminary screens, VU487 was confirmed to inhibit Kif15-N420, but its lipid like structure deemed it unlikely to be a true inhibitor and instead was used as a control for assay variability (Figure 4.1 C). Compound concentration was set to 10 µM and was incubated with 30 nM of Kif15-N420 + 5 µM MTs for 15 minutes. The reaction was then

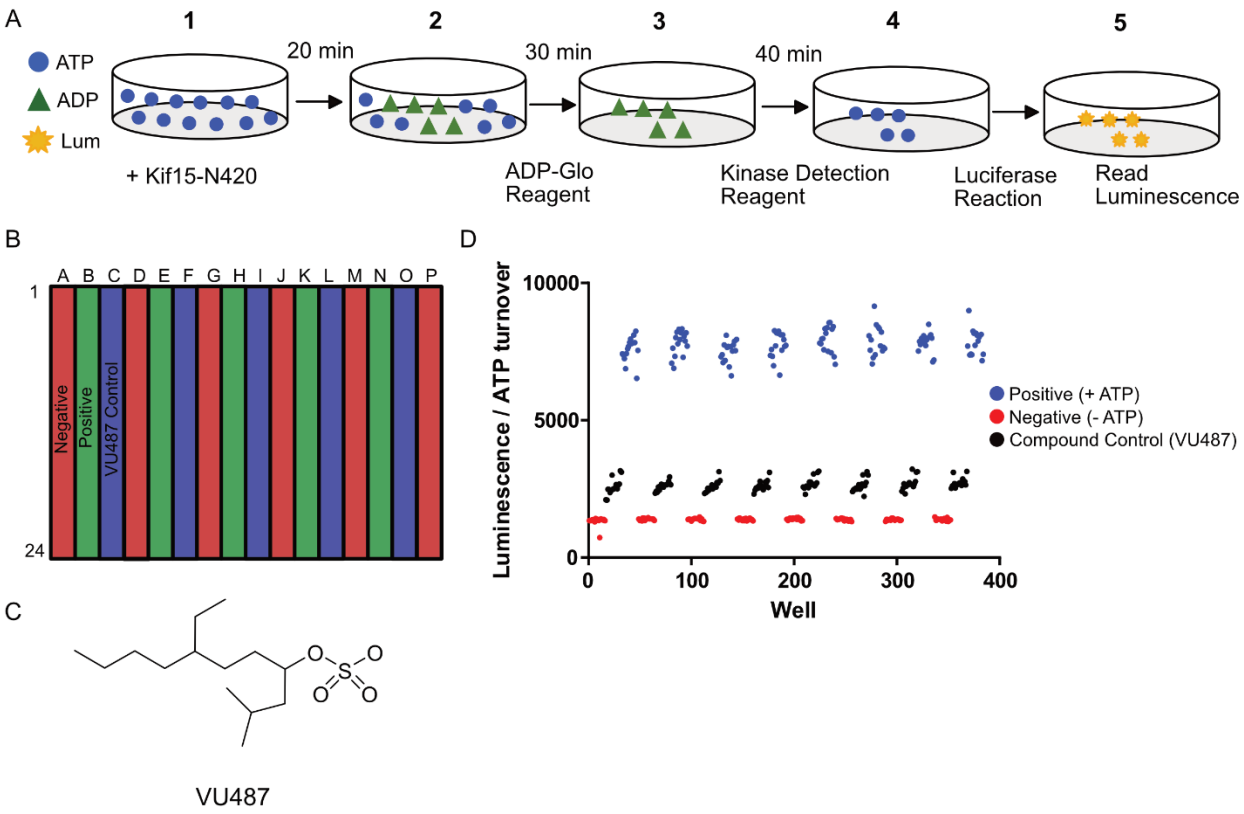

Figure 4.1 Testing ADP-Glo ATPase assay conditions. A) Schematic of the ADP-Glo assay used to measure Kif15-N420 ATPase activity. Kif15-N420 is incubated with microtubules for 20 minutes (**Step 1**) and hydrolyzes ATP to ADP (**Step 2**). ADP-Glo reagent is added to quench the reaction and deplete remaining ATP (**Step 3**). Kinase detection reagent is added (**Step 4**) to convert ADP to ATP, which drives luciferase activity (**Step 5**). Luminescence signal directly correlates with ATPase activity of Kif15-N420. B) Schematic of plate map used for Triple Checkerboard testing. Red, green, and blue indicate negative (- ATP), positive (+ ATP) and control (VU487) reactions, respectively. C) Structure of VU0656487. D) Representative Triple Checkerboard raw luminescence values from single assay plate.

incubated with 10 µM ATP for 20 minutes to stimulate the ATPase activity of Kif15-N420. Next,

kit reagents were added as described in the Materials and Methods and luminescence was measured (Figure 4.1 A). Using the positive and negative controls, the Z-factor (Z') was calculated to be 0.75 (Table 4.1). Z' is common statistical measure of assay quality and a Z' > 0.5 is considered a robust assay (Zhang et al. 1999). Furthermore, we found the % CV of the positive, negative and control compounds reactions were all be below 10, indicating little variation (Figure 4.1 D & Table 4.1).

Screening the GlaxoSmithKline Published Kinase Inhibitor Set

To identify chemical scaffolds that target Kif15 as a starting point for tool compound development, we screened the GlaxoSmithKline (GSK) Published Kinase Inhibitor Set (PKIS). The PKIS is a panel of kinase inhibitors made publicly available to researchers to stimulate development of tools that inhibit untargeted kinases within the kinome (Knapp et al. 2013). The PKIS was screened in duplicate and the compounds were randomized in the assay plates each day (Figure 2 A & B).

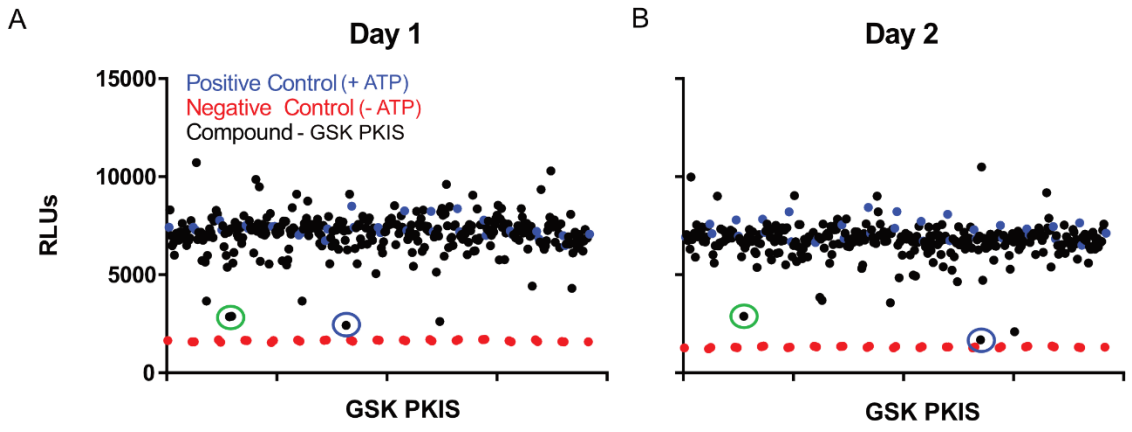

Figure 4.2 Screening the GSK PKIS. Luminescence signal directly correlates with ATPase activity of Kif15-N420. A) Day 1 and B) Day 2 raw luminescence values from GSK PKIS screened in duplicate. Compounds were randomly distributed in the assay plate on both screening days to account for any plate

effect. Positive and negative controls are Kif15-N420 + MTs +/- ATP, respectively. Highlighted in green and blue is GW108X and VU669 (Figure 4.3).

Experiment	Z-factor (Z')	CMPD % CV	Negative % CV	Positive %CV
Triple Checkerboard	0.75	8	5	6
GSK – Day 1	0.74	13.6	2.76	6.18
GSK – Day 2	0.73	12	2.68	7.04

Table 4.1 Statistical analysis of assay development and screening conditions.

The % inhibition, Z-score, and B-score was calculated for each compound on each screening day (see Materials and Methods) and the top 10 compounds between the two screening days were cherry picked for concentration response analysis (Figure 4.3 & 4.5). The top five compounds from the screen reproducibly exhibited a % inhibition > 60%, Z-score < -3 and B-score < -8 (Figure 4.3). These top five compounds were further characterized for their ability to inhibit Kif15 using the MT gliding assay. For these assays, we used Kif15-N700, a longer construct that robustly glides MTs (Sturgill et al. 2014). The two oxindoles, VU674 (herein called GW108X) and VU669, significantly inhibited Kif15 MT gliding (Figure 4.4). Both compounds contain an oxindole core and a halogenated phenol ring on the right-hand side of the molecule. They differ most at the 5-position of the oxindole, with GW108X being an acylfuran and VU669 being an iodide (Figure 4.3). GW108X and VU669 were first described as potent c-Raf1 inhibitors and have since been extensively characterized by GSK, with GW108X reported as being a promiscuous kinase and GPCR inhibitor (Elkins et al. 2016; Lackey et al. 2000; Richters et al. 2015). We decided to pursue GW108X for further analysis because of its sub-micromolar IC_{50} (Figure 4.3). Furthermore, the inhibitory activity of GW108X against Kif15 was scored by calculating the velocity of MT gliding over a range of inhibitor concentrations to generate a concentration

Compound	Structure	Avg % Inh (@ 10 uM)	Z-Score	B-Score	IC_{50} (uM)	Graph
VU669	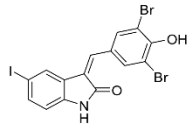	87 ± 0	-5.3 ± 0.6	-12.4 ± 1.4	2.5	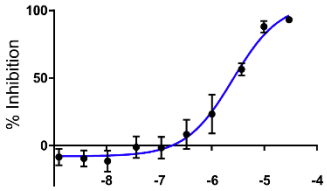
VU691	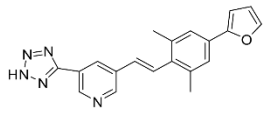	88 ± 8	-5.4 ± 1.1	-12.2 ± 2.5	0.6	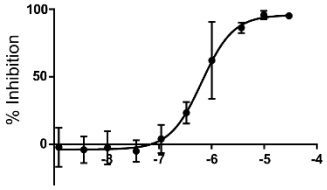
GW108X	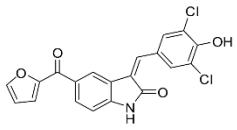	76 ± 4	-4.6 ± 0.2	-9.9 ± 1.6	0.8	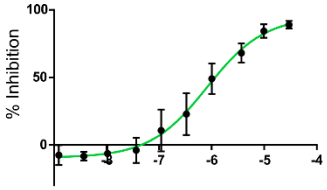
VU681	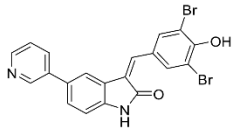	70 ± 11	-4.1 ± 0.3	-10.4 ± 0.3	5.1	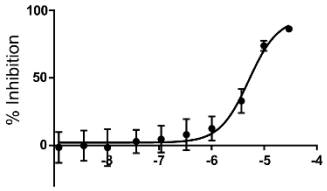
VU724	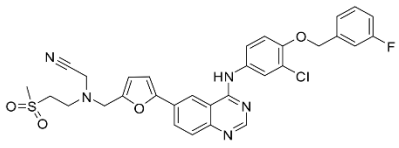	62 ± 3	-3.7 ± 0.1	-8.7 ± 0.0	5.3	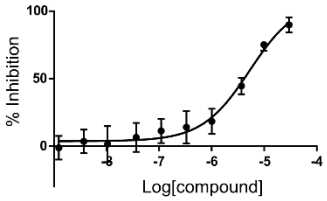

Figure 4.3. Summary of the top five compounds from PKIS screen. Compound name, structure, average % inhibition between two GSK screening days, Z-Score, B-Score, and IC_{50} of top five compounds from GSK screen. Graph shows concentration response curve (CRC) generated from the ATPase assay, developed from 10 concentrations from 30 to 0.001 μM. Each concentration was repeated in triplicate. Error bars show SEM.

response curve (CRC). The IC_{50} using this assay was 734 nM, similar to that calculated using the ATPase assay (Figure 4.4 B).

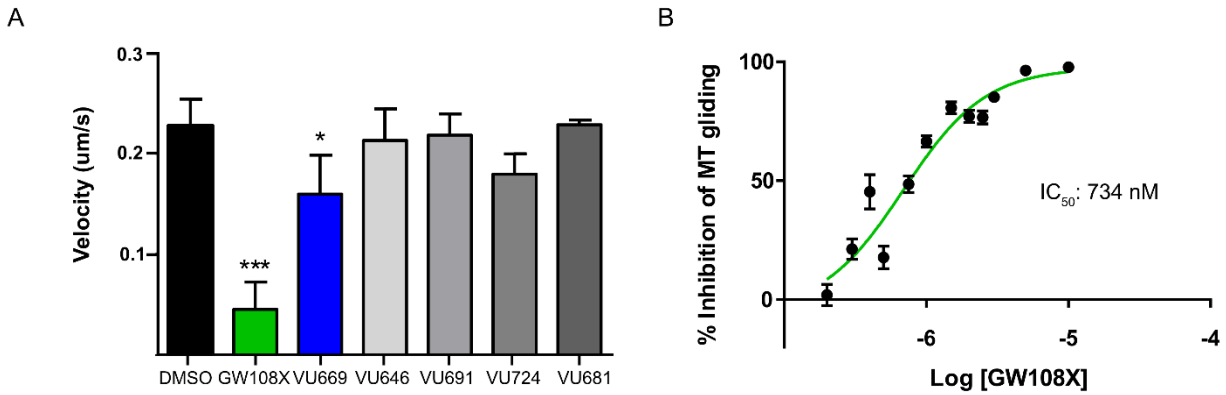

Figure 4.4. Characterization of top five compounds in the MT gliding assay and IC_{50} of GW108X. Top five compounds from Figure 4.3 analyzed using the MT gliding assay at 30 μM. Data is the average MT gliding velocity of Kif15-N700 with each compound. Every compound was tested in triplicate the n≥ 30, except VU724, which was tested in duplicate with an n ≥ 20. C) CRC generated from the MT gliding assay, developed from 12 concentrations from 10 to 0.2 μM.

First Round of Structure-Activity Relationship (SAR) Analysis

To probe the relationship between structure and Kif15 inhibition activity of GW108X, we synthesized a small library of derivatives with modifications to both the furan and phenol regions of the molecule. To start, a set of five compounds was synthesized that contained domain swaps between GW108X and VU669 (compounds **2** & **5**) or contained different halogens on the ortho position of the phenol (compounds **1**, **3** & **4**). To compare the activity of these GW108X derivatives, we tested their ability to inhibit Kif15 MT-gliding at 750 nM, roughly the IC_{50} of GW108X (Figure 4.6). The halogens in the ortho position of the phenol may provide opportunities for formation of both hydrogen and halogen bonds with biomolecules. Owing to their importance, compounds **1**, **2** and **3** displayed a structure activity relationship that correlated with halogen size (Figure 4.6). The Kif15 inhibition activity of the compound improved as the halogen size increased from fluorine to bromine, with **2** inhibiting MT gliding by 65%. The larger iodines within **3**, however, were not well tolerated, and none of the compounds showed percent inhibition significantly different than that of GW108X. Not surprisingly, the compounds that resembled

VU669 and contained an iodine instead of a furan (**4** and **5**), did not significantly inhibit Kif15 in the gliding assay (Figure 4.6).

Compound	Structure	Avg % Inh (@ 10 um)	IC_{50}	Graph
VU723	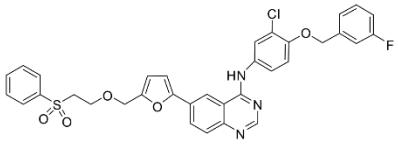	55 ± 2	3.0	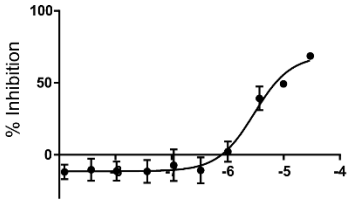
VU646	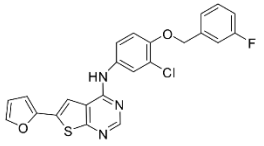	47 ± 13	2.1	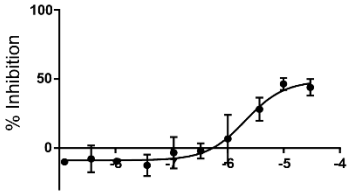
VU729	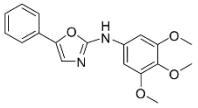	31 ± 2	2.1	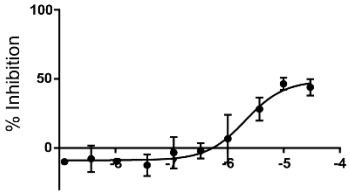
VU752	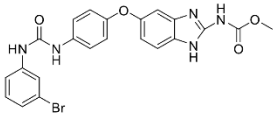	30 ± 1	5.3	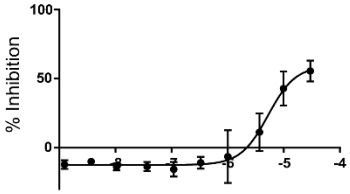
VU734	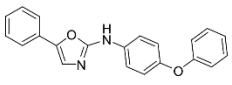	29 ± 0	40.2	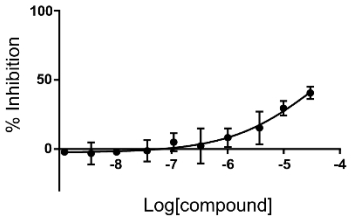

Figure 4.5 Summary of lower scoring compounds (from top 10) from PKIS. Compound name, structure, average % inhibition between two GSK screening days, Z-Score, B-Score, and IC_{50} of bottom five compounds from GSK screen. Graph shows concentration response curve (CRC) generated from the ATPase assay, developed from 10 concentrations from 30 to 0.001 μM. Each concentration was repeated in triplicate. Error bars show standard error of the mean (SEM).

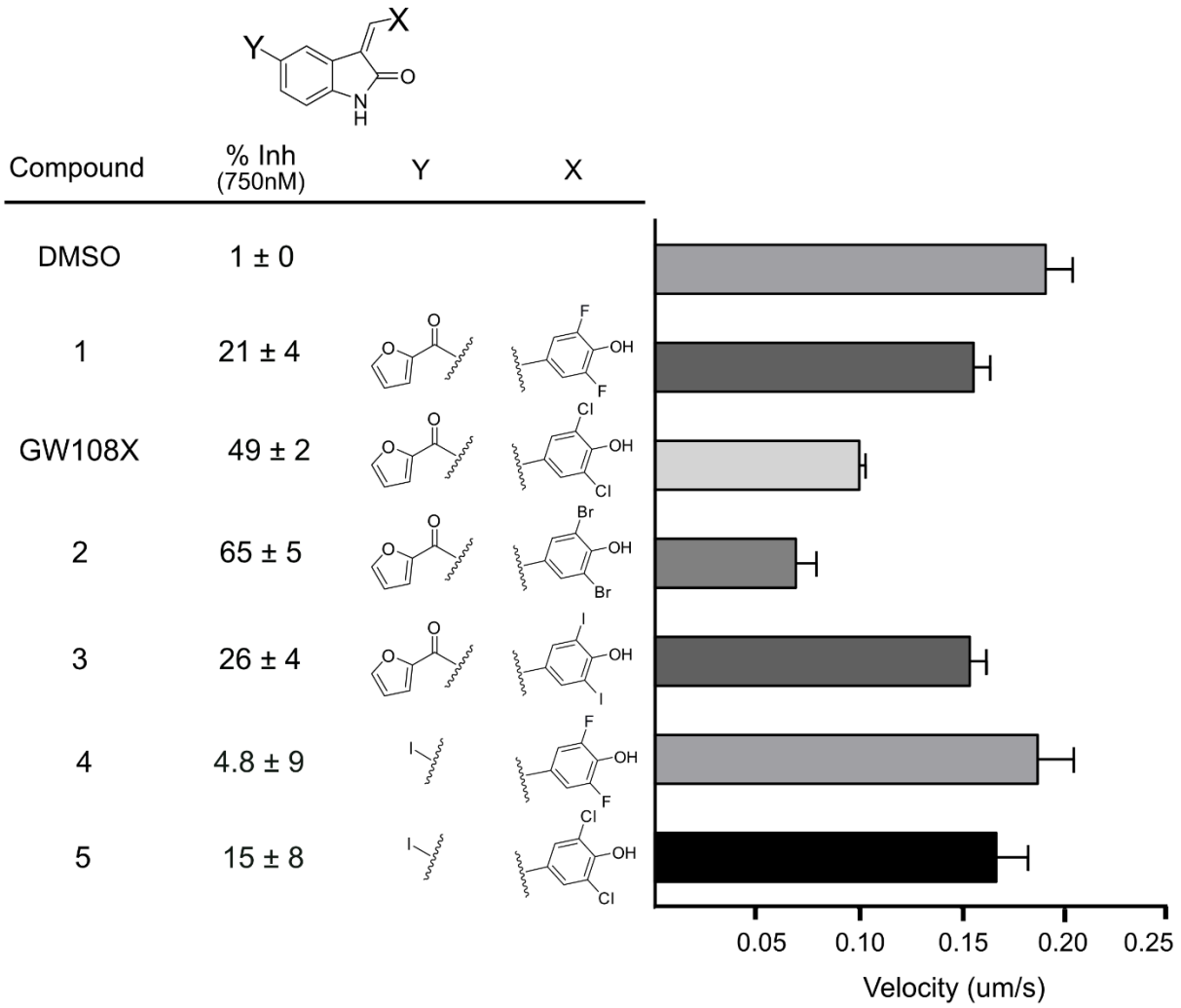

Figure 4.6 SAR analysis for GW108X derivatives. Compound structures from the first round of SAR analysis of GW108X derivatives. Data is the average microtubule gliding velocity of Kif15-N700 with each compound tested at 750 nM. Every compound was tested in triplicate with n ≥ 30 measurements for each replicate, except **3**, which was tested in duplicate. Error bars show SEM.

Second and Third Round of SAR: Modifications to the Phenol and Furan Group

The first round of SAR analysis revealed the importance of the halogens for Kif15 inhibition by GW108X. The next batch of derivatives contained modifications to only the phenol ring, leaving the furan tail unchanged. Fourteen compounds were synthesized and tested at 750 nM in the MT gliding assay (Figure 4.7). Interestingly, compounds that contain two different

halogens (**6** and **7**) showed intermediary inhibition also in line with respective halogen size. More aggressive changes in the aromatic ring substitutions served only to demonstrate the importance of the hydroxyl and halogens for robust inhibition of Kif15. For example, removal (**10**) or substitution (**19**) of the phenolic hydroxyl abolished activity. Furthermore, both halogen substituents appear to be required, as compounds with the halogens replaced with methyl groups (**12**) displayed reduced in activity (Figure 4.7).

The last round of SAR derivatives contained compounds that had modifications to the 5-position of the oxindole core. We found that the 5-position of the oxindole core was intolerant of changes, as these compounds did not robustly inhibit Kif15 MT-gliding (Figure 4.8). Available analogs of GW108X, VU669 and VU724 present in Vanderbilt HTS compound libraries were also tested to better understand the structure-activity of Kif15 inhibition. In total, 31 compounds were further tested in the ATPase assay (See Appendix Figure A1.1).

Discussion

This work describes the first published small molecule screen for Kif15 inhibitors. Extensive assay development was required not only to discover valid Kif15 inhibitors, but to provide future lab members with a reliable and robust assay for future screens. The oxindole GW108X was isolated from the GSK PKIS and exhibited a sub micromolar IC_{50} in both the ATPase and MT gliding assays. Comparable activity between these two different assays suggested GW108X may be a true Kif15 inhibitor and encouraged us to pursue GW108X derivatives. Although no derivative was superior to GW108X, the SAR campaign highlighted the importance of both the halogens and furan tail for Kif15 inhibition. The crystal structure of the motor domain

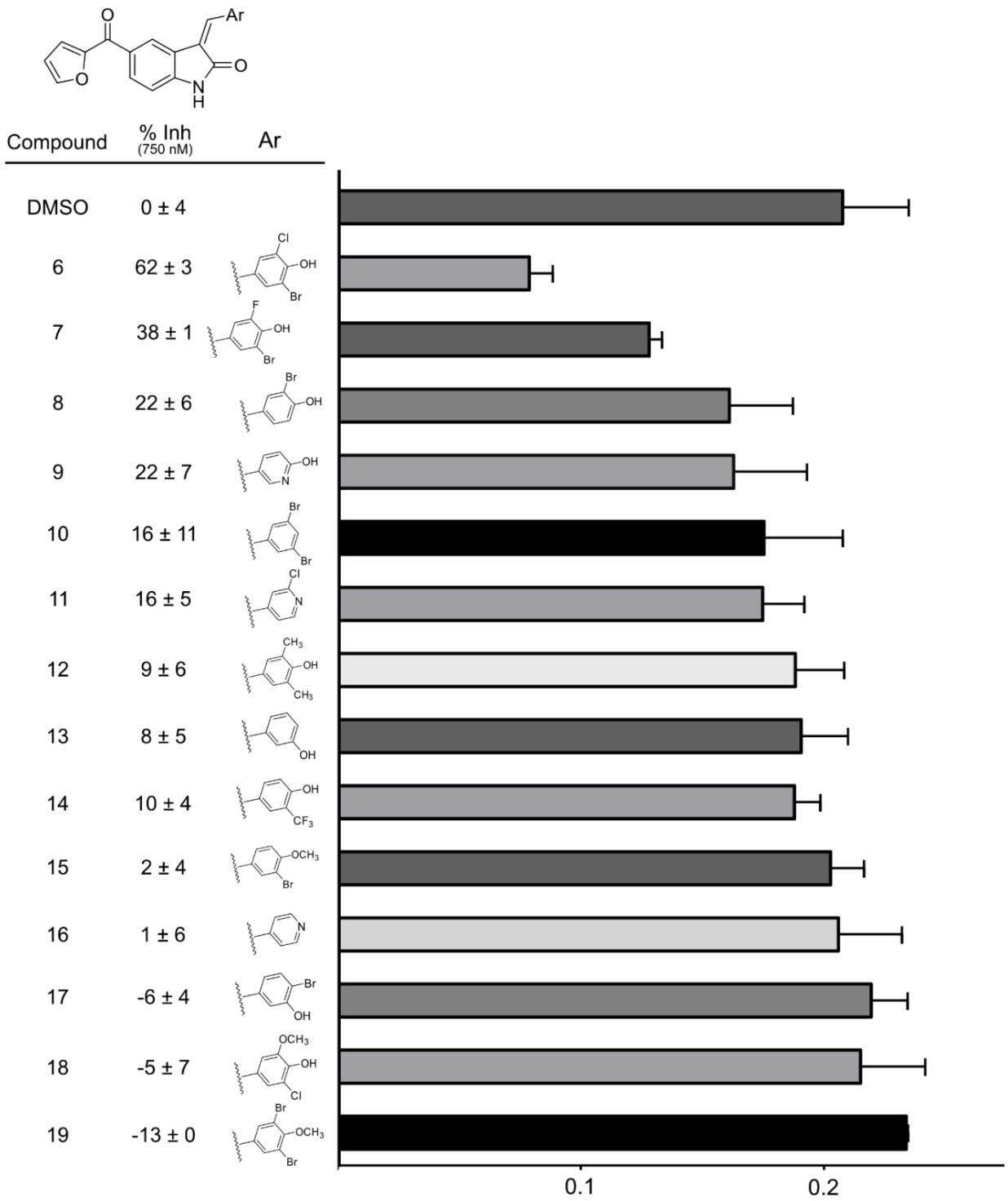

Figure 4.7 SAR analysis of the second round of GW108X derivatives. Compound structures from the second round of SAR analysis of GW108X phenol derivatives. Data is the average microtubule gliding velocity of Kif15-N700 with each compound at tested 750 nM. Every compound was tested in triplicate with n ≥ 30 measurements for each replicate, except **10**, **14**, and **19,** which were tested in duplicate. Error bars show standard deviation (SD).

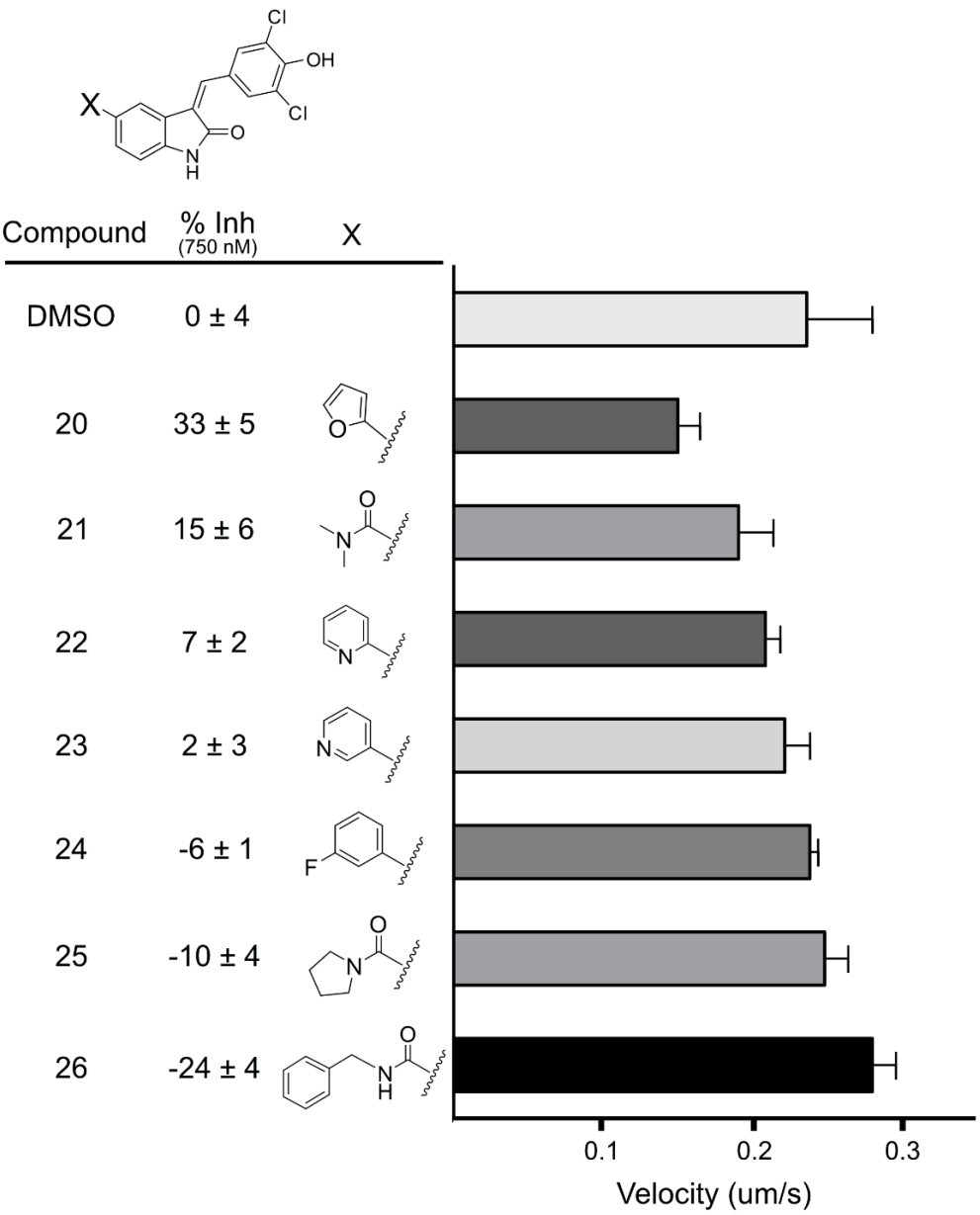

Figure 4.8 SAR analysis of third round of GW108X derivatives. Compound structures from the third round of SAR analysis of GW108X derivatives. Data is the average microtubule gliding velocity of Kif15-N700 with each compound at tested 750 nM. Every compound was tested in triplicate with n ≥ 30 measurements for each replicate, except **20**, which was tested in duplicate. Error bars show standard deviation (SD).

of Kif15 has been reported and recapitulated in collaboration with the Subramanian lab (Klejnot et al. 2014). Despite successful generation of Kif15 crystals, co crystals with GW108X did not reveal density corresponding to small molecule binding (unpublished). This is likely due to

GW108X insolubility at high concentrations (unpublished). Regardless, the crystal structure of Kif15 will be useful moving forward for any future Kif15 inhibitors discovered in the Ohi lab.

CHAPTER 5

GW108X IS A REVERSIBLE, NON-ATP COMPETITIVE INHIBITOR OF KIF15

Megan E. Dumas[1], Geng-Yuan Chen[2], George Xu[3], William Hancock[2] and Ryoma Ohi[3,4]

[1] Department of Cell and Developmental Biology, Vanderbilt University, Nashville TN
[2] Department of Biomedical Engineering, Pennsylvania State University, State College PA
[3] Department of Cell and Developmental Biology, University of Michigan Medical School, Ann Arbor MI
[4] Life Sciences Institute, University of Michigan, Ann Arbor MI

A modified version was previously published as:

Dumas, ME., Chen, GY., Kendrick, ND., Xu, G., Larsen, SA., Jana, S., Waterson, AG., Bauer, JA., Hancock, W., Sulikowski, GA., and Ohi, R. (2018) Dual inhibition of Kif15 by oxindole and quinazolinedione chemical probes. *Bioorg Med Chem Lett.* 29(2): 148-154.

Introduction

GW108X is an oxindole kinase inhibitor first developed by GSK and characterized as a potent cRaf-1 inhibitor with an IC_{50} of 40 nM (Lackey et al. 2000). A decade later, GW108X was described as a potent inhibitor of TANK-binding kinase 1 (TBK1), exhibiting an IC_{50} 300 nM (Richters et al. 2015). The most comprehensive study of GSK PKIS, including GW108X, was in 2016. In this study, the entire PKIS was characterized for its ability to inhibit 224 recombinant kinases and 24 G protein-coupled receptors (Elkins et al. 2016). Furthermore, the entire library was screened in several cellular assays measuring cell proliferation and angiogenesis. Not only did GW108X inhibit several kinases *in-vitro*, the authors specifically described GW108X as having a "complex and promiscuous GPCR activity profile" (Elkins et al. 2016).

Despite these perceived pitfalls, it is not uncommon for researchers to repurpose kinase inhibitors for novel applications. Many examples can be found in the literature using kinase inhibitor libraries to discover novel antibiotics and treatments for neglected tropical diseases (Dichiara et al. 2017; Miller et al. 2009). While these examples generally strive to target the kinome of other organisms, kinase inhibitors have been used as starting scaffolds to inhibit the molecular motor myosin (Islam et al. 2010). With these successes in mind, we decided to pursue GW0108X as a lead compound for development and drug design, characterizing its activity *in vitro* and *in vivo*.

GW108X is a Reversible Inhibitor

We used the MT gliding assay to test whether the inhibition of Kif15 by GW108X is reversible. MT gliding by Kif15 was initiated in the presence of DMSO and after roughly a minute, 10 μM of GW108X was added to the flow chamber. Treatment for 1 minute was sufficient to eliminate MT gliding. GW108X was then washed out, replaced with DMSO, and the chamber was imaged for another minute. After wash out of GW108X, MTs resumed gliding, revealing that GW108X inhibits Kif15 in a reversible manner (Figure 5.1 A). MT gliding was unaffected when only DMSO was washed in (Figure 5.1 B).

GW108X has a High Preference for Kif15

We next tested the ability of GW108X to inhibit Eg5, HSET, and Kif18A, three additional mitotic motors that differ in both structure and function (Mountain et al. 1999; Sawin et al. 1992; Stumpff et al. 2008). Despite promiscuity as a kinase inhibitor, GW108X displayed a preference for Kif15 over the other mitotic motors tested. For this set of experiments, GW108X was used at

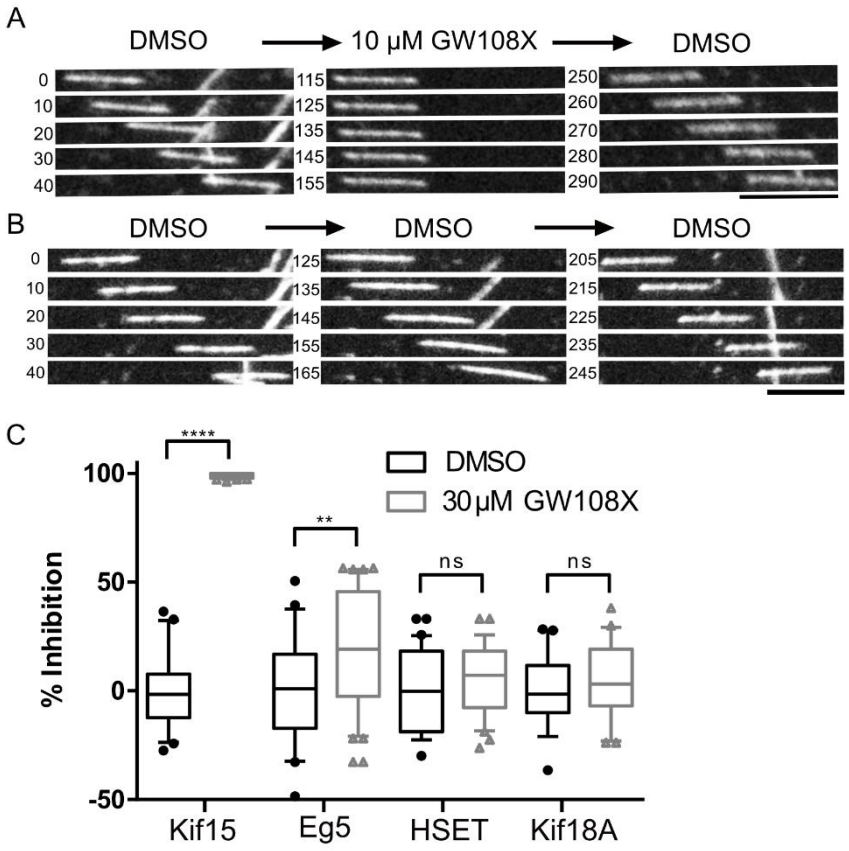

Figure 5.1 GW108X is a reversible Kif15 inhibitor and has a high preference for Kif15. A) Representative montage of fluorescent MTs from the double wash out experiment. Numbers indicate time in seconds after initial frame, which are not the same MT for each condition. Scale bar, 5 µm. B) Representative montage of fluorescent MTs from control double wash out experiment using DMSO. Each vertical frame represents 10 seconds. Scale bar, 5 µm. C) Percent inhibition of indicated mitotic motors treated with 30 µM of GW108X. n >20 for all conditions, **** $p < 0.0001$, ** $p = 0.0074$.

a concentration of 30 µM, which completely inhibits Kif15 MT gliding by 98.9% ± 0.2% while only inhibiting Eg5 by 19.8% ± 4.3%, HSET by 5.3% ± 2.9% and Kif18A by .9% ± 3.9 (mean ± SEM, Figure 5.1 C).

GW108X is a Non-Competitive ATP Inhibitor

In principle, GW108X could inhibit the MT-stimulated ATPase and MT gliding activity of Kif15 by inhibiting the motors ability to bind either ATP or MTs. To distinguish between these

possibilities, we first measured the MT-stimulated ATPase activity of Kif15-N700 at varying concentrations of ATP or MTs in the presence of GW108X. When varying the concentration of a substrate, a competitive inhibitor will change the K_M while V_{max} remains unchanged, whereas a non-competitive inhibitor will change the V_{max} with no change in the K_M. When varying ATP concentrations in the presence of GW108X at a high MT concentration, there was no change in the measured K_M^{ATP} and a decrease in the V_{max}, indicating that GW108X is not competing with ATP binding (Figure 5.2 A). In contrast, when the MT concentration was varied in the presence of saturating ATP, an increase in the K_M^{MT} was observed, suggesting that GW108X interferes with Kif15's MT binding ability (Figure 5.2 B).

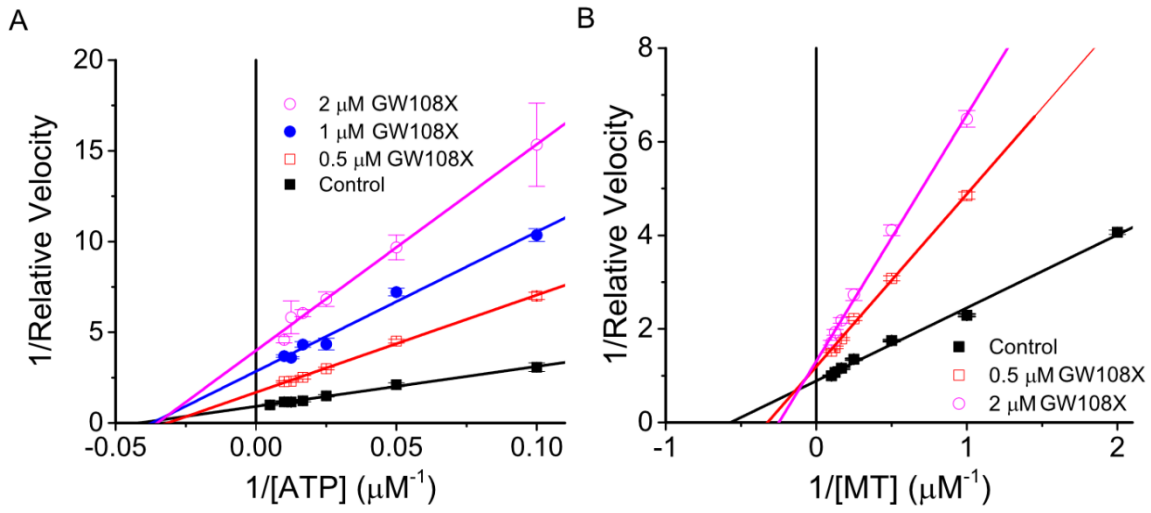

Figure 5.2 GW108X is a non-competitive ATP inhibitor. (A) Double reciprocal Lineweaver-Burk plot of ATP titration at 0.5, 1 and 2 μM GW108X. (B) Double reciprocal Lineweaver-Burk plot of MT titration at 0.5 and 2 μM GW108X (Geng-Yuan Chen).

GW108X Inhibits Spindle Assembly in K5I Resistant Cells

To determine if GW108X affects Kif15 activity in cells, we first analyzed its effects on Kif15 localization and activity in *TP53*$^{-/-}$ RPE-1 cells (Izquierdo et al. 2014). In RPE-1 cells

treated with 25 μM GW108X, 84% of pre-anaphase microtubule arrays were bipolar (n=470), similar to cells treated with DMSO (90% bipolar, n=490, Figure 5.3 B). This is consistent with previous reports that Kif15 is not normally required for spindle assembly (Sturgill and Ohi 2013; Tanenbaum et al. 2009). However, 25 μM of GW108X led to a 3-fold decrease of spindle-bound Kif15 levels compared to DMSO, as assessed by quantitative immunofluorescence microscopy (Figures 5 A and C). Decrease in spindle Kif15 levels corresponds to a ~60% decrease in Kif15 protein levels in RPE-1 cells treated with 25 μM GW108X, suggesting that GW108X treatment of cells leads to Kif15 degradation (Figure 5.3 D and E). Despite a decrease of Kif15 in RPE-1 cells treated with 25 μM GW108X, spindle lengths were unaffected (Figure 5.3 F).

To determine if GW108X inhibits the spindle assembly function of Kif15, we tested whether GW108X blocks spindle assembly in an RPE-1 cell line adapted to survive in the presence of the kinesin-5 inhibitor STLC. Cancer cell lines can acquire resistance to K5Is, and these K5I-resistant cell lines (KIRCs) all rely on Kif15 to build a bipolar spindle (Ma et al. 2014; Raaijmakers et al. 2012; Saeki et al. 2018; Sturgill et al. 2016; Sturgill and Ohi 2013). We generated the KIRC-1 cell line as a clone of *TP53*$^{-/-}$ RPE-1 cells that adapted to the presence of 10 μM STLC (see Materials and Methods). Without further perturbation, KIRC-1 cells exhibit ~50-60% monopolar spindles, consistent with previously published K5I-resistant lines listed above (Figure 5.4 B). Confirming that Kif15 is essential to complete cell division when Eg5 is inhibited, depletion of Kif15 from KIRC-1 cells by RNAi blocked bipolar spindle assembly; 99% of Kif15-depleted KIRC-1 cells contained monopolar spindles, compared to 65% in control siRNA-transfected cells (Figures 5.4 C and D). To test the effects of GW108X, we scored monopolarity in KIRC-1 cells treated with 25 μM of GW108X (in the presence of 10 μM STLC), and found that the compound increased the percent of monopolar spindles in KIRC-1 cells from 49 ± 4% to 95 ± 3% (Figure 5.4

A and B). The ability of GW108X to block spindle assembly in KIRC-1 cells was dose-dependent (Figure 5.4 D).

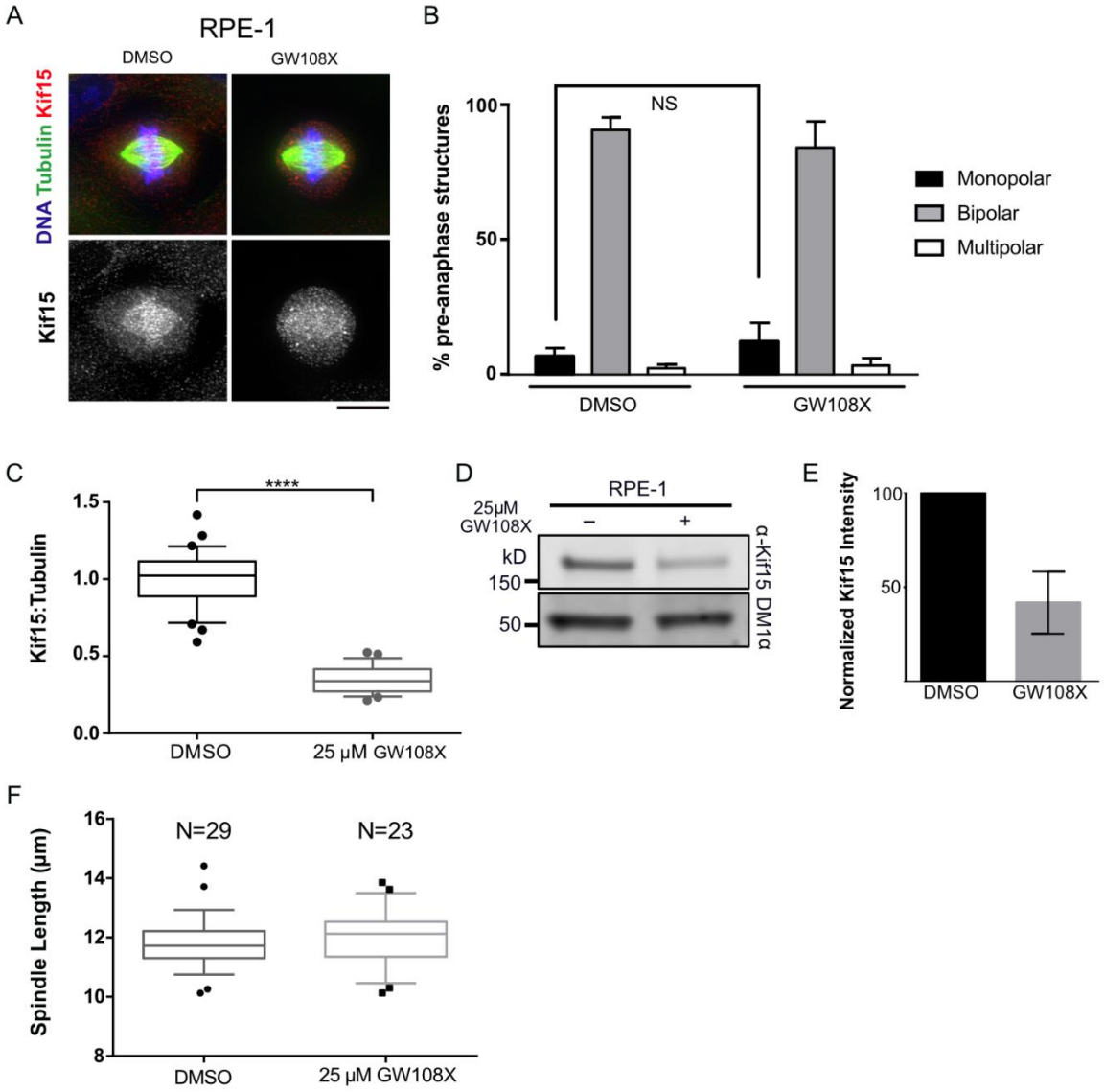

Figure 5.3 RPE-1 cells maintain spindle bipolarity when treated with GW108X. A) Max intensity z-projections of *TP53*$^{-/-}$ RPE-1 cells treated with DMSO or 25 µM GW108X for 24 hours and stained with antibodies targeting Kif15 (grayscale and red), tubulin (green) and DNA (blue). Lookup tables (LUTs) for grayscale, red, and green channel are scaled identically. Scale bar, 10 µm. B) Quantitation of % of pre-anaphase structures in *TP53*$^{-/-}$ RPE-1 cells treated with DMSO or 25 µM GW108X for 24 hours. Each condition was tested in triplicate and n ≥ 100 cells per replicate were counted. Errors bars show SD. C) Quantitation of Kif15 on metaphase MTs in *TP53*$^{-/-}$ RPE-1 cells treated with DMSO or 25 µM GW108X. Shown are ratios of Kif15 fluorescence intensities to tubulin intensities. Box-and-whisker plots describe the median value as well as the 10th, 25th, 75th and 90th percentiles. ****, $p < 0.0001$. n ≥ 25 cells from triplicate experiments. D) Western blot of whole cell lysates prepared from RPE-1 cells treated with DMSO or 25 µM

GW108X for 24 hours and probed with antibodies targeting Kif15 (α-Kif15) and tubulin (DM1α). E) Quantitation of A. Values represent levels of Kif15 protein in GW108X treated cells normalized to DMSO treatment. n = 2, error bars, SD. F) Quantitation of spindle lengths in TP53$^{-/-}$ RPE-1 cells treated with DMSO or 25 µM of GW108X for 24 hours. Box-and-whisker plots describe the median value as well as the 10th, 25th, 75th and 90th percentiles.

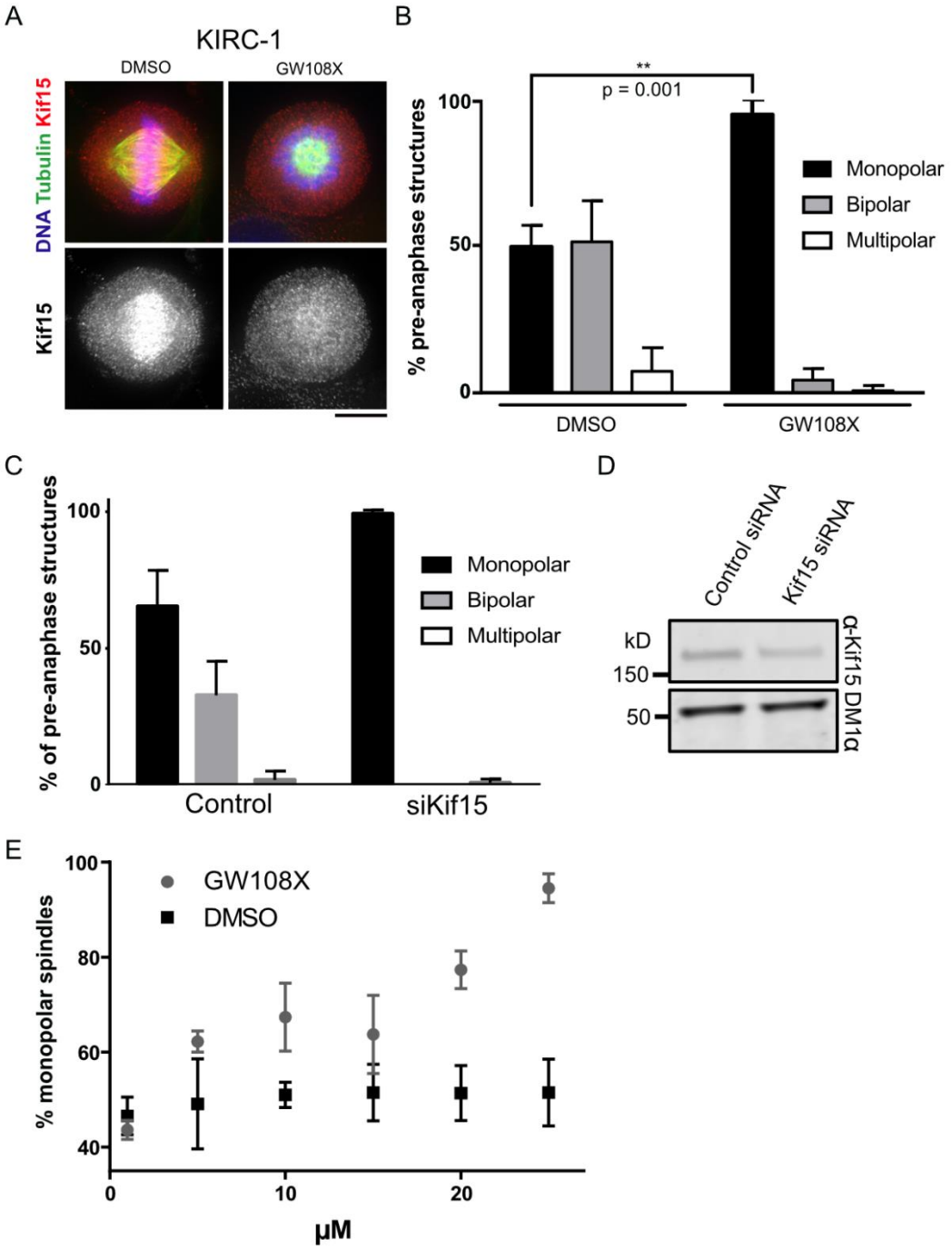

Figure 5.4 GW108X prevents spindle assembly in KIRC-1 cells. A) Max intensity z-projections of KIRC-1 cells treated with DMSO or 25 µM GW108X for 24 hours and stained with antibodies targeting Kif15

(grayscale and red), tubulin (green) and DNA (blue). Lookup tables (LUTs) for grayscale, red, and green channel are scaled identically. Scale bar, 10 µm. B) Quantitation of % of pre-anaphase structures in KIRC-1 cells treated with DMSO or 25 µM GW108X for 24 hours. Each condition was tested in triplicate and n ≥ 100 cells per replicate were counted. Errors bars show SD. C) Quantitation of pre-anaphase structures in KIRC-1 cells transfected with control or Kif15 siRNA. Each condition was repeated in triplicate and graph displays average percent from each triplicate. Error bars show SD. D) Western blot of whole cell lysates prepared from KIRC-1 cells transfected with control or Kif15 siRNA and probed with antibodies targeting Kif15 (α-Kif15) and tubulin (DM1α). E) Quantitation of monopolar spindles in KIRC-1 cells treated with varying concentrations of GW108X or DMSO. Each condition was repeated in triplicate and graph displays average percent from each triplicate. Error bars show SEM.

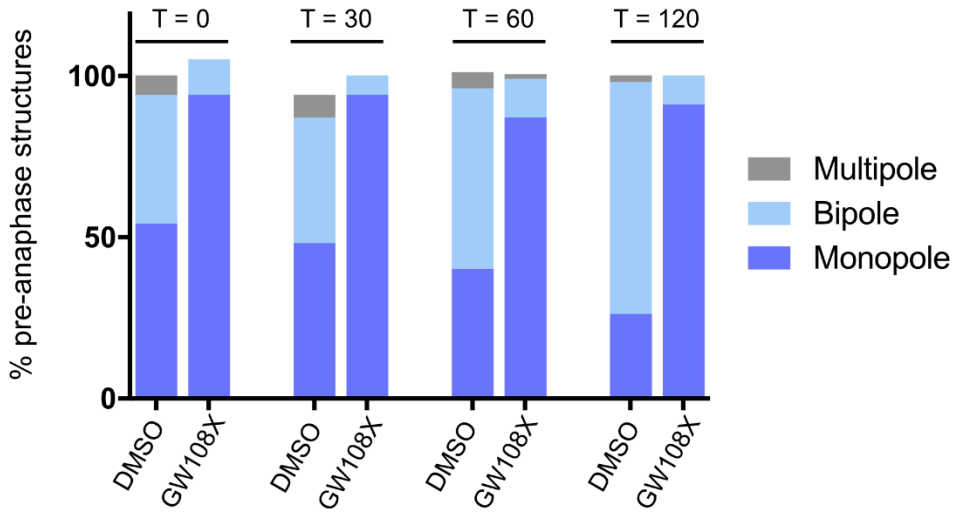

Figure 5.5 Monopolar spindles dominant 2 hours after GW108X removal. Preliminary quantitation of KIRC-1 pre-anaphase spindle structures after GW108X removal. KIRC-1 cells were treated with 25 µM GW108X for 24 hours before GW108X removal. Time indicates time after GW108X removal. N ≥ 94 for all conditions from one experimental replicate.

Discussion

Although GW108X is a kinase inhibitor, our data demonstrates that this small molecule can successfully inhibit Kif15 *in-vitro* and produces phenotypes similar to Kif15 knock-down. GW108X is reversible in the MT gliding assay, though it remains unknown if this translates into cells. If GW108X is indeed reversible in cells, it would be an exciting tool compound to temporally regulate Kif15 activity. In KIRC-1 cells, Kif15 is required for spindle bipolarity (Figure 5.4), but we cannot exclude the possibility that the increase of monopolar spindles in the presence of

GW108X is not due to mechanisms beyond Kif15 inhibition. Since GW108X is a broad-spectrum kinase inhibitor, it is possible that a block in spindle assembly is partly due to co-inhibition of a mitotic kinase(s). Importantly, such kinase inhibitor activity is tolerated in RPE-1 cells, as spindle assembly is not prevented in the parental cell line. In HeLa K5I-resistant cell lines, monopolar spindles can arise from the combined inhibition of Eg5 and Aurora A Kinase (AURKA, Ma et al. 2014). Furthermore, phosphorylation of Kif15 by AURKA is required to target Kif15 to the spindle (van Heesbeen et al. 2017). While biochemical analysis revealed that GW108X inhibits AURKA 67% at 1 μM, it is unknown if GW108X effectively inhibits AURKA in cells (Elkins et al. 2016).

In cell-based assays, GW108X had no adverse effects on parental RPE-1 cells but significantly increased the percent of monopolar spindles in the K5I resistance KIRC-1 cell line (Figure 5.3). When RPE-1 cells were treated with 25μM of GW108X, the spindle bound Kif15 intensity in RPE-1 cells decreases 3x fold. Despite this, they are able to achieve bipolarity most likely through the activity of Eg5 (Sturgill and Ohi 2013; Tanenbaum et al. 2009). In agreement with this data, Kif15 protein levels are decreased ~60% in RPE-1 cells treated with GW108X. It is unclear why GW108X is causing Kif15 degradation. Perhaps GW108X treatment causes Kif15 destruction directly by inducing Kif15 aggregation. This could be confirmed by examining the ubiquitination of Kif15 in cells treated with GW108X.

It will be important moving forward to determine if GW108X and subsequent derivatives reach Kif15 in cells. An interesting and relatively simple experiment would be to use a Kif15-GFP cell line and use live cell microscopy to measure Kif15 loss from the spindle upon addition of GW108X. Preliminary data suggests that the acute effects of GW108X in KIRC-1 cells lasts for at least 2 hours, but further work is needed to estimate cell retention time (Figure 5.5).

Furthermore, it is critical for any potential Kif15 inhibitor to be tested in combination with K5Is to confirm that dual pharmacological inhibition of both kinesins eliminates resistant colony formation in tissue culture cells (Appendix A.2).

CHAPTER 6

KIF15-IN-1 IS AN ATP COMPETITIVE INHIBITOR OF KIF15

Megan E. Dumas[1], Geng-Yuan Chen[2], George Xu[3], William Hancock[2] and Ryoma Ohi[3,4]

[1] Department of Cell and Developmental Biology, Vanderbilt University, Nashville TN
[2] Department of Biomedical Engineering, Pennsylvania State University, State College PA
[3] Department of Cell and Developmental Biology, University of Michigan Medical School, Ann Arbor MI
[4] Life Sciences Institute, University of Michigan, Ann Arbor MI

A modified version was previously published as:

Dumas, ME., Chen, GY., Kendrick, ND., Xu, G., Larsen, SA., Jana, S., Waterson, AG., Bauer, JA., Hancock, W., Sulikowski, GA., and Ohi, R. (2018) Dual inhibition of Kif15 by oxindole and quinazolinedione chemical probes. *Bioorg Med Chem Lett.* 29(2): 148-154.

Introduction

In 2004, the company Cytokinetics submitted a patent application titled "Preparation of quinazolinediones as Kif15 kinesin inhibitors for treating cellular proliferative disorders" (McDonald et al. 2004). A patent application does not require the submission of experimental data, and since a patent was never issued, the effectiveness of these compounds remains unknown. Regardless, over 10 years later, a compound from that patent application became commercially available and called Kif15-IN-1. The first academic lab to publish experimental data with Kif15-IN-1 was the Block group at Stanford University (Milic et al. 2018). Although the paper largely reports on the mechanochemical cycle Kif15, Milic et al demonstrated that Kif15-IN-1 works synergistically with K5Is to decrease cell viability in HeLa cells. While their experiments were

thorough, the group did not investigate the effect Kif15-IN-1 had on Kif15 inside cells. To fill this gap, we purchased Kif15-IN-1 to use in several of our established Kif15 assays.

Kif15-IN-1 Displays a Sub-Micromolar IC_{50}

Kif15-IN-1 is a quinazolinedione and is reported to have an IC_{50} of 1.72 μM in the MT gliding assay (Figure 6.1 A). We repeated the MT gliding assays using the reported IC_{50} of 1.72 μM and found that this concentration abolishes Kif15-driven MT gliding (Figure 6.1 B). We used the MT gliding assay to calculate our own IC_{50}, revealing an IC_{50} of 203 nM (Figure 6.1 C). This concentration is lower than the previous reported, and possibilities for this discrepancy are highlighted in the discussion.

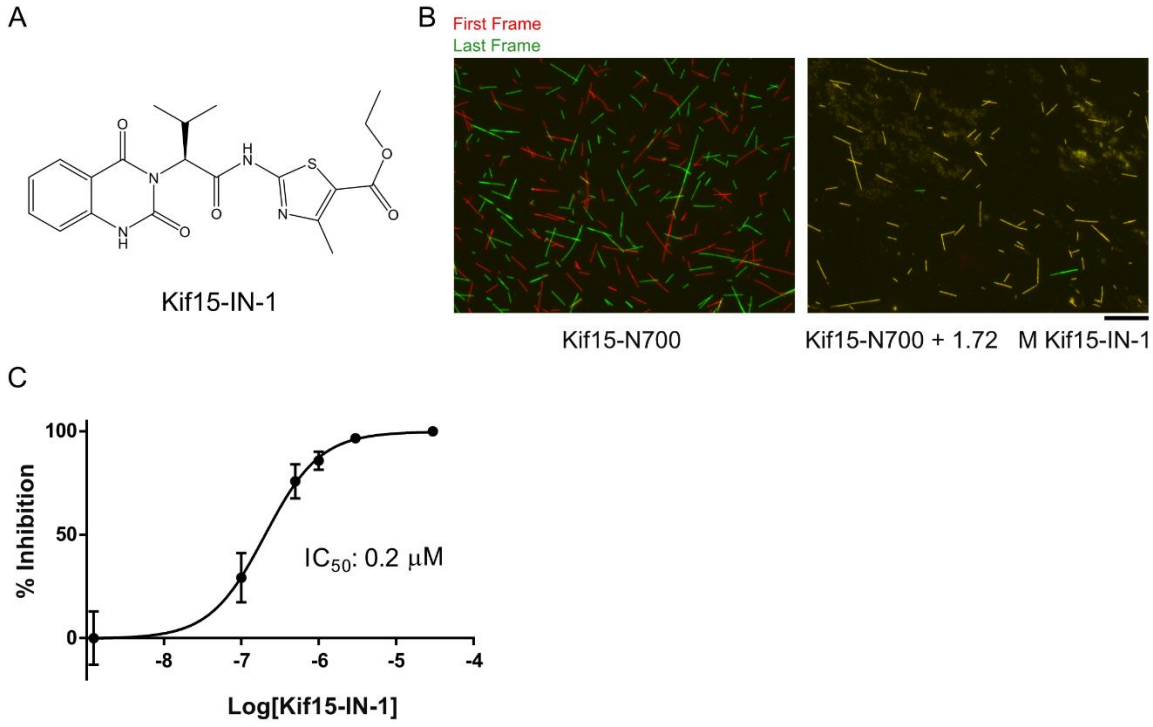

Figure 6.1 Sub-micromolar IC_{50} of Kif15-IN-1 in MT gliding assay. A) Structure of Kif15-IN-1. B) Representative still frames from MT gliding assay with or without 1.72 μM Kif15-IN-1. MTs from the first and last frame of movie are pseudo-colored in red and green, respectively. Scale bar, 20 μm. C) Concentration response curve using the MT-gliding assay, developed from 5 concentrations of Kif15-IN-1, ranging from 30 to 0.1 μM (George Xu). Error bars show SD.

Kif15-IN-1 is Reversible and Competes with ATP

The study published from the Block lab focused on understanding the mechanochemical cycle of Kif15 using single molecule optical trap assays to compare Kif15 to Eg5. They also used mixed motor MT gliding assays with recombinant Eg5 and Kif15 to understand how K5Is and Kif15-IN-1 may affect teams of mitotic motors within the spindle. Despite having all of these reagents, they did not report if Kif15-IN-1 was reversible. For this, we again turned to the MT gliding assay to determine if MTs will resume gliding when Kif15-IN-1 is washed out. Similar to GW108X, Kif15-IN-1 was reversible in the MT gliding assay (Figure 6.2 A).

We next used the steady state ATPase assay to determine if Kif15-IN-1 was ATP-competitive. In contrast to GW108X, an increase in K_M^{ATP} was observed when the ATP concentration was varied in the presence of Kif15-IN-1, indicating that instead of competing with MT binding, Kif15-IN-1 competes with ATP binding (Figure 6.2 B).

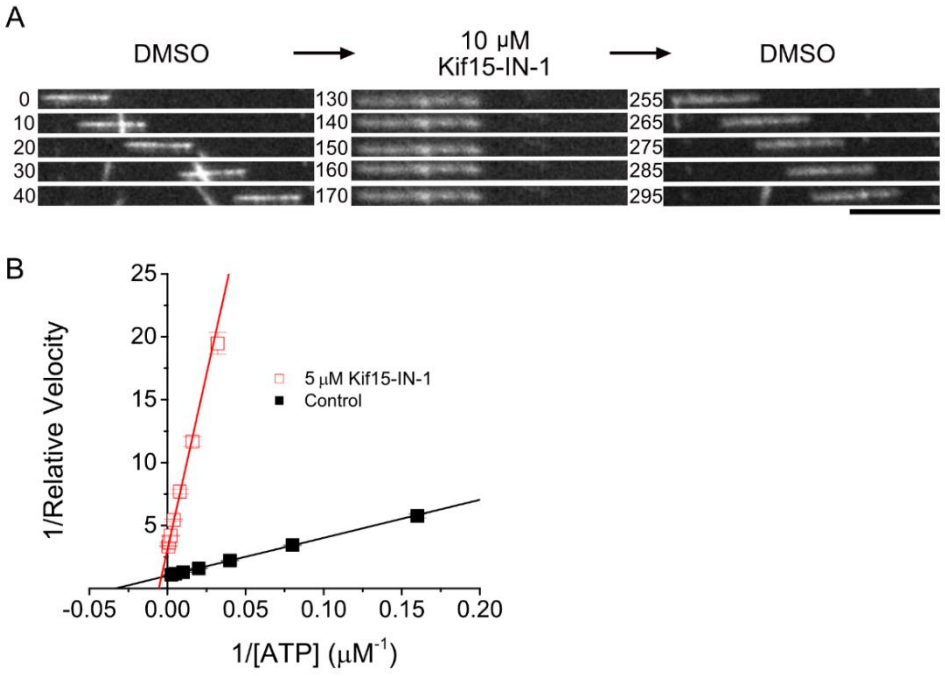

Figure 6.2 Kif15-IN-1 is a reversible, ATP competitive inhibitor of Kif15. A) Representative montage of fluorescent MTs from double wash out experiment. Each vertical frame represents 10 seconds. Scale bar, 5 μm. B) Double reciprocal Lineweaver-Burk plot of ATP titration using 5 μM Kif15-IN-1. Each reaction was performed in triplicate (Geng-Yuan Chen). Error bars shows SEM.

Kif15-IN-1 Decreases Mitotic Spindle Length

The only cellular data of Kif15-IN-1 is from cell viability assays (Milic et al. 2018). Milic et al demonstrated that K5Is and Kif15-IN-1 work synergistically to decrease HeLa cell viability, but did not characterize Kif15 localization inside cells treated with Kif15-IN-1. To start, we tested the effect of Kif15-IN-1 on Kif15 localization in RPE-1 cells. Similar to GW108X, RPE-1 cells treated with Kif15-IN-1 maintained bipolarity (Figure 6.3 A-B, DMSO: 94% bipole, n = 303, Kif15-IN-1: 96% bipole, n = 196). Unlike GW108X, Kif15-IN-1 did not reduce spindle-bound levels of Kif15 and only decreased Kif15 protein in whole cell lysates by 15% (Figure 6.3 C and E-F). Nevertheless, spindles were shorter in RPE-1 cells treated with 25 µM Kif15-IN-1 (9.9 µm ± 0.3 µm) compared to DMSO (11.4 µm ± 0.2 µm), a phenotype consistent with knock-down of Kif15 (Figure 6.3 D, Sturgill & Ohi, 2013).

Kif15-IN-1 Prevents Spindle Assembly in KIRC-1 Cells

Finally, we tested whether Kif15-IN-1 had the ability to halt spindle assembly in the KIRC-1 cell line that relies on Kif15 for bipolarity (Figure 5.4 D). In KIRC-1 cells treated with 25 µM Kif15-IN-1, the percentage of pre-anaphase microtubule arrays that were monopolar increased from 43% in DMSO (n = 260) to 84% (Figure 6.4 A and B, n = 269), similar to the increase observed with GW108X.

Discussion

The quinazolinedione Kif15-IN-1 has only been studied previously by one academic group and was found to inhibit Kif15 *in vitro* (Milic et al. 2018). Until now, it was unknown how Kif15-IN-1 may be altering Kif15 in cells. Here in, we characterized Kif15-IN-1 in both RPE-1 and

KIRC-1 cells, and compared it to GW108X. In the MT gliding assay, we estimated an IC_{50} of 203 nM for Kif15-IN-1. However, Kif15-IN-1 has previously been reported to have an IC_{50} of 1.72

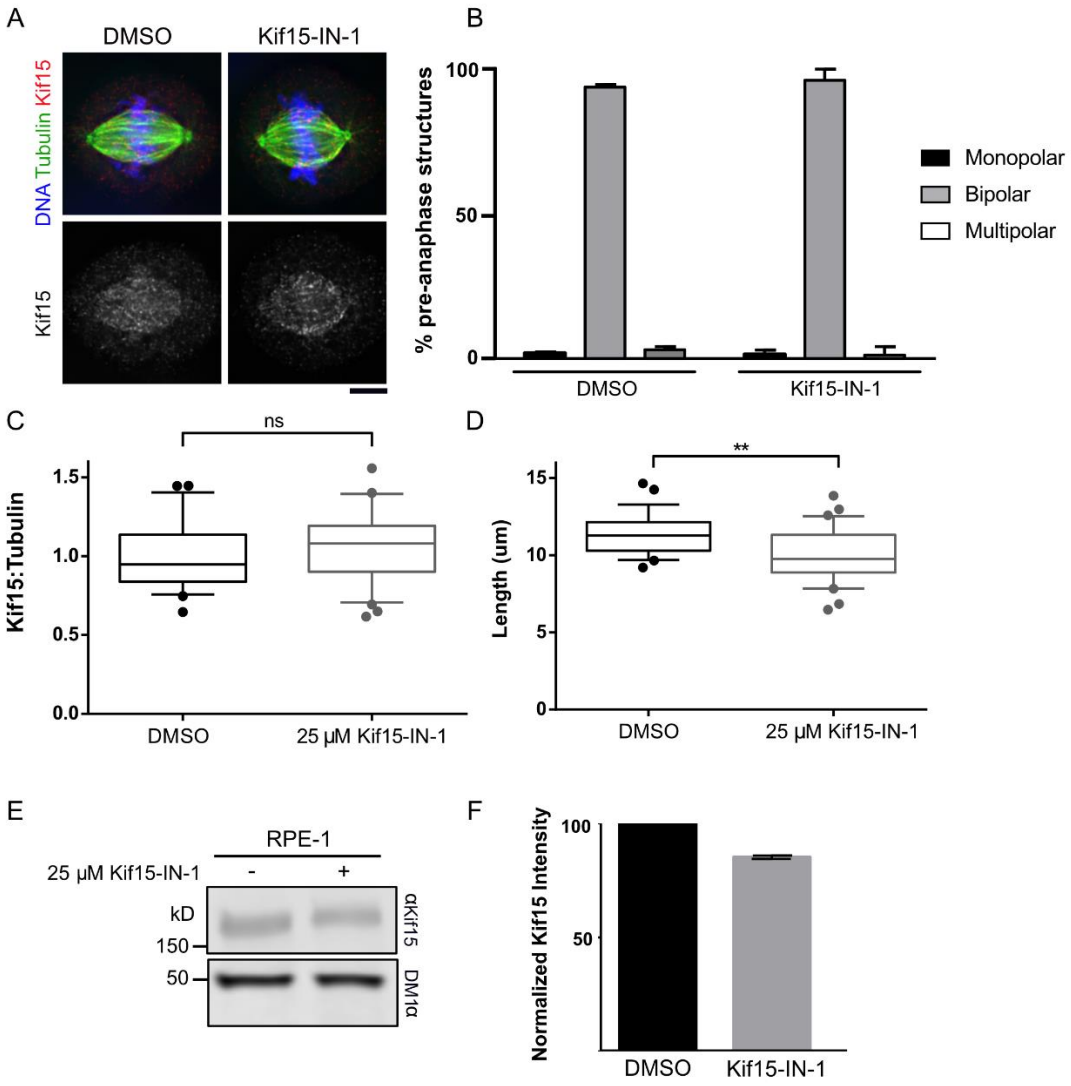

Figure 6.3 Kif15-IN-1 has no effect on Kif15 localization or protein levels in RPE-1 cells. A) Representative single optical sections of $TP53^{-/-}$ RPE-1 cells treated with DMSO or 25 µM Kif15-IN-1 for 24 hours and stained for antibodies targeting Kif15 (grayscale and red), tubulin (green) and DNA (blue). LUTs for grayscale, red and green channels are scaled identically. Scale bar, 5 µm. B) Quantitation of the % pre-anaphase structures in $TP53^{-/-}$ RPE-1 cells treated with DMSO or 25 µM Kif15-IN-1 for 24 hours. Each condition was tested in triplicate and graph displays average percent from each triplicate. Errors bars show SD. C) Quantitation of RPE-1 cells treated with DMSO or 25 µM Kif15-IN-1 for 24 hours. Shown are ratios of Kif15 fluorescence intensities to tubulin intensities. Box-and-whisker plots describe the median value as well as the 10^{th}, 25^{th}, 75^{th} and 90^{th} percentiles. n = 30 cells from triplicate experiments. D) Quantitation of spindle lengths in $TP53^{-/-}$ RPE-1 cells treated with DMSO or 25 µM of Kif15-IN-1 for 24 hours. Box-and-

whisker plots describe the median value as well as the 10th, 25th, 75th and 90th percentiles. E) Western blot of whole cell lysates prepared from TP53$^{-/-}$ RPE-1 cells treated with DMSO or 25 µM Kif15-IN-1 for 24 hours and probed with antibodies targeting Kif15 (α-Kif15) and tubulin (DM1α). F) Quantitation of E. Values represent levels of Kif15 protein in Kif15-IN-1 treated cells normalized to DMSO treatment. n = 2, error bars show SD.

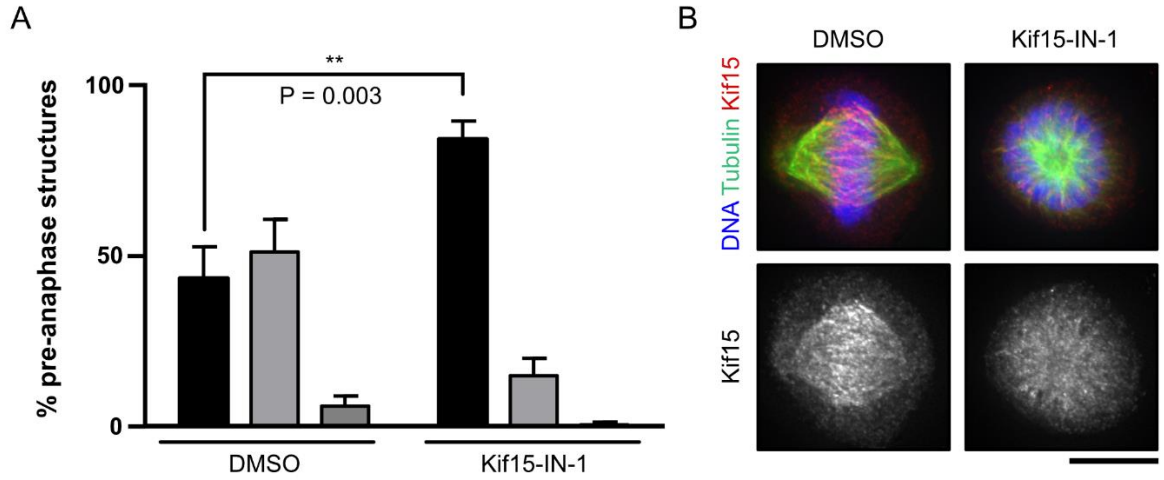

Figure 6.4 Kif15-IN-1 prevents spindle assembly in KIRC-1 cells. A) Quantitation of the % pre-anaphase structures in KIRC-1 cells treated with DMSO or 25 µM Kif15-IN-1 for 24 hours. Each condition was tested in triplicate and graph displays average percent from each triplicate. Errors bars show SD. B) Representative max intensity projection of KIRC-1 cells treated with DMSO or 25 µM Kif15-IN-1 for 24 hours and stained for antibodies targeting Kif15 (grayscale and red), tubulin (green) and DNA (blue). LUTs for grayscale (Kif15) are scaled identically. Scale bar, 10 µm.

µM in the same assay. While reasons for this discrepancy remain unclear, the most notable difference between assay conditions is the use of different Kif15-N700 constructs. We have previously characterized a Kif15-N700 construct generated from a naturally occurring mRNA variant of Kif15 that lacks the AA residues 8-21 (Sturgill et al. 2014). The Kif15 construct from the Milic study contained these AAs and exhibits ~1.5x increase in MT gliding velocity compared to our construct. Regardless, it is unlikely that these AAs are required for Kif15-IN-1 binding, as a lack of crucial AA's would only increase the predicted IC_{50}, not lower it.

In the mixed motor gliding assays with Eg5 and Kif15, Milic et al reported that when Kif15 was fully inhibited by Kif15-IN-1, Eg5 was unable to reach its characterized gliding velocity. This

observation suggests that Kif15 complexed with Kif15-IN-1 strengthens Kif15 binding to MTs, and acts as a 'brake' to Eg5 powered motility. Despite the observation that Kif15-IN-1 may rigor Kif15 to the MT lattice, we did not observe a change in Kif15 levels on the spindle (Figure 6.3 C). Furthermore, we did not observe an increase in the % of Kif15 in the pellet of a MT co pellet assay in the presence of Kif15-IN-1 (data not shown). Regardless of rigor ability, treatment of RPE-1 cells with Kif15-IN-1 displayed the characteristic short spindle phenotype of Kif15 inhibition and prevents spindle assembly in KIRC-1 cells.

Moving forward, several important experiments are necessary to fully understand the specificity of Kif15-IN-1 for Kif15 inside cells. First, a kinase inhibition profile to probe potential off target effects would determine if Kif15-IN-1 has any promiscuous kinase inhibition behavior. Furthermore, it would be useful to understand Kif15-IN-1's preference for Kif15 over other mitotic motors. Block et al demonstrated Kif15-IN-1 has no effect on Eg5 activity, but other kinesins should be tested.

CHAPTER 7

CONCLUDING REMARKS

Targeting Kif15 Intramolecular Interactions

Kinesins are the molecular work horses of the cell, uniquely able to harness and translate the energy from ATP hydrolysis into force generation. During interphase, kinesins are one of the main transport motors, using the MT highway to transport vesicles, signaling granules, and organelles (Alberts et al. 2008). During cell division, mitotic kinesins drive centrosome separation, chromosome congression, and cytokinesis (Cross and McAinsh 2014). Owing to their importance, deregulation of mitotic kinesins has been associated with the development of a variety of cancers, and are therefore attractive chemotherapeutic targets (Kozielski 2012; Qiao et al. 2018; Yu et al. 2019).

Regulating kinesin activity is paramount to prevent both kinesin hyper activity and waste of ATP. As described in the introduction, cells have a toolbox of techniques to prevent uncontrolled kinesin activity, including self-regulation, post translational modifications, and sequestration (Verhey and Hammond 2009). Kif15 is an autoinhibited motor that is regulated in a cell cycle dependent manner, whose preference for MT bundles promotes its localization to K-MTs during mitosis (Sturgill et al. 2014). Kif15 over expression promotes tumorgenicity and is correlated with poor prognosis in melanoma, breast, bladder, and lung cancers (Qiao et al. 2018; Song et al. 2018; Yu et al. 2019; Zhao et al. 2019). In tissue culture, Kif15 overexpression is one mechanism used by cells to acquire K5I resistance (Sturgill and Ohi 2013). Though not confirmed, one would predict that a subset of cancer samples from patients treated with a K5I during a clinical trial would also exhibit elevated Kif15 levels. Another mechanism to confer K5I resistance could

involve mutations that abrogate the ability of Kif15 to auto-inhibit its activity. A mutation of this nature in the gene encoding KIF21A, a kinesin that suppresses MT growth in neurons, gives rise to the congenital neurodevelopmental disorder congenital fibrosis of the extraocular muscles type 1 (Cheng et al. 2014; van der Vaart et al. 2013). Over all, knowledge of how Kif15 self regulates will shed light on how the motor regulates its activity in both space and time, and has the potential to explain a novel pathway cancer cells may use to evade the lethal effects of kinesin-5 inhibitors.

A deep understanding of the intramolecular interactions between Kif15 and its inhibitory tail may also guide the design of small molecule mimetics that exploit this region. Kif15 auto-inhibition depends on the LZ motif as well as other sequences within the last 100 AAs of the C-terminal tail (Figure 3.1 C). Knowledge of the residues key for inhibition will be critical in understanding the biochemical and structural mechanism of Kif15 auto-inhibition. Nature has already designed a Kif15 inhibitor that can be extrapolated to design small molecules that target the auto-inhibitory region within the motor domain (Peterson and Golemis 2004). Small molecule inhibitors have been designed that stabilize the inhibited conformation of self-regulated proteins as well as block antagonist activator binding interactions (Wang 2010; Wu et al. 2018). Even more promising, proof of principle studies with kinesin-1 demonstrated that small molecules can be used to manipulate the auto-inhibition state of the kinesin (Randall et al. 2017). A deep knowledge of the interaction between Kif15's tail and MD, combined with the crystal structure of Kif15, could propel Kif15 inhibitor development.

Targeting Kif15 Pharmacologically

The bipolar geometry of the mitotic spindle is both iconic and essential. Its fusiform shape is the only geometry that can successfully complete the mission of mitosis. In order to create

bipolarity, the spindle MTs must be focused within centrosomes at either end of the structure (Yang and Snyder 1992). The majority model organisms studied in the lab require Eg5 to separate the duplicated centrosomes, with the exception being *C. elegans* and *Dictyostelium* (Bishop et al. 2005; Tikhonenko et al. 2008). This seemingly universal requirement for Eg5 in spindle assembly skyrocketed its appeal as a chemotherapeutic target, with several pharmaceutical companies pouring money into K5I discovery campaigns and clinical trials (Kozielski 2012). To date, all clinical trials with K5Is have failed and several research groups have reported K5I resistance mechanisms that depend on Kif15 in tissue culture cells (Ma et al. 2014; Raaijmakers et al. 2012; Sturgill et al. 2016; Sturgill and Ohi 2013).

Using small molecule screening techniques to discover a novel function for GW108X and purchasing Kif15-IN-1, we have described and characterized two functionally unique Kif15 inhibitors. Despite being a known kinase inhibitor, GW108X is a potent and reversible inhibitor of Kif15 *in vitro*. The quinazolinedione, Kif15-IN-1, was discovered in 2004 by Cytokinetics and recently became available for scientific use. Both compounds are sub-micromolar inhibitors of Kif15 and exhibit different mechanisms of inhibition. Steady state kinetics confirmed that while Kif15-IN-1 directly competes with ATP, GW108X instead is a non-ATP competitive inhibitor and interferes with Kif15s MT binding ability. Further work is required to determine if GW108X is trapping Kif15 in a low MT affinity state by preventing ADP release or direct obstruction of Kif15's MT binding site. Since GW108X and Kif15-IN-1 display different modes of inhibition, it is unlikely that they share the same binding site within the motor and instead each offer novel chemical space for Kif15 inhibition.

This distinction in biochemical mechanism is important for two reasons. First, having multiple sites to probe for inhibition increases the likelihood of creating a truly Kif15 specific

inhibitor. If the binding site for GW108X and Kif15-IN-1 are close, it could be feasible to create a large, flexible molecule that encompasses properties of both compounds, allowing for both inhibitory regions to be engaged. Conjugation of two chemotypes might improve specificity and affinity of the inhibitor. Secondly, having two druggable sites decreases the possibility of mutations within *KIF15* bypassing drug mechanism, a common challenge of target-based chemotherapeutics (Schmitt et al. 2016). Improving the specificity and potency of both GW108X and Kif15-IN-1 relies on obtaining co-crystals of these small molecules with the Kif15 motor domain (Klejnot et al. 2014).

Mitotic kinesin inhibitors are routinely used in cell biology laboratories and allow researchers to specifically modulate a motors activity to give a predicted perturbation of MT or spindle dynamics. For example, research in Xenopus extracts using a rigor K5I (instead of the previously characterized allosteric K5Is) specifically induced loss of microtubule density at the spindle poles, unmasking a novel role for Eg5 activity in spindle pole maintenance (Groen et al. 2008). Recently, functionally distinct K5Is were shown to have differential effects on both MT dynamics *in vitro* and spindle stability in RPE-1 cells. While the canonical non-competitive loop-5 targeting K5Is result in the classic monopolar spindle phenotype, the ATP competitive inhibitor BRD9876 stabilizes MTs *in vitro* and does not cause spindle collapse (Chen et al. 2017).

Small molecule inhibitors that can modulate Kif15's mechanochemical cycle in different ways will also be powerful tools for mitosis research. In the case of Kif15, its mitotic function under normal conditions is not well understood. Kif15 localizes to kinetochore-MTs, regulating the stability and length of these bundles. When over-expressed, as in some K5I-resistant cells, Kif15 re-localizes to non-KMTs and provides outward forces required for centrosome separation (Sturgill and Ohi 2013). Small molecules that can acutely inhibit Kif15 in these different cellular

contexts through different mechanisms are likely to reveal new properties and functions of Kif15 during mitosis.

Our studies with GW108X and Kif15-IN-1 show that both compounds are useful launch points in the generation of Kif15-targeting drugs. Given that cultured cells **must** express *KIF15* in order to acquire K5I resistance and that K5Is synergize with Kif15-IN-1 to decrease in cell viability, there is clear rationale to pursue Kif15-targeting drugs for use in combination with K5Is as a chemotherapeutic strategy (Milic et al. 2018; Sturgill et al. 2016).

APPENDIX

A.1 STRUCTURE-ACTIVITY RELATIONSHIP ANALYSIS OF GW108X, VU669, AND VU724 STRUCTURAL ANALOGS

Screening of the GSK PKIS led to three potential lead compounds: GW108X, VU669 and VU724 (see Figure 4.3). The Vanderbilt High Throughput Screening facility has several commercial and private compound libraries available for researchers. Before synthesizing a GW108X derivative library, we wanted to take advantage of the large resource of compounds available for use to probe the SAR of the top three compounds. With the help of medicinal chemists, 31 compounds were selected from 11 different compound libraries and screened in triplicate at 10 μM for their ability to inhibit Kif15-N420 in the ATPase assay screen (Figure A1.1 – 1.3).

GW108X	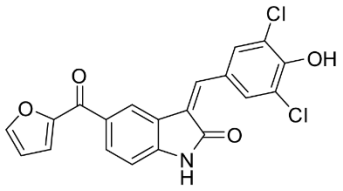	
Compound	Structure	% Inh (10 uM)
VU0472437	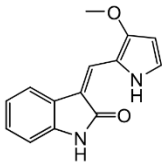	26 ± 1
VU0316618	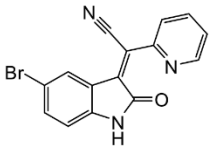	4 ± 2
VU0472452	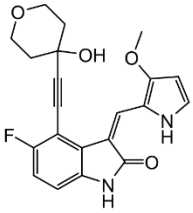	-6 ± 3
VU0472408	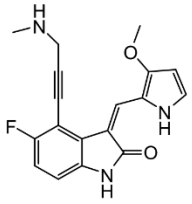	-6 ± 3
VU0472551	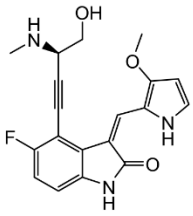	-12 ± 1

Figure A1.1 SAR analysis of GW108X structural analogs. Compounds cherry-picked from available Vanderbilt small molecule libraries that shared structural features with GW108X. Data is the average percent inhibition of Kif15-N420 with each compound using the ADP-Glo ATPase assay. Every compound was tested in triplicate.

VU669	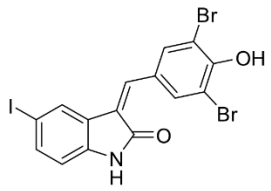	

Compound	Structure	% Inh (10 uM)
VU0482565	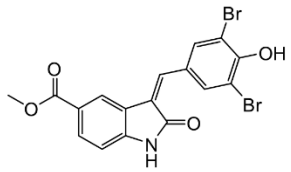	45 ± 1
VU0482559	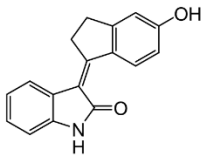	25 ± 2
VU0477482	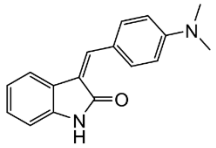	15 ± 5
VU0610974	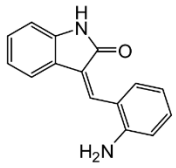	7 ± 0
VU0291597	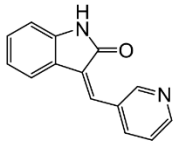	3 ± 1
VU0122765	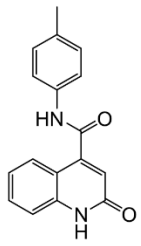	-1 ± 3

VU0320859	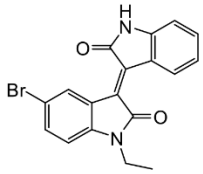	-2 ± 3
VU0341658	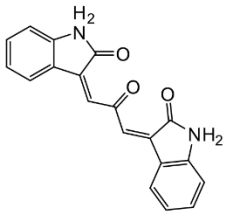	-2 ± 2
VU0287874	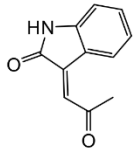	0 ± 0

Figure A1.2 SAR analysis of VU669 structural analogs. Compounds cherry-picked from available Vanderbilt small molecule libraries that shared structural features with VU669. Data is the average percent inhibition of Kif15-N420 with each compound using the ADP-Glo ATPase assay. Every compound was tested in triplicate.

VU724	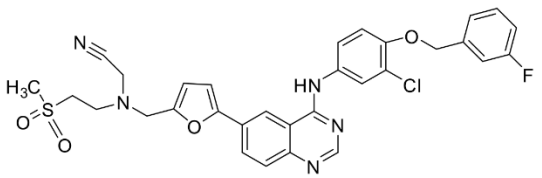

Compound	Structure	% Inh (10 uM)
VU0107550	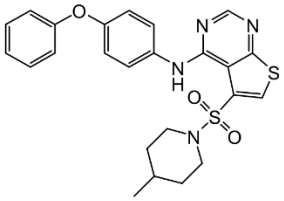	12 ± 2
VU0073990	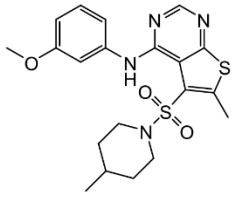	10 ± 1
VU0061547	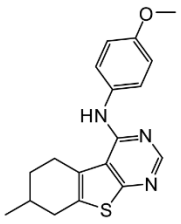	10 ± 3
VU0084767	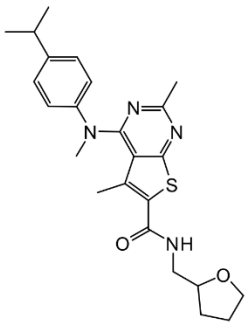	10 ± 3

VU0081027	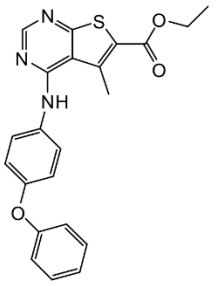	4 ± 4
VU0482571	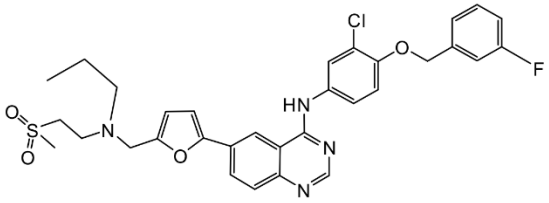	1 ± 7
VU0482569	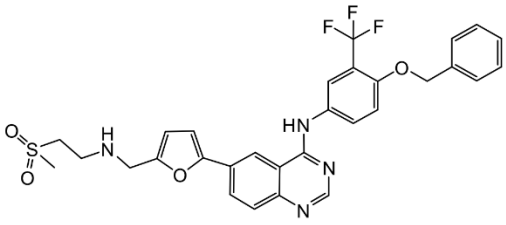	-1 ± 1
VU0778352	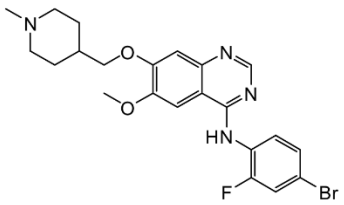	-3 ± 4
VU0778337	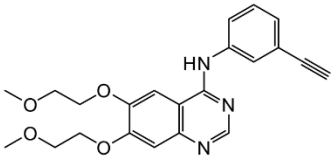	-4 ± 2
VU0081122	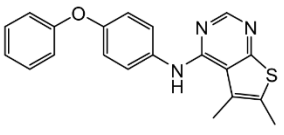	-5 ± 2

VU0084798	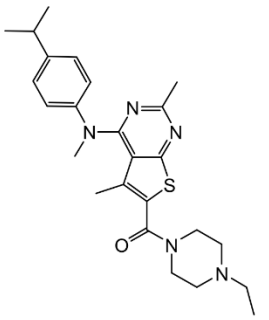	-5 ± 3
VU0778347	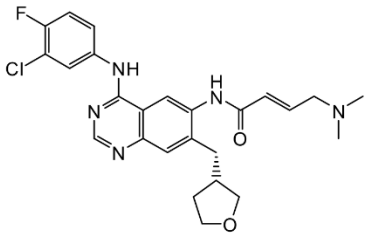	-9 ± 1
VU0778365	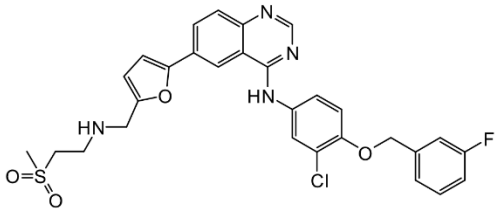	-9 ± 2
VU0778336	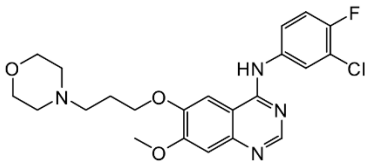	-13 ± 1
VU0482778	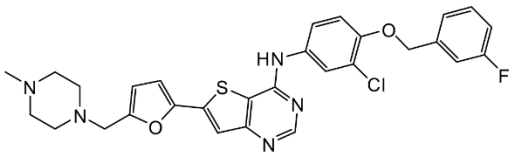	-105 ± 20

Figure A1.3 SAR analysis of VU724 structural analogs. Compounds cherry-picked from available Vanderbilt small molecule libraries that shared structural features with VU724. Data is the average percent inhibition of Kif15-N420 with each compound using the ADP-Glo ATPase assay. Every compound was tested in triplicate.

A.2 CAN GW108X OR ITS DERIVATIVES PREVENT K5I RESISTANCE IN RPE-1 CELLS?

Previous work from our lab demonstrated that pharmacological inhibition of Eg5 and genetic deletion Kif15 abolished the ability of HeLa cells to develop resistance against K5Is (Sturgill et al. 2016). This proof of principal discovery demonstrated that regardless of resistance mechanism, tissue culture cells required Kif15 to develop K5I resistance, underscoring the importance of developing Kif15 inhibitors. HeLa cells are highly aneuploid, therefore we wanted use a non-cancerous cell line to confirm that Kif15 is required for K5I resistance. We generated RPE-1 KIF15Δ cells from the diploid RPE-1$^{TP53\ -/-}$ cell line and demonstrated that K51 resistant colonies were unable to form when *KIF15* was deleted (Izquierdo et al. 2014, data not shown).

While genetic deletion of Kif15 highlighted its essential role in K5I resistance in these cells, the end goal is to eliminate K5I resistance with a small molecule. With this in mind, RPE-1$^{TP53\ +/+}$ and RPE-1$^{TP53-/-}$ cells were plated at confluency, treated with 10 μM STLC and 20 μM GW108X for 30 days and stained with crystal violet (Figure A2.1). Between the two cell lines, there were clear and unexpected differences between each experimental treatment. As expected, based off RPE-1 KIRC generation (see Chapter 5 and Materials and Methods), cells that had active p53 did not induce apoptosis when treated with STLC. Cell density decreased during the 30-day STLC treatment, but many viable cells remained by the end of the experiment. Though not confirmed, this is presumably through p53 mediated senescence (Bieging et al 2014). In contrast, RPE-1 *p53*$^{-/-}$ had massive cell death and the appearance of resistant colony formation, presumably unable to initiate senescence like their RPE-1 *p53*$^{+/+}$ counterpart. The cellular response between the cell lines is reversed in GW108X treatment, with RPE-1 *p53*$^{+/+}$ experiencing massive cell death, unlike RPE-1 *p53*$^{-/-}$. Finally, both cell lines contain viable cells after 30-day treatment with

both STLC and GW108X, with dual treatment appearing to be more effective in RPE-1 $p53^{+/+}$ cells.

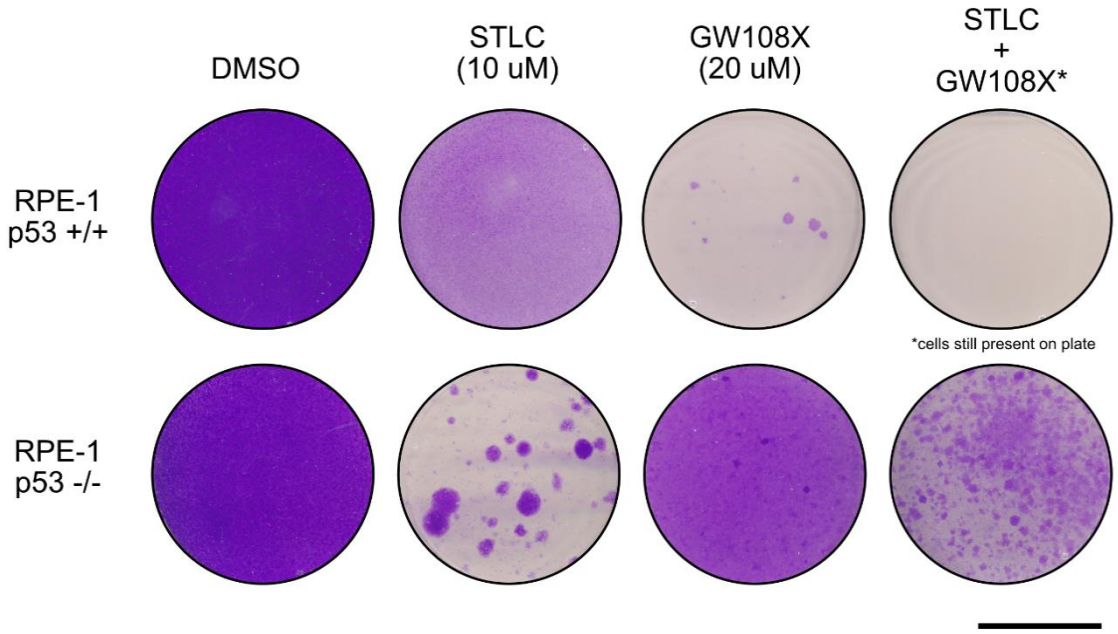

Figure A2.1 Combined STLC and GW108X Treatment. Representative images of 10 cm dishes seeded with indicated cell type and treated with STLC alone, GW108X alone, or both for 30 days and stained with crystal violet. Scale bar 5 cm.

One hypothesis for these results is that STLC and GW108X illicit different cellular responses that depend on the p53 status of the cell. When p53 is present, STLC may cause the majority of cells to senesce. Since Eg5 is a mitotic motor, STLC can only induce negative effects if a cell enters the cell cycle, thus senescence would be a logical way to bypass a catastrophic monopolar mitosis. When p53 is absent and cells are treated with STLC, senescence is not induced and the majority of the cells continue through the cell cycle with STLC present. A simple way to test this hypothesis would be to treat RPE-1 $p53^{+/+}$ and $p53^{-/-}$ with STLC and probe for senescence-associated beta-galactosidase (SA-βgal, Debacq-Chainiaux et al. 2009).

The result with GW108X is even more perplexing and likely due its ability to inhibit several kinases *in-vitro* (Elkins et al. 2016). By comparing GW10X treatment alone between the two cell lines, it seems reasonable to conclude that GW108X activates a p53 dependent apoptosis pathway. If true, one would predict that GW108X is ineffective in killing cancer tissue culture cell lines, since lack of p53 activity is a hallmark of several cancers (Alberts et al. 2008). When tested against 60 different cancer cell lines, GW108X displayed LC_{50} below 25 μM, revealing that cancer cell lines are indeed sensitive to GW108X treatment (Elkins et al. 2016). Regardless, these results demonstrate that long-term treatment with both STLC and GW108X in RPE-1 *p53*$^{-/-}$ cells produces an intermediate cellular response that is in-between what is observed with STLC or GW108X alone.

Preliminary experiments performed by Dr. Sturgill support the hypothesis that cells are forced into an evolutionary bottleneck when treated with K5Is (unpublished, Sturgill et al. 2016). Cells that survive K5I treatment can develop resistance to K5Is using different mechanisms, such as over expression of Kif15 or mutations in Eg5, but we hypothesize they require Kif15 to survive the initial bottleneck (Sturgill et al. 2016; Sturgill and Ohi 2013). Furthermore, it is possible that GW108X has off target effects or a complex relationship with STLC that manifests in resistant colony formation unrelated to Kif15. With these thoughts in mind, we redesigned the previous experiment to include variations in length of Kif15 inhibition. For this set of experiments, we hoped to conserve the GW108X stock and instead used compound **2**, which behaved similarly to GW108X in the MT gliding assay (Figure 4.6). RPE-1 *p53*$^{-/-}$ cells were treated continuously with 10 μM STLC for 30 days but with 20 μM of compound **2** for 3, 7, 10, or 14 of those days (Figure A2.2). After **2** removal, cells remained cultured with STLC until day 30.

Interestingly, the longer the treatment of compound **2**, the less sensitive cells were to Eg5 inhibition by STLC. Cells treated with compound **2** for 3 days visually had fewer viable cells after the 30-day experiment. While it is clear that STLC and GW108X or **2** have a complex relationship in cells, this preliminary data hints there may be a critical time point for Kif15 inhibition before off target effects dominant with these oxindole derivatives. Of course, the obvious caveat is the lack of knowledge regarding the *in vivo* targets for GW108X and its derivatives. Future directions include shortening the incubation with GW108X below three days to observe if resistant colony formation if further decreased.

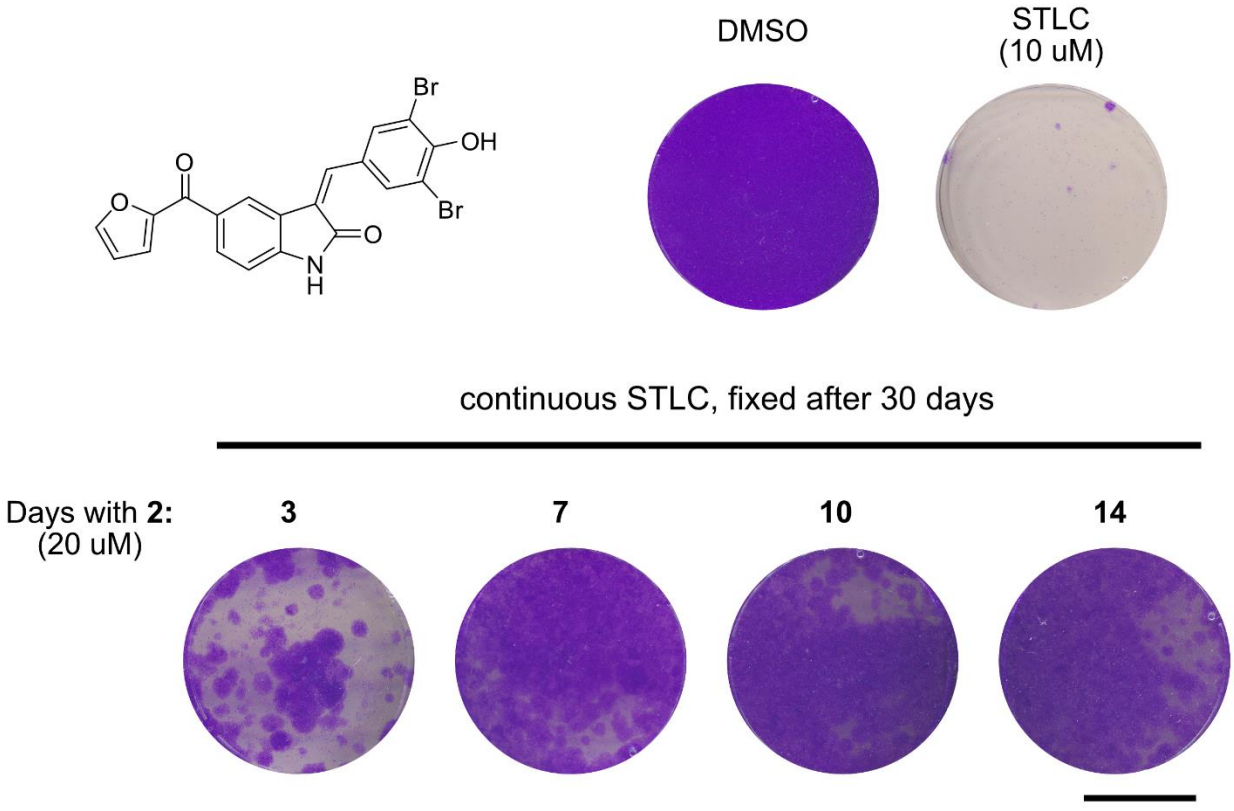

Figure A2.2. Resistant colony formation with STLC and varying incubations with compound 2. Top) Structure of **2** and representative images of 10 cm dishes of RPE-1 p53-/- cells treated with DMSO or STLC continuously for 30 days. Bottom) Representative images of 10 cm dishes treated with STLC for 30 days and **2** for the number of days listed about each dish. Scale bar 5 cm.

REFERENCES

Alberts, Bruce, Johnson Alexander, Lewis Julian, Raff Martin, Roberts Keith, and Walter Peter. 2008. "Molecular Biology of the Cell, 5th Edition by B. Alberts, A. Johnson, J. Lewis, M. Raff, K. Roberts, and P. Walter." *Biochemistry and Molecular Biology Education* 36(4):317–18.

Alushin, Gregory M., Gabriel C. Lander, Elizabeth H. Kellogg, Rui Zhang, David Baker, and Eva Nogales. 2014. "High-Resolution Microtubule Structures Reveal the Structural Transitions in Ab-Tubulin upon GTP Hydrolysis." *CELL* 157:1117–29.

Alves, Maria M., Grzegorz Burzynski, Jean-Marie Delalande, Jan Osinga, Annemieke van der Goot, Amalia M. Dolga, Esther de Graaff, Alice S. Brooks, Marco Metzger, Ulrich L. M. Eisel, Iain Shepherd, Bart J. L. Eggen, and Robert M. W. Hofstra. 2010. "KBP Interacts with SCG10, Linking Goldberg–Shprintzen Syndrome to Microtubule Dynamics and Neuronal Differentiation." *Human Molecular Genetics* 19(18):3642–51.

Asbury, Charles L. 2017. "Anaphase A: Disassembling Microtubules Move Chromosomes toward Spindle Poles." *Biology* 6(15).

Ba, Qinle, Guruprasad Raghavan, Kirill Kiselyov, and Yang Correspondence. 2018. "Whole-Cell Scale Dynamic Organization of Lysosomes Revealed by Spatial Statistical Analysis." *CellReports* 23:3591–3606.

Barbier, Pascale, Audrey Dorléans, Francois Devred, Laura Sanz, Diane Allegro, Carlos Alfonso, Marcel Knossow, Vincent Peyrot, and Jose M. Andreu. 2010. "Stathmin and Interfacial Microtubule Inhibitors Recognize a Naturally Curved Conformation of Tubulin Dimers." *The Journal of Biological Chemistry* 285(41):31672–81.

Barnum, Kevin J. and Matthew J. O'Connell. 2014. "Cell Cycle Regulation by Checkpoints." *Methods in Molecular Biology* 1170:29–40.

Bennabi, Isma, Marie-Emilie Terret, and Marie-Hélène Verlhac. 2016. "Meiotic Spindle Assembly and Chromosome Segregation in Oocytes." *The Journal of Cell Biology* 215(5):611–19.

Bhullar, Khushwant S., Naiara Orrego Lagarón, Eileen M. McGowan, Indu Parmar, Amitabh Jha, Basil P. Hubbard, and H. P. Vasantha Rupasinghe. 2018. "Kinase-Targeted Cancer Therapies: Progress, Challenges and Future Directions." *Molecular Cancer* 17(1):48.

Bieging, Kathryn T., Stephano Spano Mello, and Laura D. Attardi. 2014. "Unravelling Mechanisms of P53-Mediated Tumour Suppression." *Nature Reviews Cancer* 14(5):359–70.

Bishop, John D., Zhenbo Han, and Jill M. Schumacher. 2005. "The *Caenorhabditis Elegans* Aurora B Kinase AIR-2 Phosphorylates and Is Required for the Localization of a BimC Kinesin to Meiotic and Mitotic Spindles." *Molecular Biology of the Cell* 16(2):742–56.

Blangy, Anne, Heidi A. Lane,'t Pierre D'herin, Maryannick Harper, Michel Kress, and Erich A. Nigg. 1995. *Phosphorylation by P34-Cdc2 Regulates Spindle Association of Human Eg5, a*

Kinesin-Related Motor Essential for Bipolar Spindle Formation In Vivo. Vol. 63.

Boleti, Haralabia, Eric Karsenti, and Isabelle Vernos. 1996. "Xklp2, a Novel Xenopus Centrosomal Kinesin-like Protein Required for Centrosome Separation during Mitosis." *Cell* 84(1):49–59.

Borisy, G. G. and E. W. Taylor. 1967. "The Mechanism of Action of Colchicine. Colchicine Binding to Sea Urchin Eggs and the Mitotic Apparatus." *The Journal of Cell Biology* 34(2):535–48.

Brooks, Alice S., Aida M. Bertoli-Avella, Grzegorz M. Burzynski, Guido J. Breedveld, Jan Osinga, Ludolf G. Boven, Jane A. Hurst, Grazia M. S. Mancini, Maarten H. Lequin, Rene F. de Coo, Ivana Matera, Esther de Graaff, Carel Meijers, Patrick J. Willems, Dick Tibboel, Ben A. Oostra, and Robert M. W. Hofstra. 2005. "Homozygous Nonsense Mutations in KIAA1279 Are Associated with Malformations of the Central and Enteric Nervous Systems." *The American Journal of Human Genetics* 77(1):120–26.

Brouwers, Nathalie, Nuria Mallol Martinez, and Isabelle Vernos. 2017. "Role of Kif15 and Its Novel Mitotic Partner KBP in K-Fiber Dynamics and Chromosome Alignment" edited by D. Cimini. *PLOS ONE* 12(4):e0174819.

Carlier, M. F., T. L. Hill, and Y. Chen. 1984. "Interference of GTP Hydrolysis in the Mechanism of Microtubule Assembly: An Experimental Study." *Proceedings of the National Academy of Sciences of the United States of America* 81(3):771–75.

Catarinella, Mario, Tamara Grüner, Tobias Strittmatter, Andreas Marx, and Thomas U. Mayer. 2009. "BTB-1: A Small Molecule Inhibitor of the Mitotic Motor Protein Kif18A." *Angewandte Chemie International Edition* 48(48):9072–76.

Chen, Geng-Yuan, You Jung Kang, A. Sophia Gayek, Wiphu Youyen, Erkan Tüzel, Ryoma Ohi, and William O. Hancock. 2017. "Eg5 Inhibitors Have Contrasting Effects on Microtubule Stability and Metaphase Spindle Integrity." *ACS Chemical Biology* 12(4):1038–46.

Chen, Yalei and William O. Hancock. 2015. "Kinesin-5 Is a Microtubule Polymerase." *Nature Communications* 6(8160).

Cheng, Long, Jigar Desai, Carlos J. Miranda, Jeremy S. Duncan, Weihong Qiu, Alicia A. Nugent, Adrianne L. Kolpak, Carrie C. Wu, Eugene Drokhlyansky, Michelle M. Delisle, Wai-Man Chan, Yan Wei, Friedrich Propst, Samara L. Reck-Peterson, Bernd Fritzsch, and Elizabeth C. Engle. 2014. "Human CFEOM1 Mutations Attenuate KIF21A Autoinhibition and Cause Oculomotor Axon Stalling." *Neuron* 82(2):334–49.

Chung, Vincent, Elisabeth I. Heath, William R. Schelman, Brendan M. Johnson, Lyndon C. Kirby, Kerlin M. Lynch, Jeffrey D. Botbyl, Thomas A. Lampkin, and Kyle D. Holen. 2012. "First-Time-in-Human Study of GSK923295, a Novel Antimitotic Inhibitor of Centromere-Associated Protein E (CENP-E), in Patients with Refractory Cancer." *Cancer Chemotherapy and Pharmacology* 69(3):733–41.

Combes, G., I. Alharbi, L. G. Braga, and S. Elowe. 2017. "Playing Polo during Mitosis: PLK1 Takes the Lead." *Oncogene* 36(34):4819–27.

Coussens, Nathan P., John C. Braisted, Tyler Peryea, G. Sitta Sittampalam, Anton Simeonov, and

Matthew D. Hall. 2017. “Small-Molecule Screens: A Gateway to Cancer Therapeutic Agents with Case Studies of Food and Drug Administration-Approved Drugs.” *Pharmacological Reviews* 69(4):479–96.

Cross, Robert A. and Andrew McAinsh. 2014. “Prime Movers: The Mechanochemistry of Mitotic Kinesins.” *Nature Reviews Molecular Cell Biology* 15(4):257–71.

Debacq-Chainiaux, Florence, Jorge D. Erusalimsky, Judith Campisi, and Olivier Toussaint. 2009. “Protocols to Detect Senescence-Associated Beta-Galactosidase (SA-Bgal) Activity, a Biomarker of Senescent Cells in Culture and in Vivo.” *Nature Protocols* 4(12):1798–1806.

Desai, Arshad, Suzie Verma, Timothy J. Mitchison, and Claire E. Walczak. 1999. “Kin I Kinesins Are Microtubule-Destabilizing Enzymes.” *Cell* 96(1):69–78.

Dichiara, Maria, Agostino Marrazzo, Orazio Prezzavento, Simona Collina, Antonio Rescifina, and Emanuele Amata. 2017. “Repurposing of Human Kinase Inhibitors in Neglected Protozoan Diseases.” *ChemMedChem* 12(16):1235–53.

Dogertom, Marileen and Bernard Yurke. 1997. “Measurement of the Force-Velocity Relation for Growing Microtubules.” *Science Reports* 278:856–60.

Doxsey, Stephen. 2001. “Re-Evaluating Centrosome Function.” *Nature Reviews Molecular Cell Biology* 2(9):688–98.

Drewry, David, Timothy Willson, and William Zuercher. 2014. “Seeding Collaborations to Advance Kinase Science with the GSK Published Kinase Inhibitor Set (PKIS).” *Current Topics in Medicinal Chemistry* 14(3):340–42.

Du, Yaqing, Chauca A. English, and Ryoma Ohi. 2010. “The Kinesin-8 Kif18A Dampens Microtubule Plus-End Dynamics.” *Current Biology* 20(4):374–80.

Dumas, Megan E., Geng-Yuan Chen, Nicole D. Kendrick, George Xu, Scott A. Larsen, Somnath Jana, Alex G. Waterson, Joshua A. Bauer, William Hancock, Gary A. Sulikowski, and Ryoma Ohi. 2018. “Dual Inhibition of Kif15 by Oxindole and Quinazolinedione Chemical Probes.” *Bioorganic & Medicinal Chemistry Letters* 29:148–54.

Dumont, Sophie and Timothy J. Mitchison. 2009. “Review Force and Length in the Mitotic Spindle.” *Current Biology* 19:R749–61.

Elkins, Jonathan M., Vita Fedele, Marta Szklarz, Kamal R. Abdul Azeez, Eidarus Salah, Jowita Mikolajczyk, Sergei Romanov, Nikolai Sepetov, Xi-Ping Huang, Bryan L. Roth, Ayman Al Haj Zen, Denis Fourches, Eugene Muratov, Alex Tropsha, Joel Morris, Beverly A. Teicher, Mark Kunkel, Eric Polley, Karen E. Lackey, Francis L. Atkinson, John P. Overington, Paul Bamborough, Susanne Müller, Daniel J. Price, Timothy M. Willson, David H. Drewry, Stefan Knapp, and William J. Zuercher. 2016. “Comprehensive Characterization of the Published Kinase Inhibitor Set.” *Nature Biotechnology* 34(1):95–103.

Espeut, Julien, Amaury Gaussen, Peter Bieling, Violeta Morin, Susana Prieto, Didier Fesquet, Thomas Surrey, and Ariane Abrieu. 2008. “Phosphorylation Relieves Autoinhibition of the Kinetochore Motor Cenp-E.” *Molecular Cell* 29(5):637–43.

Firestone, Ari J., Joshua S. Weinger, Maria Maldonado, Kari Barlan, Lance D. Langston, Michael

O'donnell, Vladimir I. Gelfand, Tarun M. Kapoor, and James K. Chen. 2012. "Small-Molecule Inhibitors of the AAA1 ATPase Motor Cytoplasmic Dynein." *Nature* 484.

Florian, Stefan and Timothy J. Mitchison. 2016. "Anti-Microtubule Drugs." Pp. 403–21 in. Humana Press, New York, NY.

Gaglio, Tirso, Mary A. Dionne, and Duane A. Compton. 1997. "Mitotic Spindle Poles Are Organized by Structural and Motor Proteins in Addition to Centrosomes." *The Journal of Cell Biology* 138(5).

Ganem, Neil J., Zuzana Storchova, and David Pellman. 2007. "Tetraploidy, Aneuploidy and Cancer." *Current Opinion in Genetics & Development* 17(2):157–62.

Gibbons, I. R. and A. J. Rowe. 1965. *Dynein: A Protein with Adenosine Triphosphatase Activity from Cilia*. Vol. 149.

Gill, Steven R., Trina A. Schroer, Illya Szilak, Eric R. Steuer, Michael P. Sheetz, and Don W. Cleveland. n.d. "Dynactin, a Conserved, Ubiquitously Expressed Component of an Activator of Vesicle Motility Mediated by Cytoplasmic Dynein."

Goshima, Gohta, Mirjam Mayer, Nan Zhang, Nico Stuurman, and Ronald D. Vale. 2008. "Augmin: A Protein Complex Required for Centrosome-Independent Microtubule Generation within the Spindle." *The Journal of Cell Biology* 181(3):421–29.

Goshima, Gohta and Ronald D. Vale. 2005. "Cell Cycle-Dependent Dynamics and Regulation of Mitotic Kinesins in *Drosophila* S2 Cells." *Molecular Biology of the Cell* 16(8):3896–3907.

Green, Rebecca A., Ewa Paluch, and Karen Oegema. 2012. "Cytokinesis in Animal Cells." *Annual Review of Cell and Developmental Biology* 28(1):29–58.

Groen, Aaron C., Daniel Needleman, Clifford Brangwynne, Christain Gradinaru, Brandon Fowler, Ralph Mazitschek, and Timothy J. Mitchison. 2008. "A Novel Small-Molecule Inhibitor Reveals a Possible Role of Kinesin-5 in Anastral Spindle-Pole Assembly." *Journal of Cell Science* 121(Pt 14):2293–2300.

Gruss, Oliver J. and Isabelle Vernos. 2004. "The Mechanism of Spindle Assembly: Functions of Ran and Its Target TPX2." *The Journal of Cell Biology JCB The Journal of Cell Biology* 166(7):949–55.

Le Guellec, R., J. Paris, A. Couturier, C. Roghi, and M. Philippe. 1991. "Cloning by Differential Screening of a Xenopus CDNA That Encodes a Kinesin-Related Protein." *Molecular and Cellular Biology* 11(6):3395–98.

Hackney, D. D. and M. F. Stock. 2000. "Kinesin's IAK Tail Domain Inhibits Initial Microtubule-Stimulated ADP Release." *Nature Cell Biology* 2(5):257–60.

Heald, Rebecca, Regis Tournebize, Thiemo Blankt, Raphael Sandaltzopoulost, Peter Beckert, Anthony Hyman, and Eric Karsenti. 1996. *Self-Organization of Microtubules into Bipolar Spindles around Artificial Chromosomes in Xenopus Egg Extracts*. Vol. 382.

van Heesbeen, Roy G. H. P., Jonne A. Raaijmakers, Marvin E. Tanenbaum, Vincentius A. Halim, Daphne Lelieveld, Cor Lieftink, Albert J. R. Heck, David A. Egan, and René H. Medema.

2017. “Aurora A, MCAK, and Kif18b Promote Eg5-Independent Spindle Formation.” *Chromosoma* 126(4):473–86.

Hinshaw, Stephen M. and Stephen C. Harrison. 2018. “Kinetochore Function from the Bottom Up.” *Trends in Cell Biology* 28(1):22–33.

Hirokawa, N. and Yosuke Tanaka. 2015. “Kinesin Superfamily Proteins (KIFs): Various Functions and Their Relevance for Important Phenomena in Life and Diseases.” *Experimental Cell Research* 334(1):16–25.

Holy, Timothy E. and Stanislas Leibler. 1994. *Dynamic Instability of Microtubules as an Efficient Way to Search in Space*. Vol. 91.

Inoue, Shinya. 1953. “Polarization Optical Studies of the Mitotic Spindle.” *Chromosoma* 5(1):487–500.

Islam, Kabirul, Adrian O. Olivares, Lauren P. Saunders, Enrique M. De, La Cruz, and Tarun M. Kapoor. 2010. “Myosin V Inhibitor Based on Privileged Chemical Scaffolds **.” *Angewandte Chemie International Edition* 49(45):8484–88.

Izquierdo, Denisse, Won-Jing Wang, Kunihiro Uryu, and Meng-Fu Bryan Tsou. 2014. “Stabilization of Cartwheel-Less Centrioles for Duplication Requires CEP295-Mediated Centriole-to-Centrosome Conversion.” *Cell Reports* 8(4):957–65.

Kaan, H. Y. K., D. D. Hackney, and F. Kozielski. 2011. “The Structure of the Kinesin-1 Motor-Tail Complex Reveals the Mechanism of Autoinhibition.” *Science* 333(6044):883–85.

Kajtez, Janko, Anastasia Solomatina, Maja Novak, Bruno Polak, Kruno Vukušic, Vukušic´ Vukušic´3, Jonas Rüdiger, Gheorghe Cojoc, Ana Milas, Ivana S. ˇ. Umanovac, S. ˇ. Estak, Patrik Risteski, Federica Tavano, Anna H. Klemm, Emanuele Roscioli, Julie Welburn, Daniela Cimini, Matko Glunčic, Glunčic´ Glunčic´2, Nenad Pavin, Iva M. Tolic´1, and Tolic´ Tolic´1. 2016. “ARTICLE Overlap Microtubules Link Sister K-Fibres and Balance the Forces on Bi-Oriented Kinetochores.” *Nature Communications* 7.

Kalab, Petr and Rebecca Heald. 2008. “The Ran-GTP Gradient - a GPS for the Mitotic Spindle.” *Journal of Cell Science* 121:1577–86.

Kalab, Petr, Karsten Weis, and Rebecca Heald. 2002. “Visualization of a Ran-GTP Gradient in Interphase and Mitotic Xenopus Egg Extracts.” *Science (New York, N.Y.)* 295(5564):2452–56.

Kantarjian, H. M., S. Padmanabhan, W. Stock, M. S. Tallman, G. A. Curt, J. Li, A. Osmukhina, K. Wu, D. Huszar, G. Borthukar, S. Faderl, G. Garcia-Manero, T. Kadia, K. Sankhala, O. Odenike, J. K. Altman, and M. Minden. 2012. “Phase I/II Multicenter Study to Assess the Safety, Tolerability, Pharmacokinetics and Pharmacodynamics of AZD4877 in Patients with Refractory Acute Myeloid Leukemia.” *Investigational New Drugs* 30(3):1107–15.

Kapitein, Lukas C., Erwin J. G. Peterman, Benjamin H. Kwok, Jeffrey H. Kim, Tarun M. Kapoor, and Christoph F. Schmidt. 2005. “The Bipolar Mitotic Kinesin Eg5 Moves on Both Microtubules That It Crosslinks.” *Nature* 435(7038):114–18.

Kapoor, T. M., T. U. Mayer, M. L. Coughlin, and T. J. Mitchison. 2000. “Probing Spindle

Assembly Mechanisms with Monastrol, a Small Molecule Inhibitor of the Mitotic Kinesin, Eg5." *The Journal of Cell Biology* 150(5):975–88.

Kaverina, I., K. Rottner, and J. V Small. 1998. "Targeting, Capture, and Stabilization of Microtubules at Early Focal Adhesions." *The Journal of Cell Biology* 142(1):181–90.

Kaverina, Irina, Olga Krylyshkina, and J. Victor Small. 1999. *Microtubule Targeting of Substrate Contacts Promotes Their Relaxation and Dissociation*. Vol. 146.

Kevenaar, Josta T., Sarah Bianchi, Myrrhe van Spronsen, Natacha Olieric, Joanna Lipka, Cátia P. Frias, Marina Mikhaylova, Martin Harterink, Nanda Keijzer, Phebe S. Wulf, Manuel Hilbert, Lukas C. Kapitein, Esther de Graaff, Anna Ahkmanova, Michel O. Steinmetz, and Casper C. Hoogenraad. 2016. "Kinesin-Binding Protein Controls Microtubule Dynamics and Cargo Trafficking by Regulating Kinesin Motor Activity." *Current Biology* 26(7):849–61.

Khodjakov, Alexey, Richard W. Cole, Berl R. Oakley, and Conly L. Rieder. 2000. "Centrosome-Independent Mitotic Spindle Formation in Vertebrates." *Current Biology* 10(2):59–67.

Khodjakov, Alexey and Conly L. Rieder. 1996. "Kinetochores Moving Away from Their Associated Pole Do Not Exert a Significant Pushing Force on the Chromosome." *Journal of Cell Biology* 135(2):315–27.

Klejnot, Marta, Aditi Falnikar, Venkatasubramanian Ulaganathan, Robert A. Cross, Peter W. Baas, and Frank Kozielski. 2014. "The Crystal Structure and Biochemical Characterization of Kif15: A Bifunctional Molecular Motor Involved in Bipolar Spindle Formation and Neuronal Development." *Acta Cryst* 70:123–33.

Knapp, Stefan, Paulo Arruda, Julian Blagg, Stephen Burley, David H. Drewry, Aled Edwards, Doriano Fabbro, Paul Gillespie, Nathanael S. Gray, Bernhard Kuster, Karen E. Lackey, Paulo Mazzafera, Nicholas C. O. Tomkinson, Timothy M. Willson, Paul Workman, and William J. Zuercher. 2013. "A Public-Private Partnership to Unlock the Untargeted Kinome." *Nature Chemical Biology* 9(1):3–6.

Kozielski, F. 2012. *Kinesins and Cancer*. Vol. 12.

Kurasawa, Yasuhiro, William C. Earnshaw, Yuko Mochizuki, Naoshi Dohmae, and Kazuo Todokoro. 2004. "Essential Roles of KIF4 and Its Binding Partner PRC1 in Organized Central Spindle Midzone Formation." *The EMBO Journal* 23:3237–48.

Kwon, Mijung, Susana A. Godinho, Namrata S. Chandhok, Neil J. Ganem, Ammar Azioune, Manuel Thery, and David Pellman. 2008. "Mechanisms to Suppress Multipolar Divisions in Cancer Cells with Extra Centrosomes." *Genes & Development* 22(16):2189–2203.

Laan, Liedewij, Nenad Pavin, Julien Husson, Guillaume Romet-Lemonne, Martijn Van Duijn, Magdalena Preciado Ló Pez, Ronald D. Vale, Frank Jü, Samara L. Reck-Peterson, and Marileen Dogterom. 2012. "Cortical Dynein Controls Microtubule Dynamics to Generate Pulling Forces That Position Microtubule Asters."

Lackey, Karen, Michael Cory, Ronda Davis, Stephen V. Frye, Philip A. Harris, Robert N. Hunter, David K. Jung, O. Bradle. McDonald, Robert W. McNutt, Michael R. Peel, Randy D. Rutkowske, James M. Veal, and Edgar R. Wood. 2000. "The Discovery of Potent CRaf1 Kinase Inhibitors." *Bioorganic & Medicinal Chemistry Letters* 10(3):223–26.

Lee, T., K. J. Langford, J. M. Askham, A. Brüning-Richardson, and E. E. Morrison. 2008. “MCAK Associates with EB1.” *Oncogene* 27(17):2494–2500.

Liu, Xiaoqi and Raymond L. Erikson. 2007. “The Nuclear Localization Signal of Mitotic Kinesin-like Protein Mklp-1: Effect on Mklp-1 Function during Cytokinesis.” *Biochemical and Biophysical Research Communications* 353(4):960–64.

Lombillo, Vivian A., Russel J. Stewart, and J. Richard McIntosh. 1995. *Minus-End-Directed Motion of Kinesin-Coated Microspheres Driven by Microtubule Depolymerization*. Vol. 373.

Ma, Hoi Tang, Sergio Erdal, Shan Huang, and Randy Y. C. Poon. 2014. “Synergism between Inhibitors of Aurora A and KIF11 Overcomes KIF15-Dependent Drug Resistance.” *Molecular Oncology* 8(8):1404–18.

Malaby, Heidi LH, Megan E. Dumas, Ryoma Ohi, and Jason Stumpff. 2019. “Kinesin-Binding Protein Ensures Accurate Chromosome Segregation by Buffering KIF18A and KIF15.”

Manning, G., D. B. Whyte, R. Martinez, T. Hunter, and S. Sudarsanam. 2002. “The Protein Kinase Complement of the Human Genome.” *Science* 298(5600):1912–34.

Mansoori, Behzad, Ali Mohammadi, Sadaf Davudian, Solmaz Shirjang, and Behzad Baradaran. 2017. “The Different Mechanisms of Cancer Drug Resistance: A Brief Review.” *Adv Pharm Bull* 7(3):339–48.

Mastronarde, D. N., K. L. McDonald, R. Ding, and J. R. McIntosh. 1993. “Interpolar Spindle Microtubules in PTK Cells.” *The Journal of Cell Biology* 123(6 Pt 1):1475–89.

Mayer, T. U., T. M. Kapoor, S. J. Haggarty, R. W. King, S. L. Schreiber, and T. J. Mitchison. 1999. “Small Molecule Inhibitor of Mitotic Spindle Bipolarity Identified in a Phenotype-Based Screen.” *Science (New York, N.Y.)* 286(5441):971–74.

Mayr, Monika I., Stefan Hümmer, Jenny Bormann, Tamara Grüner, Sarah Adio, Guenther Woehlke, and Thomas U. Mayer. 2007. “The Human Kinesin Kif18A Is a Motile Microtubule Depolymerase Essential for Chromosome Congression.” *Current Biology : CB* 17(6):488–98.

McDonald, Andrew, Gustave Bergnes, and DJ Morgans. 2004. “US 20040053948A.”

Milic, Bojan, Anirban Chakraborty, Kyuho Han, Michael C. Bassik, and Steven M. Block. 2018. “KIF15 Nanomechanics and Kinesin Inhibitors, with Implications for Cancer Chemotherapeutics.” *Proceedings of the National Academy of Sciences of the United States of America* 115(20):E4613–22.

Miller, J. Richard, Steve Dunham, Igor Mochalkin, Craig Banotai, Matthew Bowman, Susan Buist, Bill Dunkle, Debra Hanna, H. James Harwood, Michael D. Huband, Alla Karnovsky, Michael Kuhn, Chris Limberakis, Jia Y. Liu, Shawn Mehrens, W. Thomas Mueller, Lakshmi Narasimhan, Adam Ogden, Jeff Ohren, J. V. N. Vara Prasad, John A. Shelly, Laura Skerlos, Mark Sulavik, V. Hayden Thomas, Steve VanderRoest, LiAnn Wang, Zhigang Wang, Amy Whitton, Tong Zhu, and C. Kendall Stover. 2009. “A Class of Selective Antibacterials Derived from a Protein Kinase Inhibitor Pharmacophore.” *Proceedings of the National Academy of Sciences of the United States of America* 106(6):1737–42.

Mimori-Kiyosue, Yuko, Nobuyuki Shiina, and Shoichiro Tsukita. 2000. “The Dynamic Behavior

of the APC-Binding Protein EB1 on the Distal Ends of Microtubules." *Current Biology* 10(14):865–68.

Mitchison, T. and M. Kirschner. 1984. "Dynamic Instability of Microtubule Growth." *Nature*.

Mitchison, Timothy J. 2012. "The Proliferation Rate Paradox in Antimitotic Chemotherapy." 23.

Mogilner, A. and George Oster. 1999. "The Polymerization Ratchet Model Explains the Force-Velocity Relation for Growing Microtubules." *European Biophysics Journal* 28(3):235–42.

Mountain, V., C. Simerly, L. Howard, A. Ando, G. Schatten, and D. A. Compton. 1999. "The Kinesin-Related Protein, HSET, Opposes the Activity of Eg5 and Cross-Links Microtubules in the Mammalian Mitotic Spindle." *The Journal of Cell Biology* 147(2):351–66.

Neef, Rüdiger, Ulf R. Klein, Robert Kopajtich, and Francis A. Barr. 2006. "Cooperation between Mitotic Kinesins Controls the Late Stages of Cytokinesis." *Current Biology* 16(3):301–7.

Noble, R. L., C. T. Beer, and J. H. Cutts. 1958. "ROLE OF CHANCE OBSERVATIONS IN CHEMOTHERAPY: *VINCA ROSEA* *." *Annals of the New York Academy of Sciences* 76(3):882–94.

Norris, Stephen R., Seungyeon Jung, Prashant Singh, Claire E. Strothman, Amanda L. Erwin, Melanie D. Ohi, Marija Zanic, and Ryoma Ohi. 2018. "Microtubule Minus-End Aster Organization Is Driven by Processive HSET-Tubulin Clusters." *Nature Communications* 9(1).

Nurse, Paul. 2000. "A Long Twentieth Century of the Cell Cycle and Beyond." *Cell* 100(1):71–78.

Oakley, C. Elizabeth and Berl R. Oakley. 1989. "Identification of γ-Tubulin, a New Member of the Tubulin Superfamily Encoded by MipA Gene of Aspergillus Nidulans." *Nature* 338(6217):662–64.

Oakley, Derl R., C. Elizabeth Oakley, Yisang Yoon, and M. Katherine Jung. 1990. *Y-Tubulin Is a Component of the Spindle Pole Body That Is Essential for Microtubule Function in Aspergillus Nidulans*. Vol. 61.

Ohi, Ryoma, Tanuj Sapra, Jonathan Howard, and Timothy J. Mitchison. 2004. "Differentiation of Cytoplasmic and Meiotic Spindle Assembly MCAK Functions by Aurora B-Dependent Phosphorylation." *Molecular Biology of the Cell* 15(6):2895–2906.

Perez, Ignacio, De Castro, Yannick Arlot, Spiros Linardopoulos, and Vassilios Bavetsias. 2015. "Aurora Kinase Inhibitors: Current Status and Outlook." 5.

Peskin, C. S., G. M. Odell, and G. F. Oster. 1993. "Cellular Motions and Thermal Fluctuations: The Brownian Ratchet." *Biophysical Journal* 65(1):316–24.

Peterson, Jeffrey R. and Erica A. Golemis. 2004. "Autoinhibited Proteins as Promising Drug Targets." *Journal of Cellular Biochemistry* 93:68–73.

Qian, Xiangping, Andrew Mcdonald, Han-Jie Zhou, Nicholas D. Adams, Cynthia A. Parrish, Kevin J. Duffy, Duke M. Fitch, Rosanna Tedesco, Luke W. Ashcraft, Bing Yao, Hong Jiang, Jennifer K. Huang, Melchor V Marin, Carrie E. Aroyan, Jianchao Wang, Seyed Ahmed,

Joelle L. Burgess, Amita M. Chaudhari, Carla A. Donatelli, Michael G. Darcy, Lance H. Ridgers, Ken A. Newlander, Stanley J. Schmidt, Deping Chai, Mariela Col, Michael N. Zimmerman, Latesh Lad, Roman Sakowicz, Stephen Schauer, Lisa Belmont, Ramesh Baliga, Daniel W. Pierce, Jeffrey T. Finer, Zhengping Wang, Bradley P. Morgan, David J. Morgans, Kurt R. Auger, Chiu-Mei Sung, Jeff D. Carson, Lusong Luo, Erin D. Hugger, Robert A. Copeland, David Sutton, John D. Elliott, Jeffrey R. Jackson, Kenneth W. Wood, Dashyant Dhanak, Gustave Bergnes, and Steven D. Knight. 2010. "Discovery of the First Potent and Selective Inhibitor of Centromere-Associated Protein E: GSK923295." *Chem. Lett* 1:30–34.

Qiao, Yuan, Jingtao Chen, Chao Ma, Yingmin Liu, Peitong Li, Yalin Wang, Lin Hou, and Ziling Liu. 2018. "Increased KIF15 Expression Predicts a Poor Prognosis in Patients with Lung Adenocarcinoma." *Cellular Physiology and Biochemistry* 51(1):1–10.

Raaijmakers, Jonne A., Roy Ghp Van Heesbeen, Johnathan L. Meaders, Erica F. Geers, Belen Fernandez-Garcia, René H. Medema, and Marvin E. Tanenbaum. 2012. "Nuclear Envelope-Associated Dynein Drives Prophase Centrosome Separation and Enables Eg5-Independent Bipolar Spindle Formation." *The EMBO Journal* 31:4179–90.

Randall, Thomas S., Yan Y. Yip, Daynea J. Wallock-Richards, Karin Pfisterer, Anneri Sanger, Weronika Ficek, Roberto A. Steiner, Andrew J. Beavil, Maddy Parsons, and Mark P. Dodding. 2017. "A Small-Molecule Activator of Kinesin-1 Drives Remodeling of the Microtubule Network." *Proceedings of the National Academy of Sciences* 114(52):13738–43.

Reinemann, Dana N., Emma G. Sturgill, Dibyendu Kumar Das, Miriam Steiner Degen, Zsuzsanna Vörös, Wonmuk Hwang, Ryoma Ohi, and Matthew J. Lang. 2017. "Collective Force Regulation in Anti-Parallel Microtubule Gliding by Dimeric Kif15 Kinesin Motors." *Current Biology* 27(18):2810–2820.e6.

Richters, André, Debjit Basu, Julian Engel, Meryem S. Ercanoglu, Hyatt Balke-Want, Roberta Tesch, Roman K. Thomas, and Daniel Rauh. 2015. "Identification and Further Development of Potent TBK1 Inhibitors." *ACS Chemical Biology* 10(1):289–98.

Rowinsky, E. K., E. A. Eisenhauer, V. Chaudhry, S. G. Arbuck, and R. C. Donehower. 1993. "Clinical Toxicities Encountered with Paclitaxel (Taxol)." *Seminars in Oncology* 20(4 Suppl 3):1–15.

Saeki, Eri, Shinji Yasuhira Id, Masahiko Shibazaki Id, Hiroshi Tada, Minoru Doita, Tomoyuki Masuda, and Chihaya Maesawa. 2018. "Involvement of C-Terminal Truncation Mutation of Kinesin-5 in Resistance to Kinesin-5 Inhibitor."

Salmela, Anna-Leena and Marko J. Kallio. 2013. "Mitosis as an Anti-Cancer Drug Target." *Chromosoma* 122(5):431–49.

Sawin, K. E. and T. J. Mitchison. 1995. "Mutations in the Kinesin-like Protein Eg5 Disrupting Localization to the Mitotic Spindle." *Proceedings of the National Academy of Sciences of the United States of America* 92(10):4289–93.

Sawin, Kenneth E., Katherine Leguellect, Michel Philippet, and Timothy J. Mitchison. 1992. *Mitotic Spindle Organization by a Plus-End-Directed Microtubule Motor*.

Schiff, Peter B., Jane Fant, and Susan B. Horwitz. 1979. “Promotion of Microtubule Assembly in Vitro by Taxol.” *Nature* 277(5698):665–67.

Schmitt, Michael W., Lawrence A. Loeb, and Jesse J. Salk. 2016. “The Influence of Subclonal Resistance Mutations on Targeted Cancer Therapy.” *Nature Reviews Clinical Oncology* 13(6):335–47.

Scholey, Jonathan, Gul Civelekoglu-Scholey, Ingrid Brust-Mascher, Jonathan M. Scholey, Gul Civelekoglu-Scholey, and Ingrid Brust-Mascher. 2016. “Anaphase B.” *Biology* 5(4):51.

Segbert, Christoph, Rosemarie Barkus, Jim Powers, Susan Strome, William M. Saxton, and Olaf Bossinger. 2003. “KLP-18, a Klp2 Kinesin, Is Required for Assembly of Acentrosomal Meiotic Spindles in Caenorhabditis Elegans □ V.” *Molecular Biology of the Cell* 14:4458–69.

Sigal, Alex, Ron Milo, Ariel Cohen, Naama Geva-Zatorsky, Yael Klein, Yuvalal Liron, Nitzan Rosenfeld, Tamar Danon, Natalie Perzov, and Uri Alon. 2006. “Variability and Memory of Protein Levels in Human Cells.” *Nature* 444(7119):643–46.

Song, Xiaowei, Tengfang Zhang, Xiangkun Wang, Xiwen Liao, Chuangye Han, Chengkun Yang, Ka Su, Wenlong Cao, Yizhen Gong, Zhu Chen, Quanfa Han, and Jiehua Li. 2018. “Distinct Diagnostic and Prognostic Values of Kinesin Family Member Genes Expression in Patients with Breast Cancer.”

Stumpff, Jason, George von Dassow, Michael Wagenbach, Charles Asbury, and Linda Wordeman. 2008. “The Kinesin-8 Motor Kif18A Suppresses Kinetochore Movements to Control Mitotic Chromosome Alignment.” *Developmental Cell* 14(2):252–62.

Stumpff, Jason, Yaqing Du, Chauca A. English, Zoltan Maliga, Michael Wagenbach, Charles L. Asbury, Linda Wordeman, and Ryoma Ohi. 2011. “A Tethering Mechanism Controls the Processivity and Kinetochore-Microtubule Plus-End Enrichment of the Kinesin-8 Kif18A.” *Molecular Cell* 43(5):764–75.

Sturgill, Emma G., Dibyendu Kumar Das, Yoshimasa Takizawa, Yongdae Shin, Scott E. Collier, Melanie D. Ohi, Wonmuk Hwang, Matthew J. Lang, and Ryoma Ohi. 2014. “Kinesin-12 Kif15 Targets Kinetochore Fibers through an Intrinsic Two-Step Mechanism.” *Current Biology* 24(19):2307–13.

Sturgill, Emma G. and Ryoma Ohi. 2013. “Article Kinesin-12 Differentially Affects Spindle Assembly Depending on Its Microtubule Substrate.” *Current Biology* 23:1280–90.

Sturgill, Emma, Stephen Norris, Yan Guo, and Ryoma Ohi. 2016. “Kinesin-5 Inhibitor Resistance Is Driven by Kinesin-12.” *Journal of Cell Biology* 213(2):213–27.

Subramanian, Radhika, Shih-Chieh Ti, Lei Tan, Seth A. Darst, and Tarun M. Kapoor. 2013. “Marking and Measuring Single Microtubules by PRC1 and Kinesin-4.” *Cell* 154(2):377–90.

Talapatra, Sandeep K., Nahoum G. Anthony, Simon P. Mackay, and Frank Kozielski. 2013. “Mitotic Kinesin Eg5 Overcomes Inhibition to the Phase I/II Clinical Candidate SB743921 by an Allosteric Resistance Mechanism.” *Journal of Medicinal Chemistry* 56(16):6317–29.

Tanenbaum, Marvin E., Libor Macůrek, Aniek Janssen, Erica F. Geers, Mónica Alvarez-

Fernández, and René H. Medema. 2009. “Kif15 Cooperates with Eg5 to Promote Bipolar Spindle Assembly.” *Current Biology* 19(20):1703–11.

Tanenbaum, Marvin E., Ronald D. Vale, and Richard J. McKenney. 2013. “Cytoplasmic Dynein Crosslinks and Slides Anti-Parallel Microtubules Using Its Two Motor Domains.” *ELife* 2.

Tao, Weikang, Victoria J. South, Yun Zhang, Joseph P. Davide, Linda Farrell, Nancy E. Kohl, Laura Sepp-Lorenzino, and Robert B. Lobell. 2005. “Induction of Apoptosis by an Inhibitor of the Mitotic Kinesin KSP Requires Both Activation of the Spindle Assembly Checkpoint and Mitotic Slippage.” *Cancer Cell* 8(1):49–59.

Thyberg, Johan L. and Stanislaw Moskalewski. 1985. *Microtubules and the Organization of the Golgi Complex*. Vol. 159.

Tikhonenko, Irina, Dilip K. Nag, Nora Martin, and Michael P. Koonce. 2008. “Kinesin-5 Is Not Essential for Mitotic Spindle Elongation in Dictyostelium.” *Cell Motility and the Cytoskeleton* 65(11):853–62.

Uehara, Ryota, Ryu-suke Nozawa, Akiko Tomioka, Sabine Petry, Ronald D. Vale, Chikashi Obuse, and Gohta Goshima. 2009. “The Augmin Complex Plays a Critical Role in Spindle Microtubule Generation for Mitotic Progression and Cytokinesis in Human Cells.” *Proceedings of the National Academy of Sciences of the United States of America* 106(17):6998–7003.

Vale, Ronald D., Thomas S. Reese, and Michael P. Sheetz. 1985. *Identification of a Novel Force-Generating Protein, Kinesin, Involved in Microtubule-Based Motility*. Vol. 42.

van der Vaart, Babet, Wilhelmina E. van Riel, Harinath Doodhi, Josta T. Kevenaar, Eugene A. Katrukha, Laura Gumy, Benjamin P. Bouchet, Ilya Grigoriev, Samantha A. Spangler, Ka Lou Yu, Phebe S. Wulf, Jingchao Wu, Gideon Lansbergen, Eljo Y. van Battum, R. Jeroen Pasterkamp, Yuko Mimori-Kiyosue, Jeroen Demmers, Natacha Olieric, Ivan V. Maly, Casper C. Hoogenraad, and Anna Akhmanova. 2013. “CFEOM1-Associated Kinesin KIF21A Is a Cortical Microtubule Growth Inhibitor.” *Developmental Cell* 27(2):145–60.

Vanneste, David, Masatoshi Takagi, Naoko Imamoto, and Isabelle Vernos. 2009. “The Role of Hklp2 in the Stabilization and Maintenance of Spindle Bipolarity.” *Current Biology* 19(20):1712–17.

Verde, Fulvia, Marileen Dogterom, Ernst Stelzer, Eric Karsenti, and Stanislas Leibler. 1992. “Control of Microtubule Dynamics and Length by Cyclin A-and Cyclin B-Dependent Kinases in Xenopus Egg Extracts.” *Journal of Cell Biology* 118(5):1097–1108.

Verhey, Kristen J. and Jennetta W. Hammond. 2009. “Traffic Control: Regulation of Kinesin Motors.” *Nature Reviews Molecular Cell Biology* 10.

Vukušić, Kruno, Renata Buđa, Agneza Bosilj, Ana Milas, Nenad Pavin, and Iva M. Tolić. 2017. “Microtubule Sliding within the Bridging Fiber Pushes Kinetochore Fibers Apart to Segregate Chromosomes.” *Developmental Cell* 43(1):11–23.e6.

Walczak, Claire E., Suzie Verma, and Timothy J. Mitchison. 1997. “XCTK2: A Kinesin-Related Protein That Promotes Mitotic Spindle Assembly in Xenopus Laevis Egg Extracts.” *The Journal of Cell Biology* 136(4):859–70.

Walker, R. A., E. T. O'Brien, N. K. Pryer, M. F. Soboeiro, W. A. Voter, H. P. Erickson, and E. D. Salmon. 1988. "Dynamic Instability of Individual Microtubules Analyzed by Video Light Microscopy: Rate Constants and Transition Frequencies." *The Journal of Cell Biology* 107(4):1437–48.

Walsh, Vivien and Jordan Goodman. 2010. "Medical Anthropology From Taxol to Taxol®: The Changing Identities and Ownership of an Anti-Cancer Drug."

Wang, Shaomeng. 2010. "Design of Small-Molecule Smac Mimetics as IAP Antagonists." Pp. 89–113 in. Springer, Berlin, Heidelberg.

Wani, Mansukhlal C., Harold Lawrence Taylor, Monroe E. Wall, Philip Coggon, and Andrew T. McPhail. 1971. "Plant Antitumor Agents. VI. Isolation and Structure of Taxol, a Novel Antileukemic and Antitumor Agent from Taxus Brevifolia." *Journal of the American Chemical Society* 93(9):2325–27.

Waterman-Storer, Clare M., Rebecca A. Worthylake, Betty P. Liu, Keith Burridge, and E. D. Salmon. 1999. "Microtubule Growth Activates Rac1 to Promote Lamellipodial Protrusionin Fibroblasts." *Nature Cell Biology* 1(1):45–50.

Weaver, Lesley N., Stephanie C. Ems-McClung, Jane R. Stout, Chantal LeBlanc, Sidney L. Shaw, Melissa K. Gardner, and Claire E. Walczak. 2011. "Kif18A Uses a Microtubule Binding Site in the Tail for Plus-End Localization and Spindle Length Regulation." *Current Biology* 21(17):1500–1506.

Welburn, Julie P. I. 2013. "The Molecular Basis for Kinesin Functional Specificity during Mitosis." *Cytoskeleton* 70(9):476–93.

Wignall, Sarah M. and Anne M. Villeneuve. 2009. "Lateral Microtubule Bundles Promote Chromosome Alignment during Acentrosomal Oocyte Meiosis." *Nat Cell Biol* 11(7):839–44.

Wozniak, Marcin J., Martina Melzer, Cornelia Dorner, Hans-Ulrich Haring, and Reiner Lammers. 2005. "The Novel Protein KBP Regulates Mitochondria Localization by Interaction with a Kinesin-like Protein." *BMC Cell Biology* 6(1):35.

Wu, Xiaoqin, Gang Xu, Xiaobo Li, Weiren Xu, Qianjin Li, Wei Liu, Karen A. Kirby, Mignon L. Loh, Jun Li, Stefan G. Sarafianos, and Cheng-Kui Qu. 2018. "Small Molecule Inhibitor That Stabilizes the Autoinhibited Conformation of the Oncogenic Tyrosine Phosphatase SHP2."

Yang, C. H. and M. Snyder. 1992. "The Nuclear-Mitotic Apparatus Protein Is Important in the Establishment and Maintenance of the Bipolar Mitotic Spindle Apparatus." *Molecular Biology of the Cell* 3(11):1259–67.

Yu, Xiaoyu, Xiaoyu He, L. M. Heindl, Xin song, Jiayan Fan, and Renbing Jia. 2019. "KIF15 Plays a Role in Promoting the Tumorigenicity of Melanoma." *Experimental Eye Research*.

Zasadil, Lauren M., Kristen A. Andersen, Dabin Yeum, Gabrielle B. Rocque, Lee G. Wilke, Amye J. Tevaarwerk, Ronald T. Raines, Mark E. Burkard, and Beth A. Weaver. 2014. "Cytotoxicity of Paclitaxel in Breast Cancer Is Due to Chromosome Missegregation on Multipolar Spindles." *Science Translational Medicine* 6(229):229ra43-229ra43.

Zegzouti, H., J. Alves, T. Worzella, G. Vidugiris, G. Cameron, J. Vidugiriene, and S. Goueli. 2011.

"Screening and Profiling Kinase Inhibitors with a Luminescent ADP Detection Platform." *Promega Corporation*. Retrieved March 15, 2019 (https://www.promega.com/resources/pubhub/screening-and-profiling-kinase-inhibitors-with-a-luminescent-adp-detection-platform/).

Zhai, Ye, Paul J. Kronebusch, and Gary G. Borisy. 1995. "Kinetochore Microtubule Dynamics and the Metaphase-Anaphase Transition." *Journal of Cell Biology* 131(3):721–34.

Zhang, J. H., Thomas D. Y. Chung, and Kevin R. Oldenburg. 1999. "A Simple Statistical Parameter for Use in Evaluation and Validation of High Throughput Screening Assays." *Journal of Biomolecular Screening* 4(2):67–73.

Zhao, Hongda, Qiyu Bo, Zonglong Wu, Qinggang Liu, Yan Li, Ning Zhang, Hu Guo, and Benkang Shi. 2019. "KIF15 Promotes Bladder Cancer Proliferation via the MEK–ERK Signaling Pathway." *Cancer Management and Research* Volume 11:1857–68.

Zheng, Yixian, Mei Lie Wong, Bruce Alberts, and Tim Mitchison. 1995. "Nucleation of Microtubule Assembly by a γ-Tubulin-Containing Ring Complex." *Nature* 378(6557):578–83.